ABSTRACT

Title of dissertation: THE NATURE OF ASYMMETRY
                           IN FLUID CRITICALITY

                           Jingtao Wang, Doctor of Philosophy, 2006

Dissertation directed by: Professor Mikhail A. Anisimov
                           Institute for Physical Science and Technology and
                           Department of Chemical and Biomolecular Engineering

This dissertation deals with an investigation of the nature of asymmetry in fluid criticality, especially for vapor-liquid equilibra in one-component fluids and liquid-liquid equilibra in binary fluid mixtures. The conventional mixing of physical variables in scaling theory introduces an asymmetric term in diameters of coexistence curves that asymptotically varies as $\left| \Delta \widetilde{T} \right|^{1-\alpha}$, where $\Delta \widetilde{T} = (T - T_{\mathrm{c}})/T_{\mathrm{c}}$ is the relative distance of the temperature T from the critical temperature T_{c}. "Complete scaling" implies the presence of an additional asymmetric term proportional to $\left| \Delta \widetilde{T} \right|^{2\beta}$ in diameters which is more dominant near the critical point. To clarify the nature of vapor-liquid asymmetry, we have used the thermodynamic freedom of a proper choice for the critical entropy to simplify "complete scaling" to a form with only two independent mixing coefficients and developed a procedure to obtain these two coefficients, responsible for the two different singular sources for the asymmetry, from mean-field equations of state. By analyzing some classical equations of state

we have found that the vapor-liquid asymmetry in classical fluids near the critical point can be controlled by molecular parameters, such as the degree of association and the strength of three-body interactions. By combining accurate vapor-liquid coexistence and heat-capacity data, we have obtained the unambiguous evidence for "complete scaling" from existing experimental and simulation data. A number of systems, real fluids and simulated models have been analyzed. Furthermore, we have examined the consequences of "complete scaling" when extended to liquid-liquid co-existence in binary mixtures. The procedure for extending "complete scaling" from one-component fluids to binary fluid mixtures follows rigorously the theory of iso-morphism of critical phenomena. We have shown that the "singular" diameter of liquid-liquid coexistence also originates from two different sources. Finally, we have studied special phase equilibria that can only be described by including non-linear mixing of physical fields into the scaling fields. Based on scaling and isomorphism, an approach is presented to represent closed-loop coexistence curves and expressions to describe the critical lines near a double critical point (DCP) are derived. The results demonstrate the practical significance of applying scaling and isomorphism theory to the treatment of phase equilibria in chemical engineering.

THE NATURE OF ASYMMETRY IN FLUID CRITICALITY

by

Jingtao Wang

Dissertation submitted to the Faculty of the Graduate School of the
University of Maryland, College Park in partial fulfillment
of the requirements for the degree of
Doctor of Philosophy
2006

Advisory Committee:
Professor Mikhail A. Anisimov, Chair/Advisor
Professor Jan V. Sengers
Professor Sandra C. Greer
Professor Srinivasa R. Raghavan
Professor John D. Weeks

ACKNOWLEDGMENTS

TABLE OF CONTENTS

LIST OF TABLES

LIST OF FIGURES

CHAPTER 1

INTRODUCTION

A variety of physical systems exhibit critical phenomena which have been a popular subject of many theoretical and experimental studies since the 19th century. Among them, studies of critical phenomena in fluids, such as vapor-liquid critical phenomena and liquid-liquid critical phenomena, are very important for chemical engineering.

It is well known that the thermodynamic properties of fluids exhibit anomalous behavior near the critical point. Asymptotic non-analytic behaviors near the critical point can be described by asymptotic power laws. For example, the isothermal compressibility obeys a power law with an exponent larger than unity, and the isochoric heat capacity diverges at the critical point.[1, 2] Another important principle is critical-point universality, which means that the effects of the microscopic structure of fluids on thermodynamic properties become unimportant in the critical region.[4, 5] Both the nonanalytic singular behavior of the thermodynamic properties and critical-point universality are consequences of the presence of long-range critical fluctuations of an order parameter (density in one-component fluids or concentration in liquid mixtures). In the vicinity of a critical point the spatial extent (correlation length) of these long-range fluctuations is much larger than any molecular length scale. This is the physical origin of critical-point universality. Furthermore, because the correlation length diverges at the critical point, the behavior of the thermodynamic properties becomes singular. However, the asymptotic scaling laws are only

valid in a narrow range around the critical point. Corrections to the scaling laws are necessary if thermodynamic-property data are to be represented in a larger range.[6]

The long-range fluctuations of the order parameter can be neglected far away from the critical point. Then, classical (mean-field) models, such as the Van der Waals equation or a Landau expansion, may be appropriate to describe the state of fluids. The earliest qualitative explanation of critical phenomena was proposed by Van der Waals who presented his famous equation of state in 1873. This equation, as well as all its further modifications, implies a quadratic parabolic coexistence curve and a finite jump in the isochoric heat capacity.[7] Although it can not describe quantitatively the anomalous behavior of fluids near the critical point, the Van der Waals equation of state is still notable and remarkable because of its great conceptual importance and simplicity.

Between the immediate vicinity of the critical point and the range in which the mean-field theory is valid, a so-called "crossover model" is needed in order to accommodate the correct critical behavior near the critical point and properly cross over to the regular behavior in the mean-field region.[8] Nicoll *et al.*[9, 10] and Chen *et al.*[11, 12] have developed a procedure to implement the crossover by incorporating the critical fluctuations into a truncated classical Landau expansion. Within the critical domain, the crossover is the so-called "asymptotic crossover", which is the crossover between asymptotic scaling behavior and asymptotic classical critical behavior. However, to deal with global crossover behavior of fluids with short range forces, nonasymptotic aspects of crossover behavior are to be considered.[4] Among nonasymptotic effects the vapor-liquid asymmetry plays an important role, which

must be correctly incorporated into the crossover procedure.

It has been over one hundred years since the law of the rectilinear diameter was first proposed by Cailletet and Mathias.[13] It states that the diameter of a vapor-liquid coexistence curve is a linear function of the temperature T. In the early 70's several theoretical models predicted non-analytic deviations from the rectilinear diameter. These models, such as Mermin's decorated lattice-gas model[14] and Widom and Rowlinson's penetrable-sphere model,[15, 16] all predict that the temperature derivative of diameter should diverge as the specific heat at constant volume C_V. The heat capacity diverges as $C_V \sim \left|\Delta\widetilde{T}\right|^{-\alpha}$, where $\Delta\widetilde{T} = (T - T_c)/T_c$ and $\alpha = 0.109$ an universal critical exponent. Pestak $et\ al.$[17] analyzed accurate data of vapor-liquid equilibria near the critical point in several normal fluids. They concluded that the slope of the diameter far from the critical point and the amplitude of a deviation from the law of rectilinear diameter within the critical region increase systematically with the increase of T_c and are proportional to the critical polarizability product, which is a dimensionless measure of three- versus two-body interactions. However, after studying the rectilinear diameter for a larger number of normal fluids, Singh and Pitzer[18] found that the slope shows a linear dependence on the acentric factor and concluded that the shape of the pair potential is the primary factor in determining the slope of the diameter, rather than the relative strength of three-body interactions. They also argued that close to the critical point the shape of the two-body potential should have equally important effect on the increase of the amplitude of $\left|\Delta\widetilde{T}\right|^{1-\alpha}$ term.

From analyzing heat capacity data in two phase region for propane (C_3H_8)

and carbon dioxide (CO_2), Fisher and coworkers,[19, 20] proposed that both $d^2\widetilde{\mu}_{\mathrm{cxc}}/d\widetilde{T}^2$ and $d^2\widetilde{P}_{\mathrm{cxc}}/d\widetilde{T}^2$ diverge like the specific heat when approaching the critical point along the phase boundary, where μ is chemical potential, P is pressure and "cxc" means the path along the vapor-liquid coexistence. This is known as the so-called Yang-Yang anomaly.[22] To account for this phenomenon, Fisher *et al.*[19, 21, 20] have developed a concept of "complete scaling" in which the pressure is mixed into the scaling fields equally with the temperature and the chemical potential. As a result of "complete scaling", a new $\left|\Delta\widetilde{T}\right|^{2\beta}$ term where $\beta = 0.325$, which dominates the $\left|\Delta\widetilde{T}\right|^{1-\alpha}$ term near the critical point, should contribute to the diameter of vapor-liquid coexistence curves. The strength of the Yang-Yang anomaly is directly related to the linear pressure mixing coefficient in ordering field.

Anisimov *et al.*[23, 24] have developed a general isomorphism approach to describe a relation between vapor-liquid critical phenomena in one-component fluids and liquid-liquid critical phenomena in binary liquid mixtures. This is accomplished by generalizing the scaling fields to linear combinations of three physical field variables related to the temperature, pressure and the chemical potentials of the components.[23, 24] This approach provides a powerful tool to predict the thermodynamic properties of fluid mixtures in the critical region.

Liquid-liquid phase equilibrium with an upper critical point or a lower critical point is exhibited by many liquid mixtures, which has been studied by many investigators, such as Greer,[25] Ley-Koo and Green,[26] and Kumar *et al.*.[27] In 1983 Greer and coworkers[28] analyzed the diameters of the liquid-liquid coexistence curves of several binary liquid mixtures to study the deviation from the law of rectilinear

diameter. They concluded that the diameter in some systems could have a singular term with an exponent $1 - \alpha$ following the theoretical prediction at that time, but also a term with an exponent 2β, because of the "wrong" choice of the order parameter. Damay and Leclercq[29] studied the molecular size effect on the asymmetry of the coexistence curve in binary mixtures. They argued that the asymmetry of the liquid-liquid coexistence is either due to a molecular-size difference between components that produces a $\left| \Delta \widetilde{T} \right|^{2\beta}$ term or to the conventional mixing scaling that produces a $\left| \Delta \widetilde{T} \right|^{1-\alpha}$ term. Recently, Cerdeiriña $et\ al.$[30] extended the "complete scaling" to liquid-liquid coexistence in binary mixtures and examined the experimental consequences.

Some systems show the phase transition twice upon increase of temperature and finally return to a state which is macroscopically similar to the initial state.[32] An example is a liquid mixture that possesses a closed solubility loop with both an upper critical point and a lower critical point. With the change of an external variable, such as pressure or a chemical potential, the upper critical point and lower critical point may approach each other and the closed-loop may shrink until they converge into a double critical point (DCP).[32] A simple approach is developed to describe liquid-liquid closed-loop coexistence curves,[31] in which the reduced temperature is $\tau_{\mathrm{UL}} = \left| (T - T_{\mathrm{L}}) (T - T_{\mathrm{U}}) / (T_{\mathrm{L}} T_{\mathrm{U}}) \right|$, where T_{L} and T_{U} are the lower critical solution temperature (LCST) and the upper critical solution temperature (UCST), respectively. Such a procedure was earlier introduced empirically by Davidovich and Shinder.[33, 34] Following Malomuzh and Veitsman[35, 36] and Anisimov et $al.$,[23, 24] we show that such a substitution follows from a specific nonlinear relation

5

between the scaling fields and the physical field variables. Based on the general isomorphism approach, we have derived equations in terms of temperature, concentration and pressure to describe the critical lines (CL). A complete description of the phase equilibrium at various pressures including the closed-loop coexistence and the critical line requires only four system-dependent parameters.[31]

Contemporarily, chemical engineers often use various molecular models for process and product design. One popular class of theoretical models is a "lattice model". It is an important question how real systems can be mapped into "lattice models". For example, the lattice-gas model is perfectly symmetric, but real fluids exhibit strong vapor-liquid asymmetry. Even when asymmetry was introduced into the "lattice model", it was not clear that all sources of vapor-liquid asymmetry were taken into account. The motivation of our research is to clarify the origin of the asymmetry in fluid criticality.

In chapter 2 the classical theory of critical phenomena, based on the Landau expansion, is discussed. The scaling laws and universality are discussed in more detail because they are the basis of the modern theory of critical phenomena. Then the crossover theory is introduced briefly. Furthermore, the scaling fields and isomorphism theory are reviewed to explain how they can be extended for a description of fluid mixtures. In chapter 3 we introduce the "complete scaling" originally formulated by Fisher and coworkers,[19] and show that only two independent mixing coefficients are responsible for the vapor-liquid asymmetry upon an approximate choice for the entropy at the critical point. We develop a method to calculate these coefficients from classical equations of state and demonstrate which molecu-

lar parameters are responsible for tuning the asymmetry. By combining accurate vapor-liquid coexistence and heat-capacity experimental and simulation data, we provide in chapter 4 the unambiguous proof for the "complete scaling". We examine a number of systems, real fluids and simulated models, and separate the two scaling-field coefficients from two different sources of the vapor-liquid asymmetry. In chapter 5 we examine experimental consequences of "complete scaling" when extended to liquid-liquid coexistence in nearly incompressible binary liquids. We have shown that "singular" diameter of liquid-liquid coexistence curves also originates from two different sources, one associated with a correlation between concentration and entropy and another one associated with a correlation between concentration and molar density. In chapter 6, we study some phase equilibria that can only be described by nonlinear scaling fields. Based on the scaling theory and isomorphism theory, an approach to describe the closed-loop curves is elucidated. In addition, expressions to describe critical lines near a double critical point (DCP) are derived from the isomorphism theory. The results of this dissertation are summarized in chapter 7.

CHAPTER 2

CRITICAL PHENOMENA

2.1 Critical points

Basic observations of critical phenomena were done almost a hundred years ago, while the modern era of critical phenomena just started in the middle of the previous century. Although a wide variety of systems exhibit critical phenomena, in this dissertation, we only discuss vapor-liquid critical phenomena in one-component fluids and liquid-liquid critical phenomena in binary mixtures.

Assuming an equation of state for fluids in the form $F(P, \rho, T) = 0$, which defines a three-dimensional surface in pressure P, density ρ, temperature T coordinates, we may consider its projection on to PT plane, as shown in Fig. 2.1. There are three separate regions in this plane, corresponding to the solid, liquid and gas phases. The liquid and gas phases are in equilibrium along the vapor-pressure curve and the triple point is the equilibrium state in which all three phases coexist. The vapor-pressure curve terminates in the critical point (CP) that is specified by a critical pressure $P_{\rm c}$, a critical density $\rho_{\rm c}$, and a critical temperature $T_{\rm c}$, which also means that one can convert a gas to a liquid continuously without crossing the vapor-liquid phase equilibrium line.[3] Since the thermodynamic potentials are continuous at the transition point, the first derivatives such as molar volume and molar entropy along isotherms or isobars are also continuous, but the second derivatives such as molar heat capacity and isothermal compressibility are discontinuous, the phase transition at the critical point is classified as a second-order phase transition. When the

8
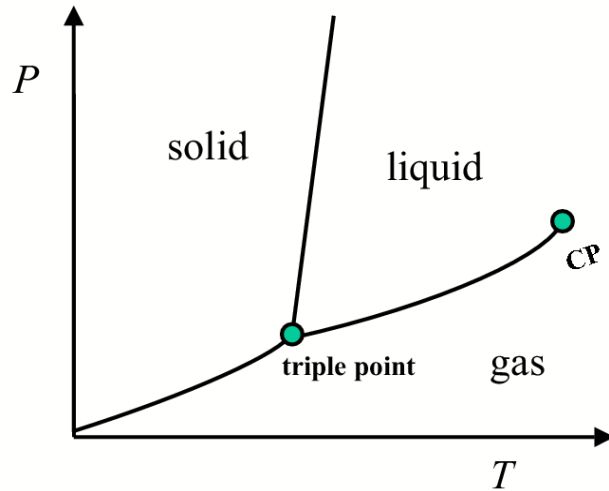
Figure 2.1: Projection of the $P\rho T$ surface in the PT plane.

critical point is approached from a temperature $T > T_{\mathrm{c}}$, some inhomogeneous re-gions appear and they may have a size of the order of the wavelength of light when it is close enough to the critical point.[3] Therefore, near critical points the light is scattered strongly, the phenomenon called critical opalescence.[3]

The critical point is the common point of a binodal and a spinodal, which means that the critical parameters are determined by $(\partial P/\partial\rho)_T = 0$ and $(\partial^2 P/\partial\rho^2)_T = 0$. Furthermore, since the isothermal compressibility is defined as $\rho^{-1}(\partial\rho/\partial P)_T$, it will diverge to infinity as the critical point is approached.[3] This divergence means that the response of the density to a very small pressure fluctuation is infinite, which causes huge density fluctuations. This is the origin of critical opalescence.

2.2   Classical (mean-field) critical behavior

The classical theory of critical behavior in fluids corresponds to the mean-field approximation which assumes that the fluctuations of density or concentration

9

are negligible near the critical point. The classical theory is commonly formulated in the form of a Landau expansion in powers of the order parameter associated with density.[43]

For a one-component fluid the molar Helmholtz energy A_{m} satisfies a differential relation

$$d\left(\rho A_{\mathrm{m}}\right) = -\rho S_{\mathrm{m}} dT + \mu d\rho = -sdT + \mu d\rho, \tag{2.1}$$

where S_{m} is the molar entropy, μ is the molar Gibbs free energy, ρ is the density and $s = \rho S_{\mathrm{m}}$ is the entropy density. We make all variables in Eq. (2.1) dimensionless as follows,

$$
\begin{aligned}
\overline{T} &= \frac{T}{T_0}, & \overline{\rho} &= \frac{\rho}{\rho_0}, & \overline{A} &= \frac{\rho A_{\mathrm{m}}}{\rho_0 R T_0}, & \overline{\mu} &= \frac{\mu}{R T_0}, \\
\overline{P} &= \frac{P}{\rho_0 R T_0}, & \overline{s} &= \frac{s}{\rho_0 R}, & \overline{C}_{\mathrm{V}} &= \frac{C_{\mathrm{V}}}{R}, & \overline{\chi} &= \frac{\chi}{R T_0 \rho_0^2}, \\
\Delta \overline{T} &= \overline{T} - 1, & \Delta \overline{\rho} &= \overline{\rho} - 1,
\end{aligned}
\tag{2.2}
$$

where C_{V} is the isochoric molar heat capacity, $A = \rho A_{\mathrm{m}}$ is the Helmholtz energy density, $\chi = (\partial^2 A / \partial \rho^2)_T$ is the susceptibility, P_0, ρ_0 and T_0 are the classical critical parameters which may be different from the actual critical parameters P_{c}, ρ_{c} and T_{c}, and R is the molar gas constant. Then expanding the thermodynamic potential $\overline{A}\left(\Delta \overline{T}, \Delta \overline{\rho}\right)$ as a power series of the order parameter $\Delta \overline{\rho}$ and temperature $\Delta \overline{T}$ at the critical point, after truncating the expansion and neglecting the asymmetric terms which are of higher-order than the 4th power term, the following equation is

10

obtained:

$$\overline{A}\left(\Delta \overline{T}, \Delta \overline{\rho}\right) = A_0\left(\Delta \overline{T}\right) + \mu_0\left(\Delta \overline{T}\right)\Delta \overline{\rho} + [\frac{1}{2}a_0 \Delta \overline{T}\Delta \overline{\rho}^2 + \frac{1}{4!}u_0 \Delta \overline{\rho}^4], \qquad (2.3)$$

where a_0, and u_0 are system-dependent coefficients. The term $A_0\left(\Delta \overline{T}\right)$ is the mechanical background and the second term (linear in $\Delta \overline{\rho}$) is the caloric background. The remaining higher-order terms constitute $\Delta \overline{A}_{\mathrm{cr}}\left(\Delta \overline{T}, \Delta \overline{\rho}\right)$, which represents the critical part of the classical Helmholtz-energy density,

$$\Delta \overline{A}_{\mathrm{cr}}\left(\Delta \overline{T}, \Delta \overline{\rho}\right) = \frac{1}{2}a_0 \Delta \overline{T}\Delta \overline{\rho}^2 + \frac{1}{4!}u_0 \Delta \overline{\rho}^4. \qquad (2.4)$$

For this symmetric equation, the following equilibrium condition that comes from the minimization of $\Delta \overline{A}_{\mathrm{cr}}$ is applicable to solve the vapor-liquid equilibrium curve,

$$\left(\frac{\partial \Delta \overline{A}_{\mathrm{cr}}}{\partial \Delta \overline{\rho}}\right)_{\Delta \overline{T}} = 0. \qquad (2.5)$$

The corresponding solution is

$$\Delta \overline{\rho}_{\mathrm{cxc}} = \frac{\rho_{\mathrm{l}} - \rho_{\mathrm{g}}}{2\rho_0} - 1 = \pm \sqrt{\frac{6a_0}{u_0}}\left|\Delta \overline{T}\right|^{1/2}, \qquad (2.6)$$

where the $\pm$ correspond to the liquid and vapor branches, respectively. It is clear that the coexistence curve in this approximation is symmetric. Higher-order odd terms are responsible for asymmetric features of $\Delta \overline{\rho}_{\mathrm{cxc}}$. Therefore, for the asym-

11

metric equation the simple equilibrium condition $\left(\partial \Delta \overline{A}_{\mathrm{cr}}/\partial \Delta \overline{\rho}\right)_{\Delta \overline{T}} = 0$ is not valid. Instead, the general phase equilibrium conditions, $T_{\mathrm{l}} = T_{\mathrm{g}}$, $P_{\mathrm{l}} = P_{\mathrm{g}}$ and $\mu_{\mathrm{l}} = \mu_{\mathrm{g}}$ should be applied to get the asymmetric coexistence curve, where subscript l and g represent the liquid and vapor phase respectively.

The reduced isochoric molar heat capacity $\overline{C}_V = \overline{T}\left(\frac{\partial \overline{S}_{\mathrm{m}}}{\partial \overline{T}}\right)_\rho = -\overline{T}\left(\frac{\partial^2 \overline{A}_{\mathrm{m}}}{\partial \overline{T}^2}\right)_\rho$ exhibits a finite jump upon crossing the critical temperature,

$$\Delta \frac{\overline{C}_{\mathrm{V}}}{\overline{T}} = \lim_{T \to T_c}\left[\frac{\overline{C}_{\mathrm{V}}}{\overline{T}}\left(T \leq T_{\mathrm{c}}\right) - \frac{\overline{C}_{\mathrm{V}}}{\overline{T}}\left(T \geq T_{\mathrm{c}}\right)\right] = \frac{3a_0^2}{u_0}. \tag{2.7}$$

The inverse dimensionless susceptibility

$$\overline{\chi}^{-1} = \left[\frac{\partial^2 \Delta \overline{A}_{\mathrm{cr}}}{\partial\left(\Delta \overline{\rho}\right)^2}\right]_{\Delta \overline{T}}. \tag{2.8}$$

varies asymptotically as

$$T \geq T_{\mathrm{c}},\ \rho = \rho_{\mathrm{c}} \qquad \overline{\chi}^{-1} = a_0\left|\Delta \overline{T}\right|, \tag{2.9}$$

$$T \leq T_{\mathrm{c}},\ \rho = \rho_{\mathrm{cxc}} \qquad \overline{\chi}^{-1} = 4a_0\left|\Delta \overline{T}\right|.$$

The nonclassical critical behavior is a consequence of the long-range critical fluctuations of the order parameter. As a result of the density fluctuations, the local density will actually be a function of the position $\vec{r}$. In the classical theory such a spatial dependence leads to the presence of a gradient term proportional to $(\nabla \overline{\rho})^2$

12

in the local Helmholtz-energy density. Therefore, the critical part of the classical local Helmholtz-energy density $\Delta \overline{A}_{\mathrm{cr}}$ corresponding to Eq. (2.4) will actually have an expansion of the form

$$\Delta \overline{A}_{\mathrm{cr}} \left(\Delta \overline{T}, \Delta \overline{\rho} \left(\overrightarrow{r} \right) \right) = \frac{1}{2} a_0 \Delta \overline{T} \left[\Delta \overline{\rho} \left(\overrightarrow{r} \right) \right]^2 + \frac{1}{4!} u_0 \left[\Delta \overline{\rho} \left(\overrightarrow{r} \right) \right]^4 + \frac{1}{2} c_0 \left(\nabla \overline{\rho} \right)^2, \quad (2.10)$$

where c_0 is an additional system-dependent coefficient which determines the amplitude of the correlation length of the density fluctuations.[44] c_0 is associated with the range of intermolecular forces and u_0 reflects the energy of interaction between fluctuations.[45] The classical expression of the correlation length ξ is proportional to the square root of the susceptibility $\overline{\chi}$

$$\xi = \left(c_0 \overline{\chi} \right)^{1/2}. \tag{2.11}$$

It thus follows from Eq. (2.9) that ξ in the one-phase region diverges along the critical isochore as

$$\xi = \overline{\xi}_0^+ \left| \Delta \overline{T} \right|^{-1/2}, \tag{2.12}$$

where $\overline{\xi}_0^+ = \left(c_0/a_0 \right)^{1/2}$ is the classical correlation length amplitude and $+$ means above the critical temperature. The presence of the gradient term does not affect the near-critical behavior of the thermodynamic properties in the first approximation. They still follow the asymptotic power laws with classical critical-exponent values. However, in the next approximation, square-root corrections appear. Thus, the

susceptibility in the one-phase region becomes[46, 45]

$$\overline{\chi} = \left(a_0 \Delta \overline{T}\right)^{-1} \left\{ 1 + \frac{u_0 v_0}{8\pi a_0^2 \left(\overline{\xi}_0^+\right)^3} \left|\Delta \overline{T}\right|^{-1/2} \right\}, \tag{2.13}$$

where v_0 is the molecular volume. Therefore, the classical theory is valid only when

$$\Delta \overline{T} >> N_{\mathrm{G}} = \frac{u_0^2 v_0^2}{64\pi^2 a_0^4 \left(\overline{\xi}_0^+\right)^6}, \tag{2.14}$$

where the parameter N_{G} is the so-called Ginzburg number. This condition for the range of validity of the classical theory is commonly referred to as the Ginzburg criterion.[47] A discussion can be found in a review by Anisimov and Sengers,[4] who give a rough estimate of $N_{\mathrm{G}} \cong 0.01$ for simple fluids near the vapor-liquid critical point so that the classical equations of state cannot be valid unless $\Delta \overline{T} >> 0.01$. If condition (2.14) is not satisfied, the fluctuations will give a major contribution to the thermodynamic properties.

2.3 Asymptotic scaling (fluctuation induced) critical behavior

For one-component fluids, the critical point is specified by the critical temperature T_{c}, critical density ρ_{c} and critical pressure P_{c}. Their thermodynamic properties near the critical point are best described by the quantities reduced by

14

critical parameters. These quantities are defined as follows:

$$
\begin{aligned}
\widetilde{T} &= \frac{T}{T_{\mathrm c}}, \qquad \widetilde{\rho} = \frac{\rho}{\rho_{\mathrm c}}, \qquad \widetilde{A} = \frac{\rho A_{\mathrm m}}{\rho_{\mathrm c} R T_{\mathrm c}}, \qquad \widetilde{\mu} = \frac{\mu}{R T_{\mathrm c}}, \qquad \widetilde{P} = \frac{P}{\rho_{\mathrm c} R T_{\mathrm c}}, \\
\widetilde{s} &= \frac{s}{\rho_{\mathrm c} R}, \quad \widetilde{C}_V = \frac{C_V}{R}, \quad \widetilde{\chi} = \frac{\chi}{R T_{\mathrm c} \rho_{\mathrm c}^2}, \quad \Delta \widetilde{T} = \widetilde{T} - 1, \quad \Delta \widetilde{\rho} = \widetilde{\rho} - 1, \\
\Delta \widetilde{\mu} &= \widetilde{\mu} - \widetilde{\mu}_{\mathrm c}, \quad \Delta \widetilde{s} = \frac{s - s_{\mathrm c}}{\rho_{\mathrm c} R}, \quad \Delta \widetilde{P} = \frac{P - P_{\mathrm c}}{\rho_{\mathrm c} R T_{\mathrm c}},
\end{aligned}
\tag{2.15}
$$

where $\widetilde{\mu}_{\mathrm c}$ is the chemical potential at the critical point.

Power laws: critical exponents and amplitudes: As the critical point is approached along selected thermodynamic paths such as the critical isotherm $\Delta \widetilde{T} = 0$, the critical isochore $\Delta \widetilde{\rho} = 0$, or the coexistence curve $\Delta \widetilde{\rho} = \Delta \widetilde{\rho}_{\mathrm{cxc}} = \frac{\rho_{\mathrm l} - \rho_{\mathrm g}}{2 \rho_{\mathrm c}} - 1$, the thermodynamic properties of one component fluids satisfy the asymptotic power laws,[43]

$$
\begin{array}{ccc}
\text{Path} & & \text{Power law} \\[4pt]
T \leq T_{\mathrm c}, \ \rho = \rho_{\mathrm{cxc}} & & \Delta \widetilde{\rho}_{\mathrm{cxc}} = \pm B_0 \left| \Delta \widetilde{T} \right|^{\beta}, \\[6pt]
T = T_{\mathrm c} & & \Delta \widetilde{\mu} = D_0 \Delta \widetilde{\rho} \, |\Delta \widetilde{\rho}|^{\delta - 1}, \\[6pt]
T \geq T_{\mathrm c}, \ \rho = \rho_{\mathrm c} & & \widetilde{C}_V^+ = A_0^+ \left| \Delta \widetilde{T} \right|^{-\alpha}, \\[6pt]
T \leq T_{\mathrm c}, \ \rho = \rho_{\mathrm c} & & \widetilde{C}_V^- = A_0^- \left| \Delta \widetilde{T} \right|^{-\alpha}, \\[6pt]
T \geq T_{\mathrm c}, \ \rho = \rho_{\mathrm c} & & \widetilde{\chi} = \Gamma_0^+ \left| \Delta \widetilde{T} \right|^{-\gamma}, \\[6pt]
T \leq T_{\mathrm c}, \ \rho = \rho_{\mathrm{cxc}} & & \widetilde{\chi} = \Gamma_0^- \left| \Delta \widetilde{T} \right|^{-\gamma},
\end{array}
\tag{2.16}
$$

where α, β, γ and δ are universal critical exponents, B_0, D_0, $A_0^{\pm}$ and $\Gamma_0^{\pm}$ are system-

dependent critical amplitudes and the superscripts $+$ and $-$ correspond to $T \geq T_{\mathrm{c}}$ and $T \leq T_{\mathrm{c}}$, respectively. The singular behavior of the thermodynamic properties near the critical point is caused by long-range fluctuations of the order parameter (density in one-component fluids and concentration in incompressible binary liquid mixtures). The magnitude and spatial character of these fluctuations are described in terms of a correlation function G, defined as[43]

$$\rho^2 G\left(\left|\overrightarrow{r} - \overrightarrow{r}'\right|\right) = \left\langle \left\{\rho\left(\overrightarrow{r}\right) - \rho\right\}\left\{\rho\left(\overrightarrow{r}'\right) - \rho\right\}\right\rangle = \left\langle \rho\left(\overrightarrow{r}\right)\rho\left(\overrightarrow{r}'\right)\right\rangle - \rho^2, \quad (2.17)$$

where the brackets $\langle \ \rangle$ indicate an equilibrium average over a grand canonical ensemble, $\rho\left(\overrightarrow{r}\right)$ is the local number density at a position $\overrightarrow{r}$ and $\rho = \left\langle \rho\left(\overrightarrow{r}\right)\right\rangle$ is the average equilibrium density which is independent of the position $\overrightarrow{r}$. The correlation function $G(r) = G\left(\left|\overrightarrow{r} - \overrightarrow{r}'\right|\right)$ measures the joint probability of finding molecules in volume elements $d\overrightarrow{r}$ and $d\overrightarrow{r}'$.[43] At the critical point the spatial correlation function $G(r)$ of the order parameter decays as

$$G(r) \sim \frac{1}{r^{d-2+\eta}} e^{-r/\xi}, \quad (2.18)$$

where $d = 3$ is the dimensionality of space and η is a universal critical exponent. The parameter ξ in the above equation is called the correlation length, which is the characteristic range of the correlation function and is defined by a normalized second moment[43, 49]

$$\xi^2 = \frac{\int r^2 G(r)\, dr}{\int G(r)\, dr}. \quad (2.19)$$

16

Critical exponent	3-d Ising system	classical value
α	0.110 ± 0.003	0
β	0.3255 ± 0.002	$1/2$
γ	1.239 ± 0.002	1
δ	4.80 ± 0.02	3
ν	0.630 ± 0.002	$1/2$
η	0.033 ± 0.004	0

Table 2.1: Universal critical exponents for three-dimensional Ising systems

The correlation length ξ diverges at the critical point according to the power law

$$T \geq T_{\mathrm{c}}, \ \rho = \rho_{\mathrm{c}} \qquad \xi = \xi_0^+ \left| \Delta \widetilde{T} \right|^{-\nu}, \tag{2.20}$$

$$T \leq T_{\mathrm{c}}, \ \rho = \rho_{\mathrm{cxc}} \qquad \xi = \xi_0^- \left| \Delta \widetilde{T} \right|^{-\nu},$$

where $\xi_0^\pm$ is a system-dependent amplitude of the order of the molecular radius and ν is a universal critical exponent.[43] All near-critical anomalies of the thermodynamic properties, shown in Eqs. (2.16) can be expressed in terms of the correlation length:

$$\widetilde{C}_V \sim \xi^{\alpha/\nu}, \qquad \Delta \widetilde{\rho}_{\mathrm{cxc}} \sim \xi^{-\beta/\nu}, \qquad \widetilde{\chi} \sim \xi^{\gamma/\nu}, \qquad \Delta \widetilde{\mu} \sim \xi^{-\beta\delta/\nu}. \tag{2.21}$$

The universal values of the six critical exponents α, β, γ, δ, ν and η for three-dimensioned Ising systems are given[44, 50, 51, 52] in Table 2.1. These six exponents are related to each other by the following exponent relations,

$$2 - \alpha = d\nu, \tag{2.22}$$

17

A_0^+/A_0^-	0.523 ± 0.009
Γ_0^+/Γ_0^-	4.95 ± 0.15
$\alpha A_0^+\Gamma_0^+/B_0$	0.0581 ± 0.001
$\Gamma_0^+ D_0 B_0^{\delta-1}$	1.57 ± 0.23
ξ_0^+/ξ_0^-	1.96 ± 0.01
$\alpha A_0^+(\xi_0^+)^3/v_0$	0.0188 ± 0.0002

Table 2.2: Universal scaling amplitude ratios for three-dimensional Ising systems

$$\beta = -\nu\left(2 - d - \eta\right)/2, \tag{2.23}$$

$$\gamma = \nu\left(2 - \eta\right), \tag{2.24}$$

$$\beta\delta = \nu\left(2 + d - \eta\right)/2. \tag{2.25}$$

Therefore, only two of the six critical exponents are independent. By taking $\nu = 0.630$ and $\eta = 0.033$, the other four exponents can be reproduced within their uncertainties.[8]

Although the values of critical amplitudes are system-dependent, they are related by universal ratios so that only two critical amplitudes are independent. The values of these ratios for 3-dimensional (3-d) Ising systems[44, 52, 53] are shown in Table 2.2.

Critical universality and scaling hypothesis: To characterize the critical behavior, systems are grouped into universality classes depending on the nature of the order parameter. It is commonly accepted that the critical behavior of fluids and fluid mixtures, regardless of variety and complexity in their microscopic structures, belong to the universality class of the 3-d Ising model because of possessing a scalar order parameter.[1] This means that they have the same universal critical exponents

18

(Table 2.1)[54] and the same critical amplitude ratios (Table 2.2),[53] which is an example of critical-point universality. The modern theory of critical phenomena predicts that the appropriate field-dependent thermodynamic potential Ψ contains a regular background contribution Ψ^{r} that depends analytically on the physical fields and a singular part Ψ_{cr},[23, 4]

$$\Psi = \Psi_{\mathrm{cr}}\left(h_1, h_2\right) \; + \; \Psi^{\mathrm{r}}. \tag{2.26}$$

Near a critical point the critical (fluctuation-induced) part Ψ_{cr} is a universal function of two scaling fields, "ordering" h_1 and "thermal" h_2:

$$\Psi_{\mathrm{cr}}\left(h_1, h_2\right) = h_2^{2-\alpha} f^{\pm}\left(\frac{h_1}{h_2^{\beta+\gamma}}\right). \tag{2.27}$$

The corresponding "order parameter" ϕ_1 and the "thermal density" ϕ_2 are defined as $\phi_1 = -\partial\left(\Psi_{\mathrm{cr}}\right)/\partial h_1$ and $\phi_2 = -\partial\left(\Psi_{\mathrm{cr}}\right)/\partial h_2$. The universal function contains two system-dependent amplitudes $f^{\pm}\left(\frac{h_1}{h_2^{\beta+\gamma}}\right)$, and the superscript $\pm$ refers to $h_2 \gtrless 0$, respectively.[4]

The Ising model, which is the simplest prototype of magnetic systems, when reformulated for the vapor-liquid transition in one-component fluids, is known as the lattice-gas model. In the lattice-gas model the field-dependent thermodynamic potential Ψ is the density of the grand thermodynamic potential $-P = \Omega/V$, where Ω is the grand thermodynamic potential. To specify the thermodynamic behavior

19

of the lattice-gas models for fluids near the critical point, we have

$$dP = sdT + \rho d\mu. \tag{2.28}$$

P is decomposed as[23]

$$P = P_{\text{cr}}\left(h_1, h_2\right) \; + \; P^{\text{r}}\left(T, \mu\right), \tag{2.29}$$

where $P^{\text{r}}\left(T, \mu\right) = P_{\text{c}} + \left(\partial P/\partial T\right)_\mu \Delta T$ is a regular background term as function of temperature T and molar Gibbs energy μ, $P_{\text{cr}}(h_1, h_2)$ is a singular function of two scaling fields, a "strong" ordering field h_1 associated with the order parameter fluctuations and a "weak" temperature-like field h_2 associated with the entropy fluctuations:[4, 54]

$$h_1 = \Delta\widetilde{\mu}, \tag{2.30}$$

$$h_2 = \Delta\widetilde{T}. \tag{2.31}$$

Thus the ordering scaling field is related to the chemical-potential difference $\Delta\widetilde{\mu}$. By definition, the ordering field is zero along the critical isochore above the critical temperature T_{c} and along the vapor-liquid coexistence curve below T_{c}. The corresponding scaling densities ϕ_1 (order parameter) and ϕ_2 conjugate to the scaling fields h_1 and h_2 are

$$\phi_1 = \Delta\widetilde{\rho}, \tag{2.32}$$

$$\phi_2 = \Delta\widetilde{s}. \tag{2.33}$$

20

Near the critical point the singular part $P_{cr}(h_1, h_2)$ satisfies a scaling law in the form,[2, 54, 55]

$$P_{cr}/\rho_c R T_c = \widetilde{P}_{cr} = h_2^{2-\alpha} f(z), \tag{2.34}$$

with

$$z = h_1/h_2^{\beta+\gamma}, \tag{2.35}$$

where $f(z)$ is a universal scaling function.

The scaling densities conjugate to h_1 and h_2 are

$$\phi_1 = \left(\frac{\partial \widetilde{P}_{cr}}{\partial h_1}\right)_{h_2} = |h_2|^\beta f'(z), \tag{2.36}$$

$$\phi_2 = \left(\frac{\partial \widetilde{P}_{cr}}{\partial h_2}\right)_{h_1} = h_2 |h_2|^{-\alpha} \psi(z), \tag{2.37}$$

where

$$f'(z) = df / dz, \tag{2.38}$$

and

$$\psi(z) = (2-\alpha)f(z) - (\beta+\gamma) z f'(z). \tag{2.39}$$

The scaling susceptibilities χ_1 (strongly divergent) and χ_2 (weakly divergent) are associated with ϕ_1 and ϕ_2

$$\chi_1 = \left(\frac{\partial \phi_1}{\partial h_1}\right)_{h_2} = |h_2|^{-\gamma} f''(z), \tag{2.40}$$

21

$$\chi_2 = \left(\frac{\partial \phi_2}{\partial h_2}\right)_{h_1} = |h_2|^{-\alpha} \Psi(z), \tag{2.41}$$

where

$$f''(z) = d^2 f / dz^2, \tag{2.42}$$

$$\Psi(z) = (1 - \alpha)\psi(z) - (\beta + \gamma) z \psi'(z), \tag{2.43}$$

$$\psi'(z) = d\psi / dz. \tag{2.44}$$

In zero field $h_1 = 0$ and in the one-phase region, the susceptibility χ_1 exhibits a strong singularity, but the reduced isochoric heat capacity density $\widetilde{C}_V$ has a weak singularity:

$$\chi_{1,\, h_1=0} = \left(\frac{\partial \phi_1}{\partial h_1}\right)_{h_2,\, h_1=0} = \Gamma_0^+ |h_2|^{-\gamma} = \Gamma_0^+ \left|\Delta \widetilde{T}\right|^{-\gamma}, \tag{2.45}$$

$$\left(\frac{\widetilde{C}_V}{\widetilde{T}}\right)_{h_1=0} = \left(\frac{\partial \phi_2}{\partial h_2}\right)_{\phi_1,\, h_1=0} = A_0^+ |h_2|^{-\alpha} = A_0^+ \left|\Delta \widetilde{T}\right|^{-\alpha}, \tag{2.46}$$

where

$$\Gamma_0^+ = f''_+(0), \tag{2.47}$$

$$A_0^+ = (2 - \alpha)(1 - \alpha) f_+(0). \tag{2.48}$$

The order parameter in zero field varies along the two branches of the phase bound-

ary below the critical temperature as

$$\phi_1 = \Delta \widetilde{\rho}_{\mathrm{cxc}} = \pm B_0 \left| h_2 \right|^{\beta} = \pm B_0 \left| \Delta \widetilde{T} \right|^{\beta},$$ (2.49)

where

$$B_0 = f'_- (0).$$ (2.50)

The system-dependent amplitudes are interrelated by the universal amplitude ratios (see Table 2.2).

Wegner corrections: In practice the scaling laws with theoretical exponent values are only valid at reduced temperatures less than 10^{-3}.[56] It is necessary to make some corrections to the asymptotic scaling laws in order to describe the data in a larger range accurately. The renormalization theory predicts the presence of confluent singularities in the dependence of the thermodynamic properties on h_2 of the order $h_2^{\Delta_{\mathrm{s}}}$, $h_2^{2\Delta_{\mathrm{s}}}$, $h_2^{3\Delta_{\mathrm{s}}}$, and so on,[6, 57] where $\Delta_{\mathrm{s}} = 0.52 \pm 0.02$ is a new independent universal correction-to-scaling exponent.[58, 59] The expansions are often referred to as Wegner expansions,[6]

$$\widetilde{P}_{\mathrm{cr}} = h_2^2 \left| h_2 \right|^{-\alpha} f_0 (z) \left[1 + h_2^{\Delta_{\mathrm{s}}} f_1 (z) + ... \right].$$ (2.51)

With the first correction to scaling, the power laws for the susceptibility along the critical isochore become

$$\chi_1 = \Gamma_0^+ \left| \Delta \widetilde{T} \right|^{-\gamma} \left[1 + \Gamma_1^+ \left| \Delta \widetilde{T} \right|^{\Delta_{\mathrm{s}}} + ... \right],$$ (2.52)

23

$$\chi_2 = A_0^+ \left| \Delta \widetilde{T} \right|^{-\alpha} \left[1 + A_1^+ \left| \Delta \widetilde{T} \right|^{\Delta_s} + ... \right]. \tag{2.53}$$

The order parameter (along the coexistence curve) is

$$\phi_1 = \Delta \widetilde{\rho}_{\mathrm{cxc}} = \pm B_0 \left| \Delta \widetilde{T} \right|^{\beta} \left[1 + B_1 \left| \Delta \widetilde{T} \right|^{\Delta_s} + ... \right]. \tag{2.54}$$

The system-dependent amplitude Γ_1^+, A_1^+ and B_1 are also interrelated by two universal amplitude ratios $A_1^+/\Gamma_1^+ = 0.9 \pm 0.1$ and $B_1/\Gamma_1^+ = 0.8 \pm 0.2$, which means that only one of these amplitudes is independent.[60, 61] In addition, the Wegner corrections are also universal: they are present in the thermodynamic properties of any systems that exhibit scaling behavior near a second-order phase transition.

In principle, including higher-order terms in the Wegner expansion might be helpful to extend the scaling procedure. However, there is evidence that the Wegner series has a poor convergence, which means that the range of applicability of a truncated Wegner series is rather restricted.[26] Therefore it is necessary to develop an alternate procedure that takes a resummation of the Wegner expansion into account in order to extend the scaling approach to a practical range of temperatures and densities.

2.4 Crossover between classical and asymptotic scaling critical behavior

The asymptotic crossover is a simple crossover problem, namely the crossover between the asymptotic singular behavior and the asymptotic classical behavior within the critical domain. Chen *et al.*[12] have developed a procedure to transform

24

an expansion of the classical Helmholtz-energy density into an equation that incorporates the fluctuation-induced singular scaling laws near the critical point and reduces to the classical expansion far away from the critical point.[99]

As a result of the order parameters fluctuations, the local density will actually be a function of the position $\overrightarrow{r}$. In the classical theory such a spatial dependence leads to the presence of a gradient term proportional to $(\nabla\overline{\rho})^2$ in the local Helmholtz-energy density. Therefore, the critical part of the classical local Helmholtz-energy density $\Delta\overline{A}_{\mathrm{cr}}$ corresponding to Eq. (2.4) will actually have an expansion of the form

$$\Delta\overline{A}_{\mathrm{cr}}\left(\Delta\overline{T},\Delta\overline{\rho}\left(\overrightarrow{r}\right)\right) = \frac{1}{2}a_0\Delta\overline{T}\left[\Delta\overline{\rho}\left(\overrightarrow{r}\right)\right]^2 + \frac{1}{4!}u_0\left[\Delta\overline{\rho}\left(\overrightarrow{r}\right)\right]^4 + \frac{1}{2}c_0\left(\nabla\overline{\rho}\right)^2, \quad (2.55)$$

where c_0 is an additional system-dependent coefficient which determines the amplitude of the correlation length of the density fluctuations. We rewrite it in a rescaled form[8]

$$\Delta\overline{A}_{\mathrm{cr}} = \frac{1}{2}tM^2 + \frac{1}{4!}u\Lambda M^4 + \frac{1}{2}\left(\nabla M\right)^2, \quad (2.56)$$

with

$$t = c_t\Delta\overline{T}, \quad M = c_\rho\Delta\overline{\rho}, \quad u = u^*\overline{u}, \quad u^*\overline{u}\Lambda = u_0/c_\rho^4, \quad (2.57)$$

where

$$c_t = a_0\left(\nu_0\right)^{2/3}/c_0, \quad c_\rho^2 = c_0\nu_0^{-2/3}, \quad c_tc_\rho^2 = a_0. \quad (2.58)$$

Here c_t and c_ρ are system-dependent scale factors. It should be emphasized that the crossover transformation is characterized by two important parameters Λ and u. The dimensionless cutoff wave number $\Lambda = q_{\mathrm{D}}/q_0 \sim q_{\mathrm{D}}\nu_0^{1/3}$ characterizes a

discrete structure of matter with spacing q_D^{-1}, where q_D is the actual maximum cutoff wave number of the fluctuations, $q_0 \sim \nu_0^{-1/3}$ is a wave number associated with the microstructure of the system and v_0 is the average molecular volume. For simple fluids $\Lambda \simeq 1$ and for a polymer solution with a high molecular weight $\Lambda \to 0$. The second parameter $u = u^* \overline{u}$ is a so-called coupling constant, where $u^* \cong 0.472$ is the fixed-point value of the universal coupling constant[48] and $\overline{u} = u/u^*$ is a reduced system-dependent coupling constant. The coupling constant is related to the strength and range of the intermolecular interaction, such as for the mean field with weak long-range interaction $\overline{u} \to 0$ and for the short-range interaction $\overline{u} \simeq 1$.

One takes approximate expressions for the rescaling functions $\mathcal{T}$, $\mathcal{D}$, $\mathcal{K}$, and $\mathcal{U}$ as:

$$\mathcal{T} = Y^{(2\nu-1)/\Delta_s}, \tag{2.59}$$

$$\mathcal{D} = Y^{-\eta\nu/\Delta_s}, \tag{2.60}$$

$$\mathcal{U} = Y^{\nu/\Delta_s}, \tag{2.61}$$

$$\mathcal{K} = \frac{\nu}{\alpha\overline{u}\Lambda}\left(Y^{-\alpha/\Delta_s} - 1\right), \tag{2.62}$$

where Y is a crossover function. Then replacing the variable t by $t\mathcal{T}\mathcal{D}\mathcal{U}^{-1/2}$, replacing the variable M in the even terms by $M\mathcal{D}^{1/2}\mathcal{U}^{1/4}$ and replacing the $\frac{1}{2}\left(\nabla M\right)^2$ by the fluctuation-induced kernel term $-\frac{1}{2}t^2\mathcal{K}$, one obtains the renormalized critical part of the Helmholtz free energy density:

$$\Delta\widetilde{A}_{\mathrm{cr}} = \frac{1}{2}tM^2\mathcal{T}\mathcal{D} + \frac{\overline{u}u^*\Lambda}{4!}M^4\mathcal{D}^2\mathcal{U} - \frac{1}{2}t^2\mathcal{K}. \tag{2.63}$$

26

The crossover function Y is to be evaluated from the equation

$$1 - (1 - \overline{u})\, Y = \overline{u} Y^{\nu/\Delta_{\mathrm{s}}} \left(1 + \frac{\Lambda^2}{\kappa^2} \right)^{1/2}, \qquad (2.64)$$

with

$$\kappa^2 = \left[\frac{\partial \Delta \widetilde{A}_{\mathrm{cr}}}{\partial \left(M \mathcal{D}^{1/2} \right)^2} \right]_t = t\mathcal{T} + \frac{\overline{u} u^* \Lambda}{2} M^2 \mathcal{D} \mathcal{U}, \qquad (2.65)$$

where κ is a measure of a distance from the critical point and related to the inverse correlation length. The critical limit corresponds to $\Lambda/\kappa \longrightarrow \infty$. From Eq. (2.64) we have

$$Y \longrightarrow \left(\frac{\kappa}{\overline{u}\Lambda} \right)^{\Delta_{\mathrm{s}}/\nu}. \qquad (2.66)$$

When $\Lambda/\kappa \longrightarrow 0$ which means that $Y = 1$ and hence $\mathcal{T} = \mathcal{D} = \mathcal{U} = 1$ and $\mathcal{K} = 0$ the classical limit is reached and the classical expression for the Helmholtz energy density is recovered. Substituting Eq. (2.59) − (2.65) into Eq. (2.63), one obtains a crossover equation for $\Delta \widetilde{A}_{\mathrm{cr}}$.

The asymptotic crossover within a critical domain ($\Delta \widetilde{T} < 10^{-2}$) is inadequate to deal with the complete crossover behavior of fluids with short-range forces. The reason is that for such fluids the classical theory does not become valid until so far from the critical point that any asymptotic critical behavior has become inadequate. Therefore, in real fluids there is no asymptotic crossover. However, in the Ising model with the various range of interactions there is an asymptotic crossover.[4] In order to deal with the extended critical region, where the correlation length is still larger than the distance between molecules, nonasymptotic aspects of the crossover

27

behavior should also be considered.[4] The nonasymptotic crossover theory has been successfully applied for a description of liquid-liquid equilibria in polymer solutions, where crossover between asymptotic scaling behavior and mean-field theta-point behavior is controlled by the polymer molecular weight.[38] In a polymer solution, like in other liquid mixtures, $\bar{u} \simeq 1$ and crossover is driven by $\Lambda \sim 1/\sqrt{N} \to 0$. However, for low-molecular weight solutions, the necessity of using the crossover approach is not as obvious as for polymer solutions. In this case, both $\bar{u}$ and Λ for liquid mixtures are usually very close to unity. The behavior of these systems is close to the Ising limit in a large range. Therefore, for phase-equilibria in many liquid solutions, especially with closed-loop coexistence, the asymptotic scaling plus first corrections to the asymptotic laws may yield reasonable and practical approximations.

2.5 Isomorphism of critical phenomena

Thermodynamics itself does not specify uniquely which set of variables is to be preferred in describing the critical behavior of fluids. Therefore, for real fluids it is unknown which variables are to be preferred in describing critical behavior, and the choice we have made is based on empirical considerations of symmetry.[43] In the lattice gas the coexistence curve would be perfectly symmetric. But in a real fluid the lack of complete symmetry is evident from the average coexisting densities, which is approximately a straight line, the rectilinear diameter, but which does not coincide with the critical isochore $\rho = \rho_c$. In fluid mixtures, additional thermodynamic variables, concentrations, appear, while the number of the theoretical scaling fields remain equal to two. Therefore, the choice of the appropriate variables become

even more ambiguous.

To understand the thermodynamic behavior of fluids and fluid mixtures near critical points, one needs to distinguish between fields that are intensive thermodynamic properties and densities that are thermodynamic properties conjugate to the fields.[117, 62] Fields (T, P, μ, $\mu_{\Delta 21}$, $etc.$) are to be the same for all coexisting phases, while densities (S, V, ρ, $x, etc.$), in contrast, differ for coexisting phases. $\mu_{\Delta 21} = \mu_2 - \mu_1$ is the difference of chemical potential between the two components in the liquid mixtures. The order parameter is always related to a corresponding density variable. The thermodynamic potentials depending on the fields and densities are transformed into each other by the Legendre transformations.

A general formulation of isomorphism has been implemented by Anisimov et $al.$[2]. The rules for choosing the isomorphic thermodynamic values for three systems, the vapor-liquid critical point of a pure fluid, and the vapor-liquid and liquid-liquid critical points of a binary liquid mixture, are presented in Table 2.3.[2]

Scaling fields and mixing of physical fields: The lattice gas has a special symmetry: the order parameter is symmetric with respect to the critical isochore and the ordering field is an anti-symmetric function of the order parameter. Real fluids approach such a symmetry only asymptotically close to the critical point. The vapor-liquid asymmetry is then commonly incorporated into the lattice-gas analogy by linear mixing of two independent physical fields (chemical potential and temper-

29

Quantity	L-G Critical Point of a one component fluid	L-G Critical Point of a binary liquid mixture	L-L Critical Point of a binary liquid mixture
Density Variable	Density $\rho = \left(\frac{\partial P}{\partial \mu}\right)_T$	Density of a mixture $\rho = \left(\frac{\partial P}{\partial \mu_1}\right)_{T,\mu_{\Delta 21}}$	Concentration of solute $x_2 = -\left(\frac{\partial \mu_1}{\partial \mu_{\Delta 21}}\right)_{T,P}$
Field Variable	Chemical Potential $\mu = A_{\mathrm{m}} + PV_{\mathrm{m}}$ $= \left(\frac{\partial \rho A_{\mathrm{m}}}{\partial \rho}\right)_T$	Chemical Potential of solvent $\mu_1 = \left(\frac{\partial \rho A^*_{\mathrm{iso}}}{\partial \rho}\right)_{T,\mu_{\Delta 21}}$	Difference of chemical potentials $\mu_{\Delta 21} = \mu_2 - \mu_1$ $= \left(\frac{\partial \mu}{\partial x_2}\right)_{T,P}$
Thermodynamic potential in density variables	$\rho A_{\mathrm{m}} = -P + \rho\mu$ $d\left(\rho A_{\mathrm{m}}\right) = -\rho S_{\mathrm{m}}dT$ $+\mu d\rho$	$\rho A^*_{\mathrm{iso}} = -P + \rho\mu_1$ $d\left(\rho A^*_{\mathrm{iso}}\right) = -\rho S_{\mathrm{m}}dT$ $+\mu_1 d\rho - \rho x_2 d\mu_{\Delta 21}$	$\mu = \mu_1 + \mu_{\Delta 21}x_2$ $d\mu = -S_{\mathrm{m}}dT+$ $V_{\mathrm{m}}dP + \mu_{\Delta 21}dx_2$
Thermodynamic potential in field variables	$\frac{\Omega}{V} = -P$ $-dP = -\rho S_{\mathrm{m}}dT$ $-\rho d\mu$	$\frac{\Omega}{V} = -P$ $-dP = -\rho S_{\mathrm{m}}dT$ $-\rho d\mu_1 - \rho x_2 d\mu_{\Delta 21}$	$\mu_1 = \mu - \mu_{\Delta 21}x_2$ $d\mu_1 = -S_{\mathrm{m}}dT+$ $V_{\mathrm{m}}dP - x_2 d\mu_{\Delta 21}$

Table 2.3: Thermodynamic potentials in terms of density and field variables

ature) into the definition of the two scaling fields[23, 63]:

$$h_1 = a_1 \Delta \widetilde{\mu} + a_2 \Delta \widetilde{T}, \tag{2.67}$$

$$h_2 = b_1 \Delta \widetilde{T} + b_2 \Delta \widetilde{\mu}. \tag{2.68}$$

where a_i and b_i are system-dependent coefficients to be determined from a comparison with experimental data. The scaling fields may be normalized in such a way that $a_1 = 1$ and $b_1 = 1$. The coefficient b_2 in expression (2.68) is often referred to as the mixing coefficient.[64] It has an important physical consequence, since it causes a nonclassical behavior of the coexistence curve diameter as discussed below.

Comparing

$$d\widetilde{P}_{\mathrm{cr}} = \widetilde{\rho} d\Delta \widetilde{\mu} + \widetilde{s} d\Delta \widetilde{T}, \tag{2.69}$$

with

$$d\widetilde{P}_{\mathrm{cr}} = \phi_1 dh_1 + \phi_2 dh_2, \tag{2.70}$$

it is easy to get

$$\Delta \widetilde{\rho} = a_1 \phi_1 + b_2 \phi_2, \tag{2.71}$$

$$\Delta \widetilde{s} = a_2 \phi_1 + b_1 \phi_2. \tag{2.72}$$

Solving above two equations, the densities conjugate to h_1 and h_2 are

$$\phi_1 = \left(\frac{\partial \widetilde{P}_{\mathrm{cr}}}{\partial h_1} \right)_{h_2} = h_2^\beta f'(z) = \frac{b_1}{a_1 b_1 - a_2 b_2} \Delta \widetilde{\rho} - \frac{b_2}{a_1 b_1 - a_2 b_2} \Delta \widetilde{s}, \tag{2.73}$$

31

$$\phi_2 = \left(\frac{\partial \widetilde{P}_{\mathrm{cr}}}{\partial h_2} \right)_{h_1} = h_2^{1-\alpha} \psi(z) = \frac{a_1}{a_1 b_1 - a_2 b_2} \Delta \widetilde{s} - \frac{a_2}{a_1 b_1 - a_2 b_2} \Delta \widetilde{\rho}, \qquad (2.74)$$

where $f'(z) = df/dz$ and $\psi(z) = (2-\alpha)f(z) - (\beta+\gamma) z f'(z)$.

It is clear that the order parameter ϕ_1 is not simply proportional to $\Delta\widetilde{\rho}$, but contains a contribution proportional to $\Delta\widetilde{s}$. As a consequence $\Delta\widetilde{\rho}$ along the two branches of the phase boundary varies asymptotically as

$$\Delta \widetilde{\rho}_{\mathrm{cxc}} = \phi_1 + b_2 \phi_2 = \pm B_0 \left| \Delta \widetilde{T} \right|^{\beta} + B_a \left| \Delta \widetilde{T} \right|^{1-\alpha}, \qquad (2.75)$$

with

$$B_0 = f'(0), \qquad (2.76)$$

$$B_{\mathrm{a}} = b_2 \left[A_0^- / (1-\alpha) \right] (P_{\mathrm{c}}/\rho_{\mathrm{c}}), \qquad (2.77)$$

where the subscript a indicates the term associated with vapor-liquid asymmetry. The term $B_{\mathrm{a}} \left| \Delta \widetilde{T} \right|^{1-\alpha}$ is an asymmetric correction to the asymptotic scaling law, especially important for fluids.

From the above derivation we know that one-component fluids are completely isomorphic to the lattice-gas model if temperature and chemical potential, being thermodynamic variables, are replaced by their linear combinations.

Generalized isomorphism approach: A second-order phase transitions is called "isomorphic" if the thermodynamic potentials of different systems have the same functional dependence on temperature and order parameters, when the variables are suitably chosen (isomorphic variables).[2] Among real systems, only the vapor-liquid

systems	Scaling field h_1 and h_2
V-L critical point of lattice gas	$h_1 = \Delta\widetilde{\mu}$ $h_2 = \Delta\widetilde{T}$
V-L critical point of one component fluid	$h_1 = a_1\Delta\widetilde{\mu} + a_2\Delta\widetilde{T}$ $h_2 = b_1\Delta\widetilde{T} + b_2\Delta\widetilde{\mu}$
V-L critical point of a binary fluid mixture	$h_1 = a_0\Delta\widetilde{\mu}_{\Delta 21} + a_1\Delta\widetilde{\mu}_1 + a_2\Delta\widetilde{T}$ $h_2 = b_0\Delta\widetilde{\mu}_{\Delta 21} + b_1\Delta\widetilde{T} + b_2\Delta\widetilde{\mu}_1$
L-L critical point of a binary liquid mixture	$h_1 = a_0\Delta\widetilde{P} + a_1\Delta\widetilde{\mu}_{\Delta 21} + a_2\Delta\widetilde{T}$ $h_2 = b_0\Delta\widetilde{P} + b_1\Delta\widetilde{T} + b_2\Delta\widetilde{\mu}_{\Delta 21}$

Table 2.4: Relations between scaling fields and physical fields in fluids

critical point of a one-component fluid is an isolated point on the phase diagram. In other cases there exist lines or even surfaces of second-order phase transitions. The thermodynamic potential near the second-order phase transition-line or surface depends on the temperature and order parameter in the same way as in the case of a system with an isolated critical point, provided that all other fields are kept constant. The number of independent critical exponents will still be two and, if an increase in the number of independent variables does not change the dimensionality of the order parameter, then the values of the critical exponents will remain the same. The isomorphism hypothesis has served as a powerful stimulus for the experimental study of binary and multicomponent mixtures and has allowed considerable extension of the class of systems belonging to the Ising model universality class.

Based on the isomorphism theory of critical phenomena mentioned above, the concept of critical point universality has been extended to binary fluid mixtures. In Table 2.4 the definitions of the scaling fields h_1 and h_2 for four different systems are listed.

(1) Vapor-liquid equilibrium for binary fluid mixtures:

For vapor-liquid equilibrium for binary liquid mixtures, according to the Table 2.3, we have

$$dP = sdT + \rho d\mu_1 + \rho_2 d\mu_{\Delta 21} \tag{2.78}$$

where $\rho_2 = \rho x_2$ is the partial density of the solute and x_2 is the molar fraction. The scaling fields are in general linear combinations of the three physical field variables $\Delta \widetilde{T} = \frac{T - T_c}{T_c}$, $\Delta \widetilde{\mu}_1 = \frac{\mu_1 - \mu_{1c}}{RT_c}$, $\Delta \widetilde{\mu}_{\Delta 21} = \frac{\mu_{\Delta 21} - \mu_{\Delta 21c}}{RT_c}$:

$$h_1 = a_0 \Delta \widetilde{\mu}_{\Delta 21} + a_1 \Delta \widetilde{\mu}_1 + a_2 \Delta \widetilde{T}, \tag{2.79}$$

$$h_2 = b_0 \Delta \widetilde{\mu}_{\Delta 21} + b_1 \Delta \widetilde{T} + b_2 \Delta \widetilde{\mu}_1, \tag{2.80}$$

where the coefficients a_i and b_i as well as the critical parameters T_c, μ_{1c}, and $\mu_{\Delta 21c}$, depend parametrically on the actual position on the critical line. This position can be specified by any of the three variables T_c, μ_{1c}, and $\mu_{\Delta 21c}$. The singular part of the pressure satisfies a scaling law

$$\frac{P_{cr}}{\rho_c^0 RT_c^0} = \widetilde{P}_{cr} = h_2^{2-\alpha} f(z), \tag{2.81}$$

where ρ_c^0 and T_c^0 are the critical density and critical temperature of the pure solvent. We have

$$\Delta \widetilde{\rho} = (\rho - \rho_{c0}) / \rho_c^0 = a_1 \phi_1 + b_2 \phi_2, \tag{2.82}$$

$$\Delta \widetilde{\rho}_2 = (\rho_2 - \rho_{2c0}) / \rho_c^0 = a_0 \phi_1 + b_0 \phi_2, \tag{2.83}$$

$$\Delta \widetilde{s} = (s - s_{c0}) / \rho_c^0 RT_c^0 = a_2 \phi_1 + b_1 \phi_2. \tag{2.84}$$

34

Thus the relevant densities ϕ_1 and ϕ_2 can be expressed as linear combinations of any two of the three physical densities $\Delta\widetilde{\rho}$, $\Delta\widetilde{\rho}_2$ and $\Delta\widetilde{s}$:

$$\phi_1 = \left[\frac{b_1}{a_1 b_1 - a_2 b_2} \Delta\widetilde{\rho} - \frac{b_2}{a_1 b_1 - a_2 b_2} \Delta\widetilde{s} \right], \tag{2.85}$$

$$\phi_1 = \left[\frac{b_2}{a_0 b_2 - a_1 b_0} \Delta\widetilde{\rho}_2 - \frac{b_0}{a_0 b_2 - a_1 b_0} \Delta\widetilde{\rho} \right], \tag{2.86}$$

$$\phi_1 = \left[\frac{b_0}{a_2 b_0 - a_0 b_1} \Delta\widetilde{s} - \frac{b_1}{a_2 b_0 - a_0 b_1} \Delta\widetilde{\rho}_2 \right], \tag{2.87}$$

$$\phi_2 = \left[\frac{a_1}{a_1 b_1 - a_2 b_2} \Delta\widetilde{s} - \frac{a_2}{a_1 b_1 - a_2 b_2} \Delta\widetilde{\rho} \right], \tag{2.88}$$

$$\phi_2 = \left[\frac{a_2}{a_2 b_0 - a_0 b_1} \Delta\widetilde{\rho}_2 - \frac{a_0}{a_2 b_0 - a_0 b_1} \Delta\widetilde{s} \right], \tag{2.89}$$

$$\phi_2 = \left[\frac{a_0}{a_0 b_2 - a_1 b_0} \Delta\widetilde{\rho} - \frac{a_1}{a_0 b_2 - a_1 b_0} \Delta\widetilde{\rho}_2 \right]. \tag{2.90}$$

(2) Liquid-liquid equilibrium for binary liquid mixtures:

For liquid-liquid equilibrium for binary liquid mixtures, according to the Table 2.3, we have

$$d\mu_1 = -S_{\mathrm{m}} dT + V_{\mathrm{m}} dP - x_2 d\mu_{\Delta 21} \tag{2.91}$$

The scaling fields are now, in general, linear combinations of the three physical field variables $\Delta\widetilde{T} = \frac{T - T_{\mathrm{c}}}{T_{\mathrm{c}}}$, $\Delta\widetilde{P} = \frac{P - P_{\mathrm{c}}}{P_{\mathrm{c}}}$, and $\Delta\widetilde{\mu}_{\Delta 21} = \frac{\mu_{\Delta 21} - \mu_{\Delta 21c}}{RT_{\mathrm{c}}}$,

$$h_1 = a_0 \Delta\widetilde{P} + a_1 \Delta\widetilde{\mu}_{\Delta 21} + a_2 \Delta\widetilde{T}, \tag{2.92}$$

$$h_2 = b_0 \Delta\widetilde{P} + b_1 \Delta\widetilde{T} + b_2 \Delta\widetilde{\mu}_{\Delta 21}. \tag{2.93}$$

When $h_1 = 0$, and $h_2 = 0$, we have the critical line (CL) in terms of temperature and pressure

$$\Delta \widetilde{T} = \left(\frac{a_1 b_0 - a_0 b_2}{a_2 b_2 - a_1 b_1} \right) \Delta \widetilde{P}, \qquad (2.94)$$

and the CL in terms of $\Delta \mu_{\Delta 21}$ and pressure

$$\Delta \widetilde{\mu}_{\Delta 21} = \left(\frac{a_2 b_0 - a_0 b_1}{a_1 b_1 - a_2 b_2} \right) \Delta \widetilde{P}. \qquad (2.95)$$

Introducing an activity, ζ, defined by[65]

$$\widetilde{\mu}_{\Delta 21} = \ln \frac{\zeta}{1 - \zeta}, \qquad (2.96)$$

and imposing the condition $x_2 = \zeta$ on the critical-point line known as the "critical line condition",[65] we have

$$\ln \frac{x_{2c}}{1 - x_{2c}} = \left(\frac{a_2 b_0 - a_0 b_1}{a_1 b_1 - a_2 b_2} \right) \Delta \widetilde{P} + \ln \frac{x_{2c0}}{1 - x_{2c0}}, \qquad (2.97)$$

where x_{2c0} is the critical concentration of a reference point. This is the two-dimensional critical point line in terms of concentration and pressure.

From Eq. (2.83), as ρ is constant for liquid-liquid equilibrium, we have

$$\Delta \widetilde{x}_{2cxc} = (x_{2cxc} - x_{2c}) / x_{2c} = a_1 \phi_1 + b_2 \phi_2 = \pm B_0 \left| \Delta \widetilde{T} \right|^\beta + B_a \left| \Delta \widetilde{T} \right|^{1-\alpha}. \qquad (2.98)$$

where

$$B_0 = a_1 f'(0),$$

<div align="right">(2.99)</div>

$$B_{\mathrm{a}} = b_2 \left[A_0^- / (1 - \alpha) \right] (P_{\mathrm{c}}/\rho_{\mathrm{c}}).$$

<div align="right">(2.100)</div>

This result is not exact, as we have neglected the effect of the regular part of the thermodynamic potential μ_1. It is well known that[2]

$$S_{\mathrm{m}} - (S_{\mathrm{m}})_{\mathrm{c}} = c_1 \left| \Delta \widetilde{T} \right|^{1-\alpha} + c_2 \left| \Delta \widetilde{T} \right|,$$

<div align="right">(2.101)</div>

where c_1 and c_2 are two coefficients. The term $c_2 \left| \Delta \widetilde{T} \right|$ results from the the regular part of the thermodynamic potential. Thus the entire expression for coexistence curve should include a diameter term,

$$\Delta \widetilde{x}_{2\mathrm{cxc}} = \pm B_0 \left| \Delta \widetilde{T} \right|^{\beta} + B_{\mathrm{a}} \left| \Delta \widetilde{T} \right|^{1-\alpha} + d_1 \Delta \widetilde{T}.$$

<div align="right">(2.102)</div>

where d_1 is the coefficient from the effect of the regular part of the thermodynamic potential.

CHAPTER 3

VAPOR-LIQUID ASYMMETRY IN FLUIDS

3.1 Fluids and lattice-gas model

An appropriate choice of order parameter is necessary to describe critical phenomena in fluids in terms of the general theory of phase transitions.[2] As shown in Fig. 3.1, the vapor-liquid coexistence curve of the Van der Waals equation of state for carbon dioxide is very asymmetric when it is described in terms of the traditional thermodynamic variables pressure P, volume V and temperature T. Thermodynamics itself does not specify uniquely which set of variables is to be preferred in describing the critical behavior of fluids.[43] Therefore, for real fluids it is unknown which variables are better in describing critical behavior, and the choice is commonly based on empirical considerations.[43] By replacing the volume V with the density ρ the vapor-liquid coexistence curve may be more symmetric, but not perfectly symmetric. The coexistence curve in the lattice gas is perfectly symmetric. But in a real fluid the lack of complete symmetry is evident from the average coexisting densities, which is approximately a straight line, the rectilinear diameter, but which does not coincide with the critical isochore $\rho = \rho_{\mathrm{c}}$.[43]

The most simple and important model to illuminate critical phenomena is the so-called lattice-gas model, which is illustrated in Fig. 3.2. Imagining that the entire fluid volume V is divided into a huge number of cells with volume v_0 which is roughly the molecular volume of the fluid. If a cell is occupied by the centre of a molecule, it is said that the cell is in the occupied state. It is not
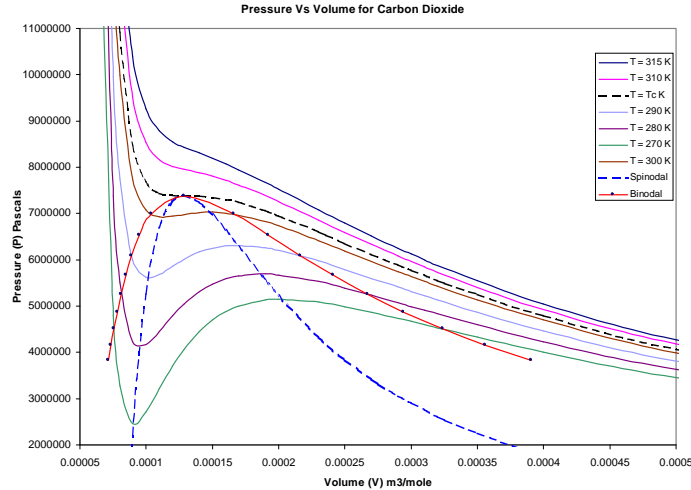
Figure 3.1: Van der Waals vapor-liquid coexistence curve in pressure P and volume V coordinates. (This figure is from homework of Ayan Ghosh for ENCH610 in 2004.)

allowed that a cell is occupied by more than one molecule since the volume of cells and molecules is roughly the same. Furthermore, it should be emphasized that the molecules themselves are not restricted to cells and the cell walls consisting of real molecules should not impede the motions of the other molecules in the fluids.[3, 16] On the contrary, every molecule moves freely and may have access to any region of the entire space. When one cell is occupied by two molecules, their interaction energy will be infinity, which is an imitation of the very strong repulsions that exist between two molecules at short distances.[16] For real molecules at intermediate distances with a negative potential energies $-\epsilon$ of interaction, the correspondence in the lattice gas is every pair of molecules occupying neighboring cells.[16] To imitate the short-range nature of intermolecular forces, it is specified that the interaction energy vanishes when two molecules are separated by one or more cells.[16]
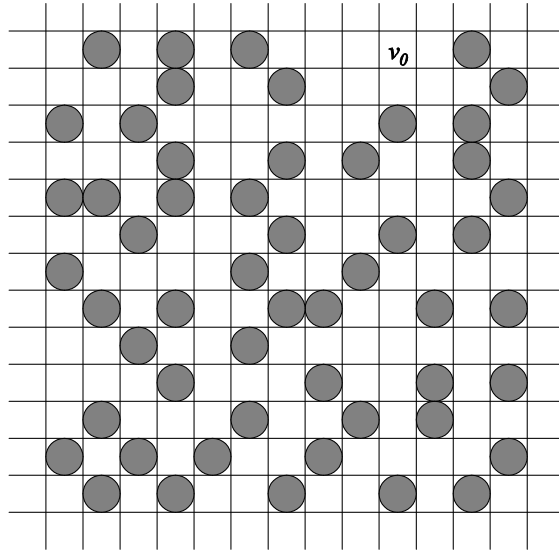
Figure 3.2: Illustration of lattice gas model.

For any configuration a in the lattice gas, there exists a corresponding anti-configuration b in which the cells filled by molecules in a are empty and the empty cells in a are occupied. Therefore, the lattice gas has a certain symmetry between any configuration, which results in a symmetric coexistence curve about the density of half filling in the temperature-density plane as shown in Fig. 3.3.[16] The density of the configuration in which half of the cells are occupied is the critical density. Thus, the coexistence curve is symmetric about the critical isochore which is also the arithmetic mean of the liquid and vapor branch and is the so-called diameter of the coexistence curve. This diameter is rectilinear and, as a matter of fact, a vertical straight line with no inclination at all. However, in real fluids, as shown in Fig. 3.4 , there does exist an inclination.[16] The data in Fig. 3.4 are from Weber[76] and the plot is from Widom.[16] The arrow on the horizontal axis in Fig. 3.4 (a) points to the location of critical density on the density axis.

40
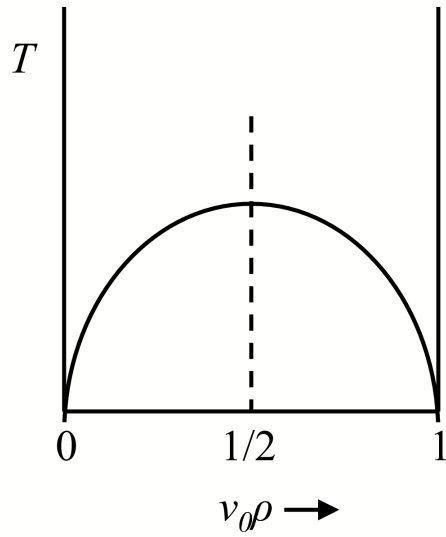
Figure 3.3: Coexistence curve and critical isochore (dash line) of the lattice gas. ρ is the number density.
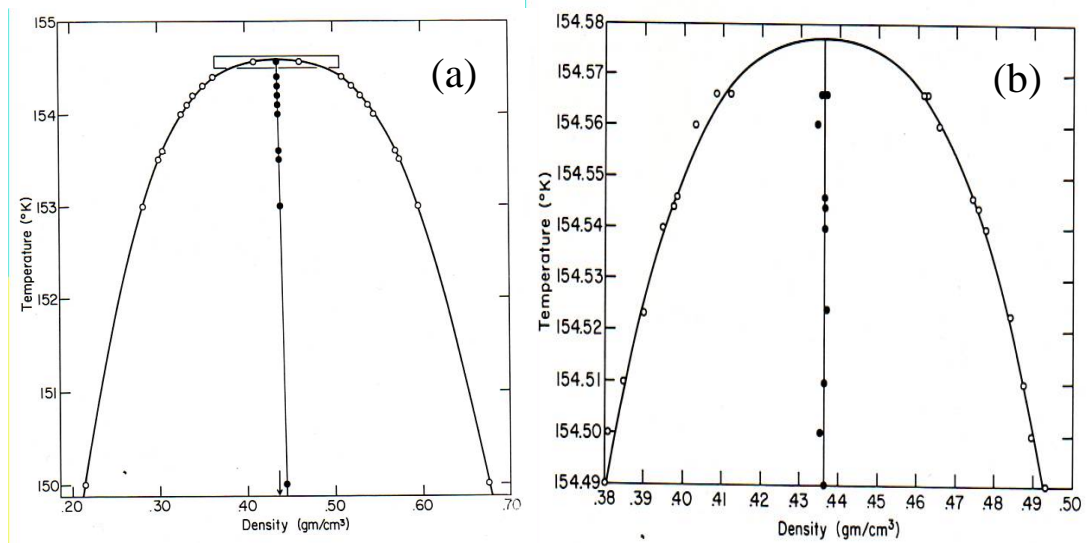
Figure 3.4: (a) Coexistence curve of oxygen in the entire temperature range.[16] (b) Coexistence curve of oxygen near the critical point corresponding to the part in rectangle in (a).[16]

41

3.2   Vapor-liquid asymmetry

It has been over one hundred years since the law of the rectilinear diameter was first proposed by Cailletet and Mathias.[13] It states that the diameter of a vapor-liquid coexistence curve is a linear function of temperature $\rho_{\mathrm{d}} = \left(\rho_{\mathrm{l}} + \rho_{\mathrm{g}}\right)/2 = \rho_{\mathrm{c}} + d\left|T - T_{\mathrm{c}}\right|$, where d is the slope, ρ_{l} and ρ_{g} are the densities of coexistent liquid and vapor. Extrapolation of this rectilinear diameter to the critical temperature is often used to obtain the critical density which is known today to be different from the real one in some cases, as shown in Fig. 3.5. Experimental data of diameters for some fluids which follow the law of the rectilinear diameter have been obtained, such as for oxygen by Weber[76] and for xenon by Närger and Balzarini.[77] Especially, the diameter of helium-3 obtained by Hahn *et al.*[78] is a straight line with an almost zero slope and this symmetry goes far beyond the range of the asymptotic power law. However, many fluids have been found whose diameters exhibit appreciable singularities near the critical point, such as Freon-113 (trifluorotrichlorethane $C_2F_3Cl_3$) as obtained by Shimanskaya *et al.*[90] Of those fluids the diameter of SF_6 reported by Weiner[79] is the first experimental evidence with sufficient precision to reveal a singular deviation from the rectilinear law.[26] Diameters for several fluids are represented in Fig. 3.6. It is clear that there exists a curvature near the critical point in the diameters of SF_6 and Freon-113. However, the diameters of nitrogen[17] and neon[17] are almost rectilinear or exhibit very small deviations from linearity.

The theoretical description of fluids diameters has been developed for several decades by many researchers. The diameters of classical fluids exactly follow the
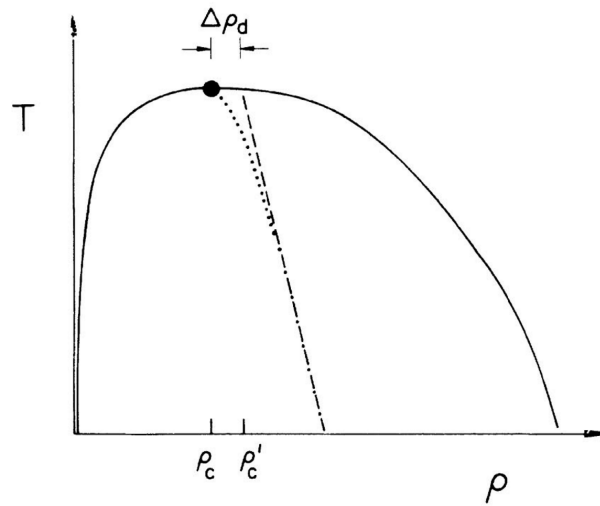
Figure 3.5: Schematic illustration of a liquid-gas coexistence curve.[17] Dashed line is the rectilinear diameter. Dotted curve is the actual diameter. ρ'_c is the critical density value extrapolated with the rectilinear diameter. ρ_c is the actual critical density.
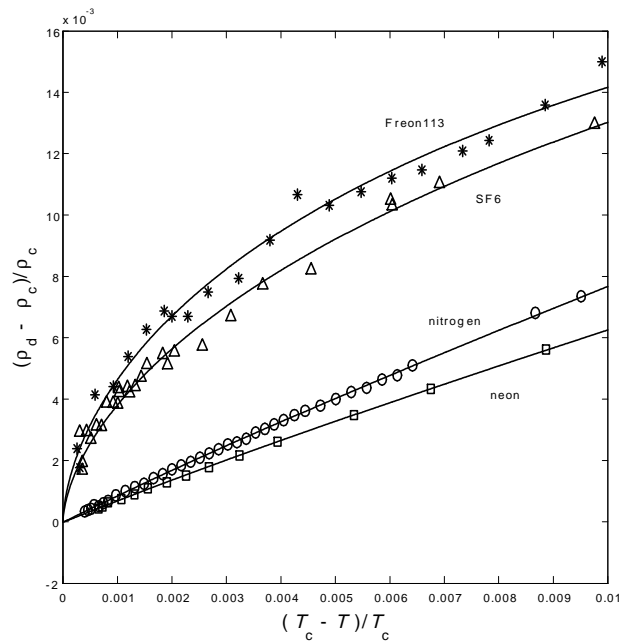
Figure 3.6: The diameters for several fluids.

43

rectilinear law with various slopes for different equation of states (EOS). In reduced form one has

$$\widetilde{\rho}_{\mathrm{d}} = \frac{\rho_{\mathrm{l}} + \rho_{\mathrm{g}}}{2\rho_{\mathrm{c}}} = 1 + D\left|\Delta\widetilde{T}\right|. \tag{3.1}$$

The lattice-gas model exhibits a perfect symmetry diameter which means the slope $D = 0$. In the early 70's several model calculations predicted singular deviations from the law of the rectilinear diameter. Those models, such as Mermin's decorated lattice-gas model[14] and Widom and Rowlinson's penetrable-sphere model,[15, 16] all show that the diameter should diverge in proportion to the specific heat at constant volume C_{V},

$$\frac{d\rho_{\mathrm{d}}}{dT} \propto C_{\mathrm{V}} \propto \left|\Delta\widetilde{T}\right|^{-\alpha}. \tag{3.2}$$

The existence of a weak singularity makes the reduced diameter behave like

$$\widetilde{\rho}_{\mathrm{d}} = \frac{\rho_{\mathrm{l}} + \rho_{\mathrm{g}}}{2\rho_{\mathrm{c}}} = 1 + D_1\left|\Delta\widetilde{T}\right|^{1-\alpha} + D_0\left|\Delta\widetilde{T}\right|. \tag{3.3}$$

However, one more term has recently been obtained in the equation for $\widetilde{\rho}_{\mathrm{d}}$ as a result of the "complete scaling" developed by Fisher and coworkers,[19, 21]

$$\widetilde{\rho}_{\mathrm{d}} = \frac{\rho_{\mathrm{l}} + \rho_{\mathrm{g}}}{2\rho_{\mathrm{c}}} = 1 + D_2\left|\Delta\widetilde{T}\right|^{2\beta} + D_1\left|\Delta\widetilde{T}\right|^{1-\alpha} + D_0\left|\Delta\widetilde{T}\right|. \tag{3.4}$$

The new singular term varying as $\left|\Delta\widetilde{T}\right|^{2\beta}$ actually dominates the earlier $\left|\Delta\widetilde{T}\right|^{1-\alpha}$ term near critical point since $2\beta < 1 - \alpha$. In this theory the pressure difference $P - P_{\mathrm{c}}$ is mixed into the scaling fields, especially into the ordering field h_1: This

feature changes the treatment of fluid asymmetry.

Pestak *et al.*[17] studied the experimental data for diameters of several normal fluids near the critical point in 1987. They concluded that the slope of the diameter far from the critical point and the amplitude of singular deviation from the law of rectilinear diameter within the critical region are all proportional to the critical polarizability product which is a dimensionless measure of the relative significance of three- versus two-body interactions. They suggested that three-body interactions play an important role in those properties relevant to the vapor-liquid symmetry of pure fluids. However, after studying the amplitude of the rectilinear diameter for a large number of normal fluids in 1990, Singh and Pitzer[18] found that the diameter slope shows a linear dependence on the acentric factor and concluded that the shape of the pair potential is the primary factor in determining the slope of the diameter rather than the relative strength of three-body interactions. They also mentioned that close to the critical point the shape of the two-body potential has the equally logical effect on the increase of the amplitude D_1 of $1 - \alpha$ term.

It is an interesting question which property of fluids is responsible for the physical origin of the singular $\left|\Delta\widetilde{T}\right|^{2\beta}$ or $\left|\Delta\widetilde{T}\right|^{1-\alpha}$ term. To clarify this, the true amplitude of each term in Eq. (3.4) must be obtained. Unfortunately, the fitted coefficients are unlikely to represent the true amplitudes of each term since they have exponents of a similar magnitude and correlate strongly in the fitting procedure.[82] Therefore, how to unambiguously separate two competing singularities in diameters is a challenge.

3.3 "Complete scaling"

It has been generally assumed that the singular critical behavior of real fluids and fluids mixtures may be characterized by the asymptotic scaling theory in terms of a strong scaling field (ordering field) and a weak scaling field (thermal field) in order to map the asymmetric fluid criticality into an symmetric lattice-gas model. However, in the primitive lattice-gas model the ordering field is only related to the reduced chemical potential difference $\Delta\widetilde{\mu}$ whose conjugate density is the strongly fluctuating order parameter $\Delta\widetilde{\rho}$ and the thermal field is merely proportional to $\Delta\widetilde{T}$ which conjugates to the more weakly fluctuating density variable $\Delta\widetilde{s}$. Therefore, this symmetric model is only a simple prototype of the vapor-liquid phase transition for one component fluids which can not describe the asymmetric criticality actually existing in most real fluids. To solve this problem, in early 70's the concept of mixing physical variables into the scaling fields was proposed.[64] According to this concept the scaling fields are linear combinations of $\Delta\widetilde{\mu}$ and $\Delta\widetilde{T}$:

$$h_1 = \Delta\widetilde{\mu} + a_2\Delta\widetilde{T}, \quad h_2 = \Delta\widetilde{T} + b_2\Delta\widetilde{\mu}, \tag{3.5}$$

where a_2 and b_2 are mixing coefficients. Furthermore, as suggested by Anisimov,[23] if the critical entropy density which is an arbitrary value is adopted as $s_{\mathrm{c}} = \rho_{\mathrm{c}}^{-1}\left(\frac{\partial P}{\partial T}\right)_{h_1=0,\rho_{\mathrm{c}}}$, the coefficient a_2 vanishes. Thus, only one mixing coefficient b_2 is left, which contributes to the asymmetric criticality in real fluids and leads to the $\left|\Delta\widetilde{T}\right|^{1-\alpha}$ term in the diameter of vapor-liquid coexistence curve. The thermodynamic potential

46

P here is a function of the independent scaling fields h_1 and h_2. In this conventional mixing model the chemical potential μ is an analytic function along the phase boundary and the critical isochore just as it is in the lattice gas, with the result that the second derivative $d^2\widetilde{\mu}_{\mathrm{cxc}}/d\widetilde{T}^2$ should remain finite at the critical temperature T_{c}, while $d^2\widetilde{P}_{\mathrm{cxc}}/d\widetilde{T}^2$ should diverge like the isochoric heat capacity $\widetilde{C}_{\mathrm{V}}$.

Recently, the conventional scaling formulation has been challenged by Fisher and coworkers[19, 20] who analyzed the heat capacity data for propane (C_3H_8) and carbon dioxide (CO_2) in the two-phase region and proposed that both $d^2\widetilde{\mu}_{\mathrm{cxc}}/d\widetilde{T}^2$ and $d^2\widetilde{P}_{\mathrm{cxc}}/d\widetilde{T}^2$ diverge like the specific heat when approaching the critical point along phase boundary. This is called the Yang-Yang anomaly.[19] To account for this phenomenon, Fisher and Orkoulas[19, 20, 21] developed a "complete scaling" in which the pressure is mixed into the scaling fields.

For a one-component fluid, the basic thermodynamic relation is

$$d\Delta\widetilde{P} = \widetilde{\rho}\, d\left(\Delta\widetilde{\mu}\right) + \widetilde{s}\, d\left(\Delta\widetilde{T}\right), \tag{3.6}$$

where P is the negative to the grand thermodynamic potential density, $-P = \Omega/V$, and

$$\widetilde{\rho} = \left(\frac{\partial\Delta\widetilde{P}}{\partial\Delta\widetilde{\mu}}\right)_{\Delta\widetilde{T}}, \quad \widetilde{s} = \left(\frac{\partial\Delta\widetilde{P}}{\partial\Delta\widetilde{T}}\right)_{\Delta\widetilde{\mu}}. \tag{3.7}$$

Therefore, the full thermodynamic description is provided by,[19, 20]

$$F(P, \mu, T) = 0. \tag{3.8}$$

47

Then the scaling hypothesis asserts that the thermodynamics may be asymptotically described by,

$$\Psi\left(\frac{h_3}{h_2^{2-\alpha}}, \frac{h_1}{h_2^{\beta+\gamma}}\right) = 0. \tag{3.9}$$

Here h_1, h_2 and h_3 are the nonlinear scaling fields which are all combinations of the three physical variables $\Delta\widetilde{T}$, $\Delta\widetilde{\mu}$ and $\Delta\widetilde{P}$. Hence, the scaling fields in linear approximation can be formulated by

$$h_1 = \Delta\widetilde{\mu} + a_2\Delta\widetilde{T} + a_3\Delta\widetilde{P}, \tag{3.10}$$

$$h_2 = \Delta\widetilde{T} + b_2\Delta\widetilde{\mu} + b_3\Delta\widetilde{P}, \tag{3.11}$$

$$h_3 = \Delta\widetilde{P} - \Delta\widetilde{\mu} - \widetilde{s}_c\Delta\widetilde{T}. \tag{3.12}$$

where a_i, and b_i $(i = 2, 3)$ are the mixing coefficients. Then the thermodynamic potential h_3 for the fluid may be obtained by solving Eq. (3.9),

$$h_3 = h_2^{2-\alpha} f^{\pm}\left(\frac{h_1}{h_2^{\beta+\gamma}}\right), \tag{3.13}$$

where $f^{\pm}$ is a scaling function and the superscript $\pm$ refers to $h_2 \lessgtr 0$. Since we have the differential relation

$$dh_3 = \phi_1 dh_1 + \phi_2 dh_2, \tag{3.14}$$

both the generalized number density and entropy density obey the simple scaling rules when they approach the critical temperature,

$$\phi_1 = \left(\frac{\partial h_3}{\partial h_1}\right)_{h_2} \sim \pm |h_2|^\beta, \quad \phi_2 = \left(\frac{\partial h_3}{\partial h_2}\right)_{h_1} \sim |h_2|^{1-\alpha}. \tag{3.15}$$

Comparing Eq. (3.14) with

$$dh_3 = d\Delta\widetilde{P} - d\Delta\widetilde{\mu} - \widetilde{s}_c d\Delta\widetilde{T}, \tag{3.16}$$

we have

$$\widetilde{\rho} = \left(\frac{\partial \Delta\widetilde{P}}{\partial \Delta\widetilde{\mu}}\right)_{\Delta\widetilde{T}} = \frac{1 + \phi_1 + b_2\phi_2}{1 - a_3\phi_1 - b_3\phi_2}, \tag{3.17}$$

$$\widetilde{s} = \left(\frac{\partial \Delta\widetilde{P}}{\partial \Delta\widetilde{T}}\right)_{\Delta\widetilde{\mu}} = \frac{\widetilde{s}_c + a_2\phi_1 + \phi_2}{1 - a_3\phi_1 - b_3\phi_2}. \tag{3.18}$$

Expanding the Eqs. (3.17) and (3.18) and neglecting the higher-order term, one obtains expressions for the reduced density and entropy density:

$$\widetilde{\rho} = 1 + (1 + a_3)\,\phi_1 + a_3\,(1 + a_3)\,\phi_1^2 + (b_2 + b_3)\,\phi_2, \tag{3.19}$$

$$\widetilde{s} = \widetilde{s}_c + (a_2 + \widetilde{s}_c a_3)\,\phi_1 + a_3\,(a_2 + \widetilde{s}_c a_3)\,\phi_1^2 + (1 + \widetilde{s}_c b_3)\,\phi_2 +$$

$$a_3^2\,(a_2 + \widetilde{s}_c a_3)\,\phi_1^3. \tag{3.20}$$

Since in Eq. (3.19) there is a new term proportional to $\phi_1^2 \sim |h_2|^{2\beta}$, the 2β term will appear in the expression for the vapor-liquid coexistence-curve diameter. Kim

49

and coworkers[21] have also derived the equations of pressure and chemical potential along the phase boundary:

$$\widetilde{P}_{\mathrm{cxc}} = p_1 \left| \Delta\widetilde{T} \right| + p_2 \left| \Delta\widetilde{T} \right|^2 + p_3 \left| \Delta\widetilde{T} \right|^{2-\alpha} + \ldots, \qquad (3.21)$$

$$\widetilde{\mu}_{\mathrm{cxc}} = u_1 \left| \Delta\widetilde{T} \right| + u_2 \left| \Delta\widetilde{T} \right|^2 + u_3 \left| \Delta\widetilde{T} \right|^{2-\alpha} + \ldots, \qquad (3.22)$$

where p_i and u_i $(i = 1, 2, 3)$ are system-dependent coefficients. The appearance of terms proportional to $\left| \Delta\widetilde{T} \right|^{2-\alpha}$ implies that $d^2\widetilde{\mu}_{\mathrm{cxc}}/d\widetilde{T}^2$ and $d^2\widetilde{P}_{\mathrm{cxc}}/d\widetilde{T}^2$ diverge like the specific heat when approaching the critical point along phase boundary. Moreover, they also clarified how the singularity in $\widetilde{C}_{\mathrm{V}}$ is shared by giving the relation between the two second order derivatives,[19, 20]

$$a_3 \frac{d^2\widetilde{P}_{\mathrm{cxc}}}{d\widetilde{T}^2} = -\frac{d^2\widetilde{\mu}_{\mathrm{cxc}}}{d\widetilde{T}^2}. \qquad (3.23)$$

and one has

$$\frac{-a_3}{1+a_3} \frac{\widetilde{C}_{\mathrm{v}}}{\widetilde{T}} = \frac{d^2\widetilde{\mu}_{\mathrm{cxc}}}{d\widetilde{T}^2}. \qquad (3.24)$$

Therefore, the strength of the Yang-Yang "anomaly" is determined by the mixing coefficient a_3.

In the "complete scaling" formulation (3.10), (3.11) and (3.12), there are four unknown mixing coefficients, which make the asymmetry effects not clearly defined. In the conventional mixing with an appropriate choice of critical entropy density s_{c}, the number of unknown mixing coefficients can be reduced from two to one. It

is natural to ask whether a proper choice of s_c may also simplify the "complete scaling" formulation.

When thermodynamic potential depends on field variable, the basic thermodynamic relation is

$$dP = \rho d\mu + sdT, \tag{3.25}$$

and at critical point it may be transformed to

$$\rho_c \left(\frac{\partial \mu}{\partial T}\right)_{h_1=0,c} + s_c - \left(\frac{\partial P}{\partial T}\right)_{h_1=0,c} = 0. \tag{3.26}$$

With the path $h_1 = 0$, it is easy to get the following relation from the definition of the ordering field in "complete scaling"

$$0 = \frac{\Delta \widetilde{\mu}}{\Delta \widetilde{T}} + a_2 + a_3 \frac{\Delta \widetilde{P}}{\Delta \widetilde{T}}. \tag{3.27}$$

As $T \longrightarrow T_c$, Eq. (3.27) becomes a partial differential relation at the critical point

$$\frac{1}{R} \left(\frac{\partial \mu}{\partial T}\right)_{h_1=0,c} + a_2 + a_3 \frac{1}{\rho_c R} \left(\frac{\partial P}{\partial T}\right)_{h_1=0,c} = 0. \tag{3.28}$$

Since s_c depends on the choice of zero entropy, we may select the critical entropy density $s_c = \left(\frac{\partial P}{\partial T}\right)_{h_1=0,c}$ and then obtain $\left(\frac{\partial \mu}{\partial T}\right)_{h_1=0,c} = 0$ as a natural result from the relation (3.26). Thus, it is straightforward to get the simple relation between a_2 and

51

a_3 from Eq. (3.28)

$$a_2 + a_3 \frac{1}{\rho_c R} \left(\frac{\partial P}{\partial T} \right)_{h_1=0,c} = a_2 + a_3 \widetilde{s}_c = 0. \tag{3.29}$$

The $\lim_{T \longrightarrow T_c} \left(\frac{h_2}{\Delta \widetilde{T}} \right) = 1$ can help reduce the number of independent mixing coefficients

further. Transforming the definition (3.11) of the thermal field in "complete scaling"

and taking $T \longrightarrow T_c$, one obtains

$$\lim_{T \longrightarrow T_c} \left(\frac{h_2}{\Delta \widetilde{T}} \right) = 1 = 1 + b_2 \frac{1}{R} \left(\frac{\partial \mu}{\partial T} \right)_{h_1=0,c} + b_3 \frac{1}{\rho_c R} \left(\frac{\partial P}{\partial T} \right)_{h_1=0,c}. \tag{3.30}$$

Since $\left(\frac{\partial \mu}{\partial T} \right)_{h_1=0,c} = 0$ and $\left(\frac{\partial P}{\partial T} \right)_{h_1=0,c} = s_c$ is not zero in vapor-liquid phase bound-

ary for pure fluids, b_3 should be necessarily zero. Thus, the "complete scaling"

fields (3.10), (3.11) and (3.12) with four unknown coefficients are simplified into the

following formulation with only two asymmetry coefficients a_3 and b_2,

$$h_1 = \Delta \widetilde{\mu} + a_3 \left(\Delta \widetilde{P} - \widetilde{s}_c \Delta \widetilde{T} \right), \tag{3.31}$$

$$h_2 = \Delta \widetilde{T} + b_2 \Delta \widetilde{\mu}, \tag{3.32}$$

$$h_3 = \Delta \widetilde{P} - \Delta \widetilde{\mu} - \widetilde{s}_c \Delta \widetilde{T}. \tag{3.33}$$

Furthermore, Eqs. (3.19) and (3.20) reduce to

$$\Delta\widetilde{\rho} = (1+a_3)\,\phi_1 + a_3\,(1+a_3)\,\phi_1^2 + b_2\phi_2,$$

$$\simeq \pm(1+a_3)\,|h_2|^\beta + a_3\,(1+a_3)\,|h_2|^{2\beta} + b_2\,|h_2|^{1-\alpha} \qquad (3.34)$$

$$\Delta\widetilde{s} = \phi_2 \sim |h_2|^{1-\alpha}. \qquad (3.35)$$

Hence, there are only two relevant coefficients that in the first approximation control the asymmetry in fluid criticality.

3.4   Experimental consequences of "complete scaling"

As a result of "complete scaling", while the order parameter in fluids is, in general, a nonlinear combination of density and entropy $\phi_1 = (\Delta\widetilde{\rho} + b_2\Delta\widetilde{s})\,/(1+a_3\Delta\widetilde{\rho})$, the weakly fluctuating scaling density ϕ_2 in first approximation is associated with the density of entropy only, $\phi_2 = \Delta\widetilde{s}$. There is an important thermodynamic consequence of "complete scaling" that can be checked from experiments. The "diameter" ρ_{d} should contain two non-analytical contributions, associated with the terms $a_3\Delta\widetilde{P}$ and $b_2\Delta\widetilde{\mu}$ in the scaling fields,

$$\widetilde{\rho}_{\mathrm{d}} - 1 = D_2\left|\Delta\widetilde{T}\right|^{2\beta} + D_1\left|\Delta\widetilde{T}\right|^{1-\alpha} + D_0\left|\Delta\widetilde{T}\right| + \ldots \qquad (3.36)$$

Note, since $2\beta < 1-\alpha$, the term $D_2\left|\Delta\widetilde{T}\right|^{2\beta}$ should dominate near the critical point. Experimental verification of "complete scaling" is very difficult. The nonanalytical contributions in the "diameter" are usually not large enough to be separated

53

unambiguously.

When applied to the two-phase region at $\Delta\widetilde{T} < 0$ and $\rho = \rho_c$, the reduced form of the Yang-Yang relation[22] is

$$\frac{\widetilde{C}_V}{\widetilde{T}} = \frac{d^2\widetilde{P}_{cxc}}{d\widetilde{T}^2} - \frac{d^2\widetilde{\mu}_{cxc}}{d\widetilde{T}^2}, \tag{3.37}$$

where the subscript "cxc" denotes the vapor-liquid phase boundary. It has been known that the heat capacity diverges as $\left|\Delta\widetilde{T}\right|^{-\alpha}$ when the critical point is approached along the coexistence curve since the observation by Voronel' and coworkers[83, 84] in 1960's. Naturally this implies that one or both of the two second derivatives $d^2\widetilde{\mu}_{cxc}/d\widetilde{T}^2$ and $d^2\widetilde{P}_{cxc}/d\widetilde{T}^2$ must behave like $\widetilde{C}_V$; that is, weakly diverge along the same path. The lattice-gas model predicts that μ_{cxc} is analytic along an isochore so that μ_{cxc}'' must remain finite. Of the three possible choices, Yang and Yang[22] preferred that both of the derivatives would diverge in real fluids. Recently, "complete scaling" has substantiated this opinion.[19, 20] Furthermore, Fisher and coworkers[19, 20] have tried to find how the singularity in $\widetilde{C}_V$ is shared, in other words, to determine the strength of the Yang-Yang "anomaly", that is, the divergence of $\mu_{cxc}''(T)$. They carefully analyzed the extensive data for two-phase heat capacity of propane (C_3H_8) and found that the singularity is split almost equally between μ_{cxc}'' and P_{cxc}''. They also studied data for carbon dioxide (CO_2) and obtained a similar result but with μ_{cxc}'' diverging in the opposite sense. In their study the Yang-Yang anomaly is measured by the ratio

$$R_\mu = \frac{a_3}{1 + a_3}, \tag{3.38}$$

54

which is obtained from the experimental data for $\widetilde{C}_V$. For propane $R_\mu \approx 0.56$ and $a_3 \approx 1.27$, while for CO_2 $R_\mu \approx -0.4$ and $a_3 \approx -0.29$. Their results have been questioned by Wyczalkowska and coworkers[100] in 2002. They have shown how such an analysis done by Fisher and coworkers[19, 20] may be affected by the presence of a small amount of impurity as well as by other nonasymptotic deviations from lattice-gas symmetry. When corrections for a small amount of impurity are applied and allowance is made for the leading asymmetric Wegner correction, the experimental $\widetilde{C}_V$ data are not inconsistent with previous treatments in which the second derivative of the chemical potential exhibits a cusplike singularity with a finite limiting value at the critical temperature. This discovery means that up to now experiments do not yield conclusively the value of R_μ, the strength of the Yang-Yang "anomaly", and further the mixing coefficient a_3.

The second derivative of the thermodynamic potential with respect to chemical potential is the susceptibility $\widetilde{\chi} = \left(\partial^2 \widetilde{P}/\partial\widetilde{\mu}^2\right)_{\widetilde{T}}$. The reduced susceptibility on the two sides of the coexistence curve is given by Kim[21]

$$\widetilde{\chi}^- = \Gamma_0^- \left|\Delta\widetilde{T}\right|^{-\gamma} \pm \Gamma_1^- \left|\Delta\widetilde{T}\right|^{\beta} \pm \Gamma_2^- \left|\Delta\widetilde{T}\right|^{\beta+\gamma-1}, \tag{3.39}$$

where the asymmetric correction amplitudes $\Gamma_1^- \propto a_3$ and $\Gamma_2^- \propto b_2$. Evidently, since $\beta < \beta+\gamma-1$, near the critical point, the pressure mixing coefficient a_3 dominates the susceptibility asymmetry. This results suggest that it may be possible to detect a_3 experimentally by measuring the susceptibilities on the two sides of the coexistence boundary.[21]

3.5 Fluid asymmetry in mean-field approximation

It has been generally accepted that fluid criticality in real fluids may be mapped into a lattice-gas model in terms of a strong scaling field h_1 which conjugates to the strongly fluctuating order parameter ϕ_1 and a weak scaling field conjugate to the weakly fluctuating ϕ_2. The lattice gas has a special symmetry: the chemical potential is antisymmetric and the order parameter is symmetric with respect to the critical isochore. Therefore, for the lattice gas the critical part of Helmholtz free energy density in the mean field has a symmetric form of Landau expansion,

$$\Delta \overline{A}_{\mathrm{cr}} = \frac{1}{2} a_0 h_2 \phi_1^2 + \frac{1}{24} u_0 \phi_1^4, \tag{3.40}$$

and the critical part of grand thermodynamic-potential density is

$$-\Delta \overline{P}_{\mathrm{cr}} = \frac{1}{2} a_0 h_2 \phi_1^2 + \frac{1}{4} u_0 \phi_1^4 - h_1 \phi_1, \tag{3.41}$$

where a_0 and u_0 are parameters. The critical part of chemical potential is of a simple form,

$$h_1 = \Delta \overline{\mu} = a_0 h_2 \phi_1 + \frac{1}{6} u_0 \phi_1^3, \tag{3.42}$$

and when $h_1 = 0$ it gives the symmetric coexistence curve,

$$\phi_1 = \pm \left(\frac{6a_0}{u_0} \right)^{\frac{1}{2}} |h_2|^{\frac{1}{2}}. \tag{3.43}$$

Simple lattice gas: In the primitive prototype the scaling fields and their conjugate density are just the physical variables:

$$h_1 = \Delta\overline{\mu}, \quad h_2 = \Delta\overline{T}, \tag{3.44}$$

$$\phi_1 = \Delta\overline{\rho}, \quad \phi_2 = \Delta\overline{s}. \tag{3.45}$$

Substituting Eqs. (3.44) and (3.45) into Eq. (3.42) and comparing it with the expansion of $\Delta\overline{\mu}$ in terms of $\Delta\overline{T}$ and $\Delta\overline{\rho}$ with only the third-order term, one obtains

$$a_0\Delta\overline{\rho}\Delta\overline{T} + \frac{1}{6}u_0\Delta\overline{\rho}^3 = \mu_{11}\Delta\overline{\rho}\Delta\overline{T} + \frac{1}{6}\mu_{30}\Delta\overline{\rho}^3 \tag{3.46}$$

where $\mu_{ij} = \frac{\partial^{i+j}\Delta\overline{\mu}}{\partial\Delta\overline{\rho}^i\Delta\overline{T}^j}$, the parameters $a_0 = \mu_{11}$ and $u_0 = \mu_{30}$.

Conventional mixing scaling: Since the early 1970's, the vapor-liquid asymmetry has been commonly incorporated into the lattice-gas analogy by linear mixing of two independent physical fields $\Delta\overline{\mu}$ and $\Delta\overline{T}$ into the both theoretical scaling fields h_1 and h_2.[14] Since the absolute value of entropy is arbitrary, mixing of $\Delta\overline{T}$ into h_1 plays no role. Contrarily, mixing of $\Delta\overline{\mu}$ (with b_2 as a mixing coefficient) into h_2 has an important consequence, known as the "singular diameter". However, the chemical potential would remain an analytical function of temperature along the vapor-liquid coexistence and fluid asymmetry would be eliminated by a redefinition of the order parameter as $\phi_1 = \Delta\overline{\rho} - b_2\Delta\overline{s}$.

With the convenient choice of the critical entropy value, the conventional

mixing scaling is described by

$$h_1 = \Delta\overline{\mu}, \quad h_2 = \Delta\overline{T} + b_2\Delta\overline{\mu}, \qquad (3.47)$$

$$\phi_1 = \Delta\overline{\rho} - b_2\Delta\overline{s}, \quad \phi_2 = \Delta\overline{s}, \qquad (3.48)$$

$$\Delta\overline{\rho} = \phi_1 + b_2\phi_2, \quad \Delta\overline{s} = \phi_2. \qquad (3.49)$$

When $\Delta\overline{\mu}$ in h_2 is expanded by $\Delta\overline{\mu} = \mu_{11}\Delta\overline{\rho}\Delta\overline{T} + \frac{1}{6}\mu_{30}\Delta\overline{\rho}^3$ and in the first approximation $\Delta\overline{s} = -\frac{1}{2}\mu_{11}\Delta\overline{\rho}^2$, we expresses h_2 and ϕ_1 in terms of $\Delta\overline{T}$ and $\Delta\overline{\rho}$. Then the Eq. (3.42) is described in terms of $\Delta\overline{T}$ and $\Delta\overline{\rho}$, neglecting the higher order terms,

$$h_1 = a_0\Delta\overline{\rho}\Delta\overline{T} + \frac{1}{6}u_0\Delta\overline{\rho}^3 + \left(\frac{a_0^2}{2} + a_0\mu_{11}\right)b_2\Delta\overline{\rho}^2\Delta\overline{T} + \left(\frac{1}{4}u_0a_0 + \frac{\mu_{30}}{6}a_0\right)b_2\Delta\overline{\rho}^4.$$

$$(3.50)$$

This expansion generates the asymmetric terms $\propto b_2\Delta\overline{\rho}^2\Delta\overline{T}$ and $\propto b_2\Delta\overline{\rho}^4$. If the mixing coefficient $b_2 = 0$, both asymmetric terms vanish. However, in the simplest equation of state that describes real fluid behavior, the van der Waals equation, the term $\propto\Delta\overline{\rho}^2\Delta\overline{T}$ is absent, while the term $\propto\Delta\overline{\rho}^4$ exists. Furthermore, in most classical equations of state $d\Delta\overline{\mu}^2/d\Delta\overline{T}^2$ along the vapor-liquid coexistence exhibits a discontinuity directly related to the existence of the independent 4th-order term in Landau expansion of chemical potential. The existence of the independent 4th-order term makes exact mapping of fluids into the lattice-gas model by the conventional mixing of physical fields impossible. This problem was recognized a long time ago[43] but was never clearly articulated. $h_1 = \Delta\overline{\mu}$ may be expanded in terms of $\Delta\overline{T}$ and

$\Delta\overline{\rho}$ with terms below the fourth order

$$h_1 = \mu_{11}\Delta\overline{\rho}\Delta\overline{T} + \frac{1}{6}\mu_{30}\Delta\overline{\rho}^3 + \frac{\mu_{21}}{2}\Delta\overline{\rho}^2\Delta\overline{T} + \frac{\mu_{40}}{24}\Delta\overline{\rho}^4. \tag{3.51}$$

Comparing Eq. (3.50) and Eq. (3.51) we may obtain $a_0 = \mu_{11}$ and $u_0 = \mu_{30}$ and the relation between μ_{21} and μ_{40}

$$\frac{2\mu_{21}}{\mu_{11}} = \frac{3\mu_{40}}{5\mu_{30}}. \tag{3.52}$$

It is impossible to get an explicit relation between b_2 and μ_{ij} since the number of equations is one more than the number of unknown variables. Only the fluids whose coefficients of the Landau expansion follow relation (3.52) will be described by the conventional mixing scaling. Thus, this scaling is not valid for those fluids with a vanishing 2nd-order term μ_{21} and non-zero 4th-order term μ_{40} in the Landau expansion for the chemical potential such as the Van der Waals fluid and most other classical fluids. Moreover, since the difference of the second derivative $d\Delta\overline{\mu}^2/d\Delta\overline{T}^2$ along the phase boundary and along the isochore above the critical temperature[43]

$$\frac{d^2\Delta\overline{\mu}_{\mathrm{cxc}}}{d\Delta\overline{T}^2} - \left(\frac{d^2\Delta\overline{\mu}}{d\Delta\overline{T}^2}\right)_{\rho_{\mathrm{c}}} = \frac{\mu_{11}^2}{\mu_{30}}\left(-\frac{2\mu_{21}}{\mu_{11}} + \frac{3\mu_{40}}{5\mu_{30}}\right), \tag{3.53}$$

it is straightforward that the discontinuity will disappear for fluids that follow relation (3.52).

"Complete scaling": In "complete scaling", the ordering field and thermal field

are constructed by mixing the physical variables $\Delta \overline{P}$, $\Delta \overline{\mu}$ and $\Delta \overline{T}$ with only two unknown mixing coefficients a_3 and b_2,

$$h_1 = \Delta \overline{\mu} + a_3 \left(\Delta \overline{P} - \widetilde{s}_c \Delta \overline{T} \right), \qquad (3.54)$$

$$h_2 = \Delta \overline{T} + b_2 \Delta \overline{\mu}. \qquad (3.55)$$

In order to obtain the expressions of a_3 and b_2 for the mean-field fluids in terms of μ_{ij}, the expansion of Eq. (3.54) as a function of $\Delta \overline{\rho}$ and $\Delta \overline{T}$ will be compared with the expansion of Eq. (3.42) term to term. Since we have $\mu_{01} = \left(\frac{\partial \Delta \overline{\mu}}{\partial \Delta \overline{T}} \right)_c = 0$, $a_2 + a_3 P_{01} = a_2 + a_3 \left(\frac{\partial \Delta \overline{P}}{\partial \Delta \overline{T}} \right)_c = 0$ and $\mu_{02} + a_3 P_{02} = \left(\frac{\partial^2 \Delta \overline{\mu}}{\partial \Delta \overline{T}^2} \right)_c + a_3 \left(\frac{\partial^2 \Delta \overline{P}}{\partial \Delta \overline{T}^2} \right)_c = 0$, the expansion of Eq. (3.54) in terms of $\Delta \overline{\rho}$ and $\Delta \overline{T}$ with terms up to 4th-order is

$$\begin{aligned} h_1 &= \left(\mu_{11} + a_3 P_{11} \right) \Delta \overline{\rho} \Delta \overline{T} + \frac{1}{6} \left(\mu_{30} + a_3 P_{30} \right) \Delta \overline{\rho}^3 + \\ &\quad \frac{1}{2} \left(\mu_{21} + a_3 P_{21} \right) \Delta \overline{\rho}^2 \Delta \overline{T} + \frac{1}{24} \left(\mu_{40} + a_3 P_{40} \right) \Delta \overline{\rho}^4. \end{aligned} \qquad (3.56)$$

The relation between the coefficients[43] μ_{ij} and P_{ij}, such as $P_{11} = \mu_{11}$, $P_{30} = \mu_{30}$, $P_{21} = \mu_{21} + \mu_{11}$ and $P_{40} = \mu_{40} + 3\mu_{30}$, may help to simplify Eq. (3.56) further,

$$\begin{aligned} h_1 &= \left(1 + a_3 \right) \mu_{11} \Delta \overline{\rho} \Delta \overline{T} + \frac{1}{6} \left(1 + a_3 \right) \mu_{30} \Delta \overline{\rho}^3 + \\ &\quad \frac{1}{2} \left[\left(1 + a_3 \right) \mu_{21} + a_3 \mu_{11} \right] \Delta \overline{\rho}^2 \Delta \overline{T} + \\ &\quad \frac{1}{24} \left[\left(1 + a_3 \right) \mu_{40} + 3 a_3 \mu_{30} \right] \Delta \overline{\rho}^4. \end{aligned} \qquad (3.57)$$

By substituting $\phi_2 = \frac{\partial \Delta \overline{P}}{\partial h_2} = -\frac{1}{2} a_0 \phi_1^2$ into Eq. (3.34), one obtains $\Delta \overline{\rho}$ to be a

60

function of ϕ_1 only,

$$\Delta\bar{\rho} = (1 + a_3)\,\phi_1 + \left[a_3\,(1 + a_3) - \frac{1}{2}\,(1 + a_3)^2\,\mu_{11}b_2\right]\phi_1^2. \tag{3.58}$$

Solving this equation one can obtain ϕ_1 as a function of $\Delta\bar{\rho}$

$$\phi_1 = \frac{1}{1 + a_3}\Delta\bar{\rho} + \left[\frac{-a_3}{(1 + a_3)^2} + \frac{1}{2\,(1 + a_3)}\mu_{11}b_2\right]\Delta\bar{\rho}^2. \tag{3.59}$$

The expansion of h_2 (3.55) with terms up to the 3rd-order yields

$$h_2 = \Delta\overline{T} + \mu_{11}b_2\Delta\bar{\rho}\Delta\overline{T} + \frac{1}{6}\mu_{30}b_2\Delta\bar{\rho}^3. \tag{3.60}$$

Then the Eq. (3.42) is expanded in terms of $\Delta\overline{T}$ and $\Delta\bar{\rho}$ by using Eqs. (3.59) and (3.60):

$$
\begin{aligned}
h_1 &= a_0 h_2 \phi_1 + \frac{1}{6}u_0\phi_1^3 \\
&= \frac{a_0}{1 + a_3}\Delta\bar{\rho}\Delta\overline{T} + \frac{1}{6}u_0\frac{1}{(1 + a_3)^3}\Delta\bar{\rho}^3 + \\
&\quad \left[\frac{a_0}{1 + a_3}\mu_{11}b_2 + \frac{-a_0 a_3}{(1 + a_3)^2} + \frac{a_0}{2}\frac{\mu_{11}}{1 + a_3}b_2\right]\Delta\bar{\rho}^2\Delta\overline{T} + \\
&\quad \frac{1}{6}\left\{\frac{a_0}{1 + a_3}\mu_{30}b_2 + 3u_0\left[\frac{-a_3}{(1 + a_3)^4} + \frac{1}{2}\frac{\mu_{11}}{(1 + a_3)^3}b_2\right]\right\}\Delta\bar{\rho}^4. \tag{3.61}
\end{aligned}
$$

The coefficients of each corresponding term between Eq. (3.57) and Eq. (3.61) must be equivalent. The comparison will give four equations with four unknown parameters a_0, u_0, a_3 and b_2. It is straightforward that terms $\sim\Delta\bar{\rho}\Delta\overline{T}$ and $\sim\Delta\bar{\rho}^3$

61

yield the relations $a_0 = (1 + a_3)^2 \mu_{11}$ and $u_0 = (1 + a_3)^4 \mu_{30}$, which make the Ising

model amplitude for the coexistence curve as

$$B_0^{\text{Ising}} = \left(\frac{6a_0}{u_0} \right)^{\frac{1}{2}} = \frac{1}{1 + a_3} B_0 = \frac{1}{1 + a_3} \left(\frac{6\mu_{11}}{\mu_{30}} \right)^{\frac{1}{2}}, \tag{3.62}$$

which is not equal to the real fluids amplitude. The comparison of each asymmetry

term, which is proportional to $\Delta \bar{\rho}^2 \Delta \bar{T}$ or $\Delta \bar{\rho}^4$ in Eq. (3.57) and Eq. (3.61), results

in two very complicated equations involving only unknown a_3 and b_2. Theoretically

these two equations may be solved to obtain the expected expressions of a_3 and b_2 in

terms of Landau expansion coefficients μ_{ij}. The slope of linear diameters in classical

fluids has been found for many years,[43]

$$D = \frac{\mu_{21}}{\mu_{30}} - \frac{3\mu_{11}\mu_{40}}{5\mu_{30}^2}, \tag{3.63}$$

which will be employed to make the task easier.

The definition, $h_1 = 0$, of the coexistence curve can be solved by iteration to

obtain the slope of the diameter. Eq. (3.57) will be considered first since only a_3

is involved in this expression. Comparing the slope obtained from Eq. (3.57) with

Eq. (3.63), the expression of a_3 in terms of μ_{ij} is obtained

$$a_3 = \frac{\frac{2}{3} \frac{\mu_{21}}{\mu_{11}} - \frac{\mu_{40}}{5\mu_{30}}}{1 - \frac{2}{3} \frac{\mu_{21}}{\mu_{11}} + \frac{\mu_{40}}{5\mu_{30}}}. \tag{3.64}$$

By transforming this expression we have a simple and clear equation which will be

used frequently in our analysis,

$$\frac{a_3}{1+a_3} = \frac{2}{3}\frac{\mu_{21}}{\mu_{11}} - \frac{1}{5}\frac{\mu_{40}}{\mu_{30}}. \tag{3.65}$$

Making Eq. (3.61) equal to zero and comparing the coefficients with Eq. (3.63), we obtain the expression of b_2 in terms of μ_{ij},

$$b_2 = \frac{1}{\mu_{11}}\left(\frac{\mu_{21}}{\mu_{11}} - \frac{1}{5}\frac{\mu_{40}}{\mu_{30}}\right). \tag{3.66}$$

Since "complete scaling" is assumed to be valid for both real fluids and classical equation of state (EOS), the expressions (3.65) and (3.66) may be checked further by comparing our classical results to the description of real fluids derived from "complete scaling". Dividing the slope of diameter in classical fluids Eq. (3.63) into two part, a_3 contribution and b_2 contribution, one obtain

$$D = \frac{a_3}{1+a_3}\frac{6\mu_{11}}{\mu_{30}} - b_2\frac{3\mu_{11}^2}{\mu_{30}}. \tag{3.67}$$

The result is equivalent to the slope found from Eq. (3.58) in the first approximation by substituting $\phi_1 = \pm\left(\frac{6a_0}{u_0}\right)^{\frac{1}{2}}\left|\Delta\overline{T}\right|^{\frac{1}{2}}$, $a_0 = (1+a_3)^2\mu_{11}$ and $u_0 = (1+a_3)^4\mu_{30}$. One may notice that $\frac{6\mu_{11}}{\mu_{30}}$ is the square of the mean-field amplitude B_0^2 and $\frac{3\mu_{11}^2}{\mu_{30}}$ is the heat capacity jump $\frac{\Delta\overline{C}_v}{\overline{T}}$ when heat capacity crosses the phase boundary from

the one-phase region at the critical density. Finally,

$$D = \frac{a_3}{1+a_3}B_0^2 - b_2\frac{\Delta\overline{C}_v}{\overline{T}}. \tag{3.68}$$

Since $\alpha = 0$ and $\beta = 0.5$ in mean field, $1 - \alpha$ and 2β term both become linear term. However, obviously in Eq. (3.68) $\frac{a_3}{1+a_3}B_0^2$ is the contribution from 2β term, while $-b_2\frac{\Delta\overline{C}_v}{\overline{T}}$ comes from $1 - \alpha$ term and linear term. Furthermore, $\left(-\frac{\Delta\overline{C}_v}{\overline{T}}\right)$ may be written down as

$$-\frac{\Delta\overline{C}_v}{\overline{T}} = \left(\frac{\overline{C}_v}{\overline{T}}\right)_{\Delta\widetilde{T}<0,c} \cdot - \left(\frac{\overline{C}_v}{\overline{T}}\right)_{\Delta\widetilde{T}>0,c} = \left(\frac{\overline{C}_v}{\overline{T}}\right)_{\Delta\widetilde{T}<0,c} - \left(\frac{\overline{C}_v}{\overline{T}}\right)_{ideal}. \tag{3.69}$$

It is clear that the ideal-gas background of the heat capacity does not contribute to the diameter. Furthermore, the contribution from the chemical potential to the isochoric heat capacity jump $\Delta\overline{C}_v/\overline{T}$ for the classical fluids is

$$\frac{-a_3}{1+a_3}\frac{\Delta\overline{C}_v}{\overline{T}} = \frac{\mu_{11}^2}{\mu_{30}}\left(-\frac{2\mu_{21}}{\mu_{11}} + \frac{3\mu_{40}}{5\mu_{30}}\right) = \frac{d^2\Delta\overline{\mu}_{cxc}}{d\Delta\overline{T}^2} - \left(\frac{d^2\Delta\overline{\mu}}{d\Delta\overline{T}^2}\right)_{\rho_c}, \tag{3.70}$$

which corresponds to the result from "complete scaling" for real fluids given by Eq. (3.24).

The critical parameters T_c, ρ_c and P_c are affected by long-range fluctuations and they have different values for different fluids. However, "the law of corresponding states", when the physical variables are reduced by the critical parameters, makes physical properties of fluids much more similar. In the definition of two fields h_1 and h_2, the physical variables $\Delta\widetilde{\mu}$, $\Delta\widetilde{T}$, and $\Delta\widetilde{P}$ are all reduced by the actual critical

64

parameters. This fact enables us to assume that the values obtained for a_3 and b_2 in the mean-field EOS may be valid in the real fluids, at least in the first approximation. This assumption implies that fluctuations of the order parameter do not strongly affect the values of a_3 and b_2 in the scaling theory.

3.6   Asymmetry coefficients from mean-field equations of state

Assuming that fluctuations do not affect the values of a_3 and b_2 we have decided to obtain these two asymmetry parameters from the classical equations of state. The earliest qualitative explanation of critical phenomena was proposed by Van der Waals.   His equation, as well as all its further modifications, imply a quadratic parabolic coexistence curve and a finite jump in the isochoric heat capacity.[7]   We shall begin with the Van der Waals fluid due to its simplicity and great conceptual importance.

Van der Waals model: The Van der Waals EOS in (P, ρ, T) variables reads

$$P = \frac{\rho RT}{1 - b\rho} - a\rho^2, \tag{3.71}$$

where a is an attraction parameter associated with the strength of the attractive intermolecular forces and b a repulsion parameter related to the effective molecular volume; both of them are system-dependent constants. Thus, $\widehat{\rho} = b\rho$ is the dimensionless density and we have

$$\frac{\widehat{P}}{RT} = \frac{\widehat{\rho}}{1 - \widehat{\rho}} - \frac{\widetilde{a}\widehat{\rho}^2}{RT}, \tag{3.72}$$

65

where $\widehat{P} = Pb$ and $\widehat{a} = a/b$. For simplicity, when there is no confusion, we will use $P = \widehat{P}$, $a = \widehat{a}$ and $\rho = \widehat{\rho}$, and the Eq. (3.72) may be written in the form

$$\frac{P}{RT} = \frac{\rho}{(1 - \rho)} - \frac{a\rho^2}{RT},\tag{3.73}$$

which is equal to Eq. (3.71) with $b = 1$. The coordinates of the critical point can be found from any pair of the stability conditions, either

$$\left(\frac{\partial P}{\partial \rho}\right)_T = \frac{RT}{(1 - \rho)^2} - 2a\rho = 0,\tag{3.74}$$

$$\left(\frac{\partial^2 P}{\partial \rho^2}\right)_T = \frac{2RT}{(1 - \rho)^3} - 2a = 0,\tag{3.75}$$

or

$$\left(\frac{\partial \mu}{\partial \rho}\right)_T = \frac{1}{\rho}\left(\frac{\partial P}{\partial \rho}\right)_T = \frac{RT}{\rho(1 - \rho)^2} - 2a = 0,\tag{3.76}$$

$$\left(\frac{\partial^2 \mu}{\partial \rho^2}\right)_T = -\frac{1}{\rho^2}\left(\frac{\partial P}{\partial \rho}\right)_T + \frac{1}{\rho}\left(\frac{\partial^2 P}{\partial \rho^2}\right)_T = -\frac{RT(1 - 3\rho)}{\rho^2(1 - \rho)^3} = 0.\tag{3.77}$$

Solving the conditions, we obtain the critical parameters

$$\frac{T_c R}{a} = \frac{8}{27}, \quad \rho_c = \frac{1}{3}.\tag{3.78}$$

By integration, one can obtain the density of the Helmholtz energy for Van der Waals fluids,

$$\frac{\rho A - \rho A_0}{RT} = \rho \ln \frac{\rho RT}{(1 - \rho)} - \rho - \frac{a\rho^2}{RT}.\tag{3.79}$$

66

where $A_0 = \int C_P^{ig}(T)\,dT - T\int C_P^{ig}(T)\frac{dT}{T}$ is the ideal-gas caloric background. Finally, we obtain the same result for the chemical potential

$$\frac{\mu - \mu_0}{RT} = \ln\frac{\rho RT}{(1-\rho)} + \frac{\rho}{(1-\rho)} - \frac{2a\rho}{RT}. \tag{3.80}$$

where $\mu_0 = A_0$ is a temperature-dependent integration constant. Taking derivatives of chemical potential with respect to density ρ and temperature T, we have

$$\frac{\partial^2\mu}{\partial\rho\partial T} = R\left[\frac{1}{\rho} + \frac{2}{1-\rho} + \frac{\rho}{(1-\rho)^2}\right], \tag{3.81}$$

$$\frac{\partial^3\mu}{\partial\rho^2\partial T} = R\left[\frac{-1}{\rho^2} + \frac{3}{(1-\rho)^2} + \frac{2\rho}{(1-\rho)^3}\right], \tag{3.82}$$

$$\frac{\partial^3\mu}{\partial\rho^3} = RT\left[\frac{2}{\rho^3} + \frac{8}{(1-\rho)^3} + \frac{6\rho}{(1-\rho)^4}\right], \tag{3.83}$$

$$\frac{\partial^4\mu}{\partial\rho^4} = RT\left[\frac{-6}{\rho^4} + \frac{30}{(1-\rho)^4} + \frac{24\rho}{(1-\rho)^5}\right]. \tag{3.84}$$

Then, we have the Landau expansion coefficients of chemical potential with respect to $\Delta\bar{\rho}$ and $\Delta\overline{T}$

$$\mu_{11} = \left(\frac{\partial^2\Delta\bar{\mu}}{\partial\Delta\bar{\rho}\,\partial\Delta\overline{T}}\right)_{\Delta\bar{\rho}=0,\Delta\overline{T}=0} = \frac{\rho_c}{R}\left(\frac{\partial^2\mu}{\partial\rho\partial T}\right)_{\rho=\rho_c,T=T_c} = \frac{9}{4}, \tag{3.85}$$

$$\mu_{21} = \left(\frac{\partial^3\Delta\bar{\mu}}{\partial\Delta\bar{\rho}^2\,\partial\Delta\overline{T}}\right)_{\Delta\bar{\rho}=0,\Delta\overline{T}=0} = \frac{\rho_c^2}{R}\left(\frac{\partial^3\mu}{\partial\rho^2\partial T}\right)_{\rho=\rho_c,T=T_c} = 0, \tag{3.86}$$

$$\mu_{30} = \left(\frac{\partial^3\Delta\bar{\mu}}{\partial\Delta\bar{\rho}^3}\right)_{\Delta\bar{\rho}=0,\Delta\overline{T}=0} = \frac{\rho_c^3}{RT_c}\left(\frac{\partial^3\mu}{\partial\rho^3}\right)_{\rho=\rho_c,T=T_c} = \frac{27}{8}, \tag{3.87}$$

$$\mu_{40} = \left(\frac{\partial^4\Delta\bar{\mu}}{\partial\Delta\bar{\rho}^4}\right)_{\Delta\bar{\rho}=0,\Delta\overline{T}=0} = \frac{\rho_c^4}{RT_c}\left(\frac{\partial^4\mu}{\partial\rho^4}\right)_{\rho=\rho_c,T=T_c} = -\frac{27}{8}. \tag{3.88}$$

Substituting $\mu_{ij} = \left[\partial^{i+j}\Delta\bar{\mu}\big/\left(\partial\Delta\bar{\rho}^i\partial\Delta\overline{T}^j\right)\right]$ into Eq. (3.63), Eq. (3.65) and Eq.

(3.66), we have the rectilinear diameter slope D, a_3 and b_2 for Van der Waals fluids

$$D = \frac{\mu_{21}}{\mu_{30}} - \frac{3\mu_{11}\mu_{40}}{5\mu_{30}^2} = \frac{2}{5}, \tag{3.89}$$

$$a_3 = \frac{1}{4}, \quad b_2 = \frac{4}{45}. \tag{3.90}$$

Mean-field lattice gas: The mean-field lattice-gas[68] is a symmetric model which

has a diameter with zero slope.

$$\frac{P}{RT} = -\ln(1 - \rho) - \frac{a\rho^2}{RT}. \tag{3.91}$$

The density of the Helmholtz energy and chemical potential are, respectively,

$$\frac{\rho A - \rho A_0}{RT} = \rho \ln \frac{\rho RT}{(1 - \rho)} - \ln(1 - \rho) - \frac{a\rho^2}{RT}, \tag{3.92}$$

$$\frac{\mu - \mu_0}{RT} = \ln \frac{\rho RT}{(1 - \rho)} - \frac{2a\rho}{RT}. \tag{3.93}$$

From the critical condition and stability condition, we find the critical parameters

$$\frac{T_c R}{a} = \frac{1}{2}, \quad \rho_c = \frac{1}{2}. \tag{3.94}$$
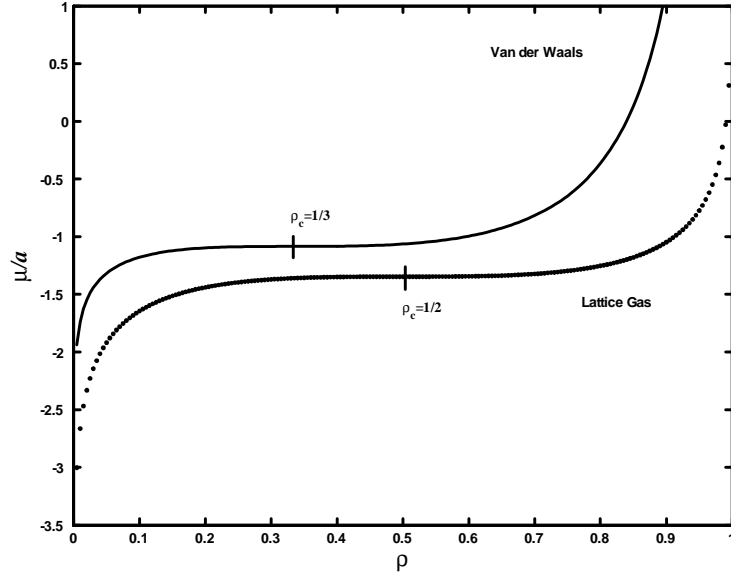
Figure 3.7: Chemical potential *vs* density of Van der Waals model and mean-field lattice gas.

From the derivatives of chemical potential we obtain the Landau expansion coefficients for lattice gas

$$\mu_{11} = 2, \quad \mu_{21} = 0, \quad \mu_{30} = 4, \quad \mu_{40} = 0. \tag{3.95}$$

Since the asymmetric coefficients both μ_{21} and μ_{40} vanish, it is straightforward that $a_3 = 0, \quad b_2 = 0$ and $D = 0$. Fig (3.7) compares the chemical potential at critical temperature between Van der Waals fluid and mean-field lattice gas. It is clear that the curve for the lattice gas is symmetric about $\rho_{\rm c} = \frac{1}{2}$, while the curve implied by the Van der Waals is not symmetric.

Other classical equations of state:

69

1. Debye-Hückel model:[69] This EOS is a general equation of state with a Debye-Hückel interaction between ions proportional to $\rho^{3/2}$.

$$\frac{P}{RT} = \frac{\rho}{1-\rho} - \frac{a\rho^{3/2}}{RT}. \tag{3.96}$$

$$\frac{\mu - \mu_0}{RT} = \ln\frac{\rho RT}{(1-\rho)} + \frac{\rho}{1-\rho} - \frac{3a\rho^{1/2}}{(RT)^{3/2}}. \tag{3.97}$$

Solving the critical condition and stability condition we have critical parameters

$$\frac{(T_c R)^{\frac{3}{2}}}{a} = 0.429, \quad \rho_c = 0.2. \tag{3.98}$$

Furthermore, one obtains the mixing coefficients

$$a_3 = 0.364, \quad b_2 = 0.043. \tag{3.99}$$

2. Redlich-Kwong EOS:[70] This is the first cubic EOS that has been widely employed to do the routine engineering calculations of the fugacity. It is also very successful for calculating properties of gas mixtures, but not adequate to model both gas and liquid phases.

$$\frac{P}{RT} = \frac{\rho}{1-\rho} - \frac{a\rho^2}{RT^{3/2}(1+\rho)}. \tag{3.100}$$

$$\frac{\mu - \mu_0}{RT} = \ln \frac{\rho RT}{(1 - \rho)} + \frac{\rho}{1 - \rho} + \frac{a}{RT^{3/2}} \left(\ln \frac{1}{1 + \rho} - \frac{\rho}{1 + \rho} \right). \qquad (3.101)$$

Solving the critical condition and stability condition we obtain the critical parameters

$$\frac{T_c^{\frac{3}{2}} R}{a} = 0.203, \quad \rho_c = 0.260. \qquad (3.102)$$

Furthermore, the mixing coefficients are

$$a_3 = 0.400, \quad b_2 = 0.068. \qquad (3.103)$$

3. Peng -Robinson EOS:[70] The Peng-Robinson EOS predicts better liquid volumes for medium-size hydrocarbons and other compounds with intermediate values of the acentric factor.

$$\begin{aligned}
\frac{P}{RT} &= \frac{\rho}{1 - \rho} - \frac{a\rho^2 \alpha}{RT(1 + 2\rho - \rho^2)} \quad T_r = \frac{T}{T_c}, \\
\alpha &= \left[1 + \left(0.37464 + 1.54226\omega - 0.26992\omega^2 \right) \left(1 - T_r^{1/2} \right) \right]^2, (3.104)
\end{aligned}$$

where ω is the acentric factor.

$$\frac{\mu - \mu_0}{RT} = \ln \frac{\rho RT}{(1 - \rho)} + \frac{\rho}{1 - \rho} + \frac{a\alpha}{RT} \left[\frac{1}{2\sqrt{2}} \ln \frac{1 + \rho \left(1 - \sqrt{2} \right)}{1 + \rho \left(1 + \sqrt{2} \right)} - \frac{\rho}{1 + 2\rho - \rho^2} \right].$$
$$(3.105)$$

Solving the critical condition and stability condition we find for the critical

Model	ρ_c	μ_{11}	μ_{21}	μ_{30}	μ_{40}	D	a_3	b_2
Lattice gas	0.5	2	0	4	0	0	0	0
Van der Waals	0.333	2.25	0	3.375	-3.375	0.4	0.25	0.089
Debye-Hückel	0.200	2.344	-1.172	0.977	-2.930	3.120	0.364	0.043
Redlich-Kwong	0.260	2.739	-0.815	2.145	-5.192	1.474	0.400	0.068
Peng-Robinson $\omega = 0$	0.221	2.266	-0.979	1.658	-5.125	1.944	0.493	0.082
$\omega = 0.1$	0.221	2.516	-1.087	1.658	-5.125	2.158	0.493	0.074
$\omega = 0.4$	0.221	3.212	-1.388	1.658	-5.125	2.755	0.493	0.058

Table 3.1: Asymmetry parameters for classical fluids

parameters

$$\frac{T_c R}{a} = 0.158, \quad \rho_c = 0.221. \tag{3.106}$$

When $\omega = 0$, one obtains $a_3 = 0.493, \quad b_2 = 0.082.$

The results are summarized in Table 3.1. One can see that for the Peng-Robinson EOS, the value of a_3 doesn't change as ω increases but b_2 decreases.

Fine-lattice discretization: Moghaddam and coworkers[87] developed a fine-lattice discretization model in 2005, which represents a crossover between the lattice gas and a continuous van der Waals fluid by introducing a discretization parameter $\zeta = a/a_0 \geq 1$,

$$\frac{P}{RT} = \zeta \ln \left(1 + \frac{\rho}{\zeta (1 - \rho)} \right) - \frac{a\rho^2}{RT}. \tag{3.107}$$

when $\zeta = 1$ is the lattice gas limit and $\zeta \longrightarrow \infty$ approaches the Van der Waals fluid, as shown in Fig. 3.8. This model makes it possible to transform a symmetric fluid system to an asymmetric one by adjusting the discretization parameter ζ.
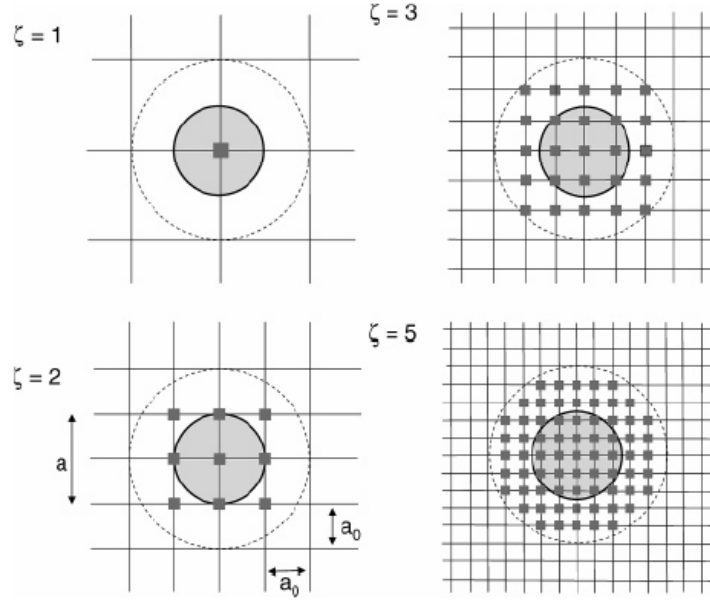
Figure 3.8: Illustration of fine-lattice discretization model.

The chemical potential of the model has the form

$$\frac{\mu - \mu_0}{RT} = \ln \frac{\rho RT}{1 + \rho\,(1/\zeta - 1)} + \zeta \ln \left[1 + \frac{\rho}{\zeta\,(1 - \rho)}\right] - \frac{2a\rho}{RT}. \tag{3.108}$$

Then the critical density and temperature are both function of parameter ζ

$$0 = -3(1/\zeta - 1)\rho_c^2 + (2/\zeta - 4)\,\rho_c + 1, \tag{3.109}$$

$$\frac{RT_c}{a} = \frac{2\rho_c}{\frac{1-\zeta}{1+(1/\zeta-1)\rho_c} + \frac{\zeta}{1-\rho_c}}, \tag{3.110}$$

which may be solved numerically. Then by substituting the critical parameters into the derivatives of chemical potential, we obtain a full picture that shows the transition of D, a_3 and b_2 from lattice gas to a continuum Van der Waals fluid, as shown in Figs 3.9 and 3.10. This fine-lattice discretization model makes it very clear

73
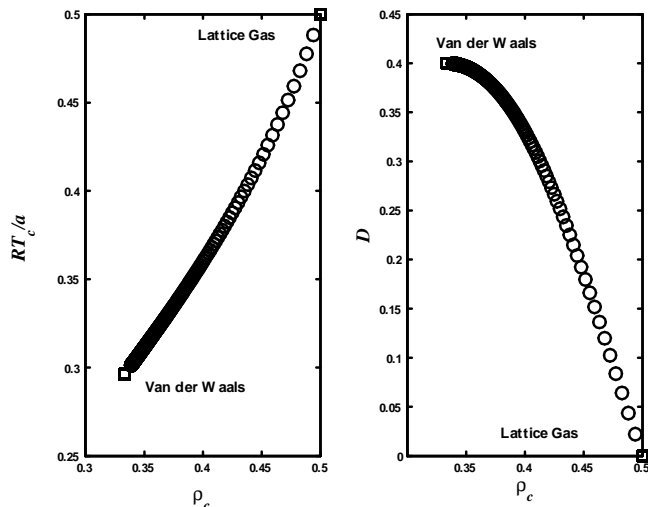
Figure 3.9: Fine-lattice gas model: crossover from lattice gas to Van der Waals fluid. T_c vs ρ_c and diameter slope D vs ρ_c.

that the ratio of molecular volume and lattice size $\zeta = a/a_0$ plays an important role in the change of fluid nature with respect to the vapor-liquid asymmetry. When the molecular volume is fixed, the smaller size of lattice increases the asymmetry in fluids. Therefore, we may imagine that the lattice size is fixed while the molecular volume changes continuously.

Effect of three-body interactions: In the fine-lattice gas model we know that by adjusting a parameter ζ, the symmetric fluid may transfer into an asymmetric fluid. It is natural to think whether there is another parameter which can play a similar role. The relative strength c of three-body interactions to two-body potentials is a good choice just as was suggested for the Van der Waals model by Pestak and coworkers.[17] The lattice-gas model with extra three-body interactions has a chemical

74
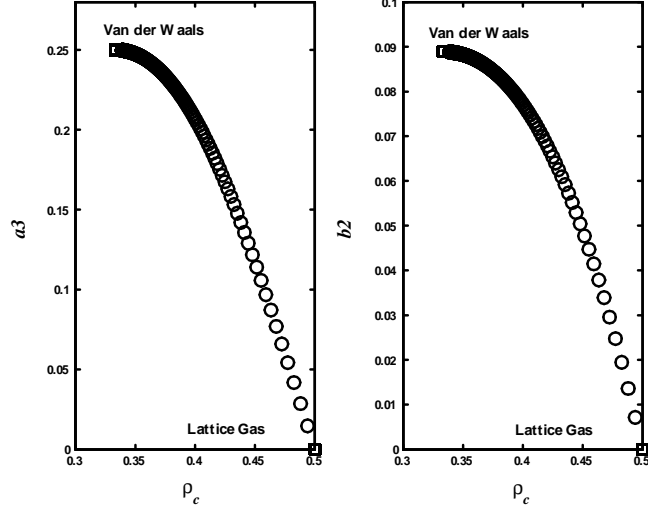
Figure 3.10: Fine-lattice gas model: crossover from lattice gas to Van der Waals fluid. a_3 *vs* ρ_c and b_2 *vs* ρ_c.

potential of the form,

$$\frac{\mu - \mu_0}{RT} = \ln \frac{\rho RT}{(1 - \rho)} - \frac{2a\rho}{RT} + c\frac{\frac{3}{2}a\rho^2}{RT}. \tag{3.111}$$

Then both the critical density and temperature depend on the parameter c:

$$0 = 9c\rho_c^2 - (6c + 4)\rho_c + 2, \tag{3.112}$$

$$\frac{RT_c}{a} = \frac{2 - 3c\rho_c}{\frac{1}{\rho_c} + \frac{1}{1 - \rho_c}}, \tag{3.113}$$

which may be solved numerically. Then upon substituting the critical parameters into the derivatives of chemical potential, we obtain a full picture that shows the effect of the relative strength c of three-body interactions to D, a_3 and b_2 for the lattice-gas model as shown in Figs 3.11 and 3.12. There is no doubt that the effect of three-body interactions on the fluids nature related to their asymmetry is rather

75
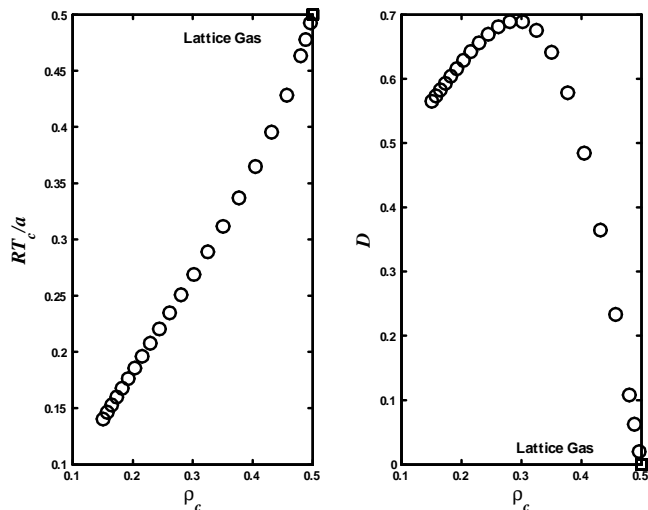
Figure 3.11: Lattice-gas model with three-body interactions: crossover from symmetric lattice gas to asymmetric lattice gas. T_c *vs* ρ_c and diameter slope D *vs* ρ_c.

large. Our calculation indicates that the asymmetry of fluids does not increase

monotonically as the three-body interactions get stronger.

Flory-Huggins model plus three-body interactions: Considering the crucial

effects of molecular volume and three-body interactions on the asymmetry in fluids,

we may construct a model which involves both of these two factors. Although the

fine-lattice discretization model is very attractive, it only accomplishes the crossover

from the lattice gas to Van der Waals fluids. The fluids with a higher asymmetry

than Van der Waals fluids cannot be represented by this model. Thus, the Flory-

Huggins model is useful; it has a fixed lattice and a changing molecular size. In

general, molecules in the Flory-Huggins model are drawn like a pearl necklace with

a flexible chain and each pearl occupies one lattice. Here, we simply treat them as

rectilinear blocks with different molecular volume as shown in Fig 3.13. When its
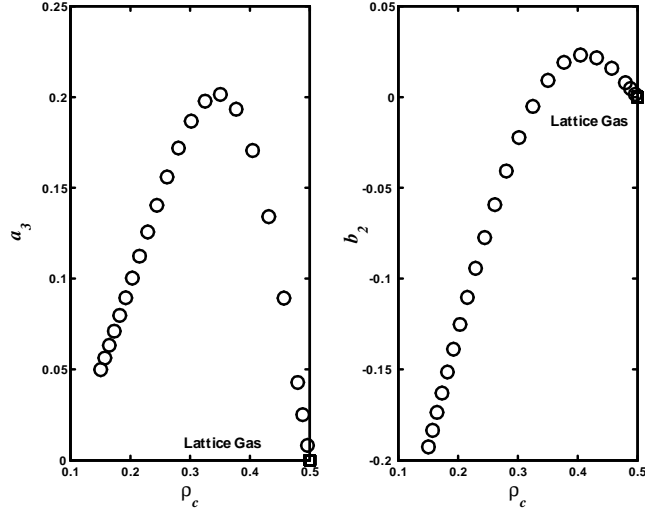
Figure 3.12: Lattice-gas model with three-body interactions: crossover from symmetric lattice gas to asymmetric lattice gas. a_3 vs ρ_c and b_2 vs ρ_c.

volume is very large, the molecule may occupy more than one lattice as shown in Fig 3.13 (d). In the opposite extreme, several molecules with very small volumes may stay in one lattice as shown in Fig 3.13 (a).

The chemical potential of the Flory-Huggins model with three-body interactions is

$$\frac{\mu - \mu_0}{RT} = \left[\frac{1}{N}\ln\rho - \ln(1-\rho)\right] - \frac{2a\rho}{RT} + c\frac{\frac{3}{2}a\rho^2}{RT}, \qquad (3.114)$$

where $N = a/a_0 > 0$ is the effective association number which is the ratio of molecular characteristic length a and the lattice size a_0 and c is the relative strength of three-body to two-body interactions. The Flory-Huggins model was formulated for $N \gg 1$. However, we will consider N here as a phenomenological parameter representing for molecular size. In contrast to the fine-lattice discretization model, the lattice size a_0 is now fixed, while the molecular volumes change for different fluids, as shown in Fig 3.13. The critical parameters ρ_c and T_c of this model are both

77
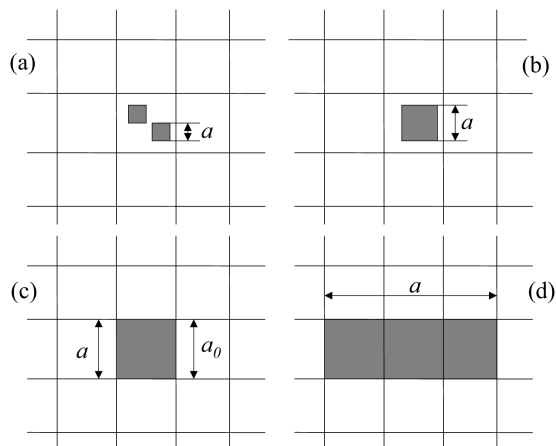
Figure 3.13: Illustration of the change of molecular volume relative to lattice size. (a) $a \ll a_0$ several molecules occupy one lattice. (b) $a < a_0$ in one lattice only one molecule. (c) $a = a_0$ molecular size is equal to lattice size. (d) $a > a_0$ molecular size is larger than lattice size and one molecule occupies more lattices.

functions of N and c:

$$0 = 6c\,(N-1)\,\rho_{\mathrm{c}}^{3} + [3c\,(2-N) - 2\,(N-1) + 6c]\,\rho_{\mathrm{c}}^{2} -$$

$$(6c+4)\,\rho_{\mathrm{c}} + 2, \tag{3.115}$$

$$\frac{RT_{\mathrm{c}}}{a} = \frac{2 - 3c\rho_{\mathrm{c}}}{\frac{1}{N\rho_{\mathrm{c}}} + \frac{1}{1-\rho_{\mathrm{c}}}}. \tag{3.116}$$

As shown in Figs. 3.14 and 3.15, the calculated results of a_3 and b_2 are very interesting. Both of them start from a small negative value when N is small (< 1) and then generally increase as the molecular volume becomes larger and larger. When N or c increases, the critical density ρ_{c} becomes smaller, which means that generally a larger molecular volume and a stronger relative strength of three-body interactions will give rise to a larger asymmetry. The solid curves in these two figures are the same as those in Fig 4.18 (a) and (b) which stand for the trend of a_3 and b_2 ob-
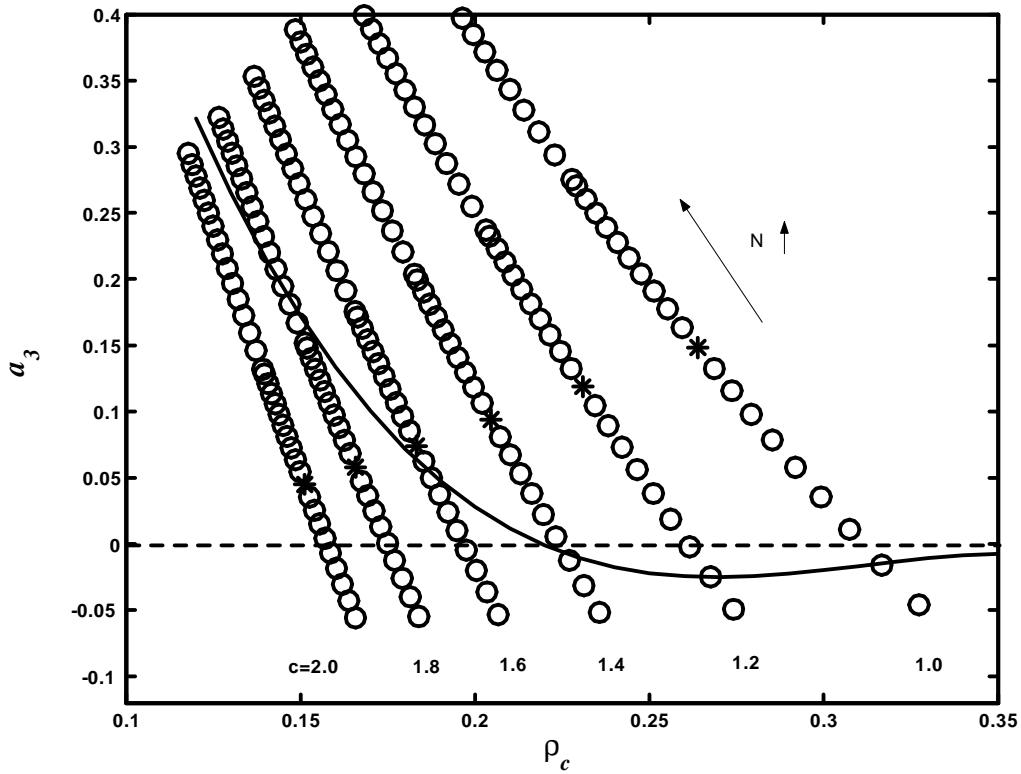
Figure 3.14: a_3 of Flory Huggins model with three-body interactions as a function of N and c. * means $N = 1$.

tained from experimental data for real fluids, which will be discussed in detail in the next chapter. From these results, we may describe real fluids by a simple classical equation of state if a proper effective association number N and a relative strength of three-body to two-body interactions c are selected.

3.7 Asymmetric criticality in a crossover Van der Waals equation of state

It is well known that since the thermodynamic properties near the critical point are strongly affected by the fluctuations of the order parameter, the classical equations, such as the Van der Waals equation of state, fail in this region. Wycza-lkowska and coworkers[99] presented a theoretical approach to correct a classical Van
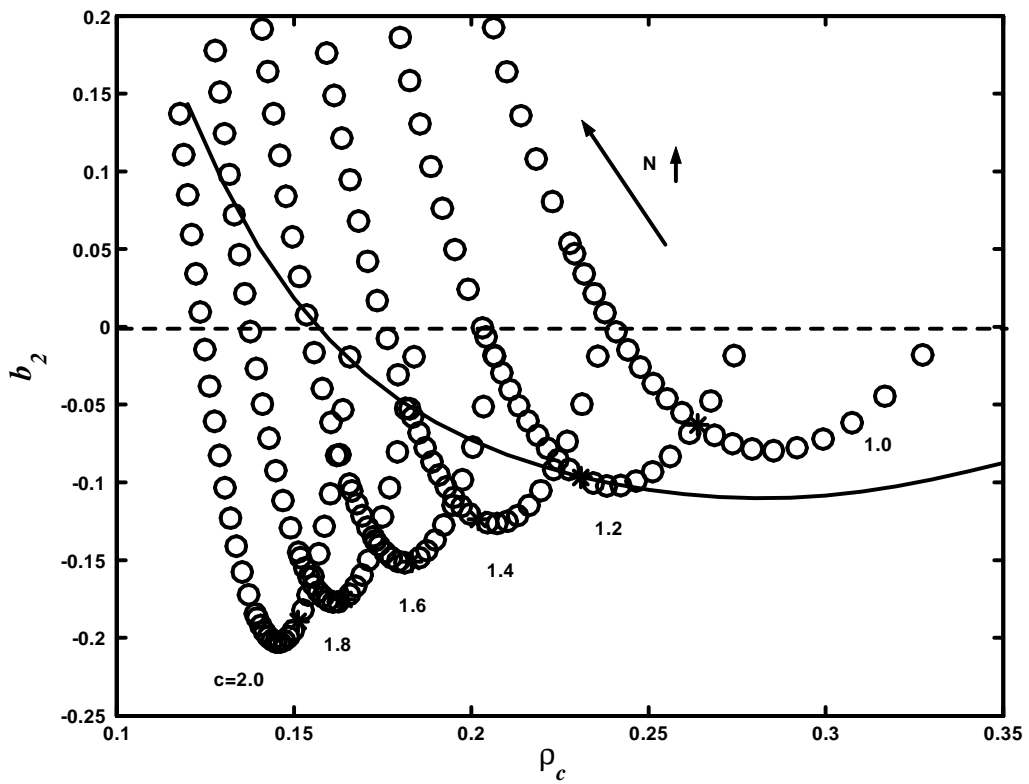
Figure 3.15: b_2 of Flory Huggins model with three-body interactions as a function of N and c. * means $N = 1$.

der Waals equation of state for the effects of critical fluctuations by utilizing a transformation deduced from the renormalization-group theory of critical phenomena. They explained how critical fluctuations lower the critical temperature, flatten the coexistence curve, induce a singularity in the isochoric heat capacity and so on. However, the vapor-liquid asymmetry, as given by "complete scaling", was not incorporated into that work.

Heat capacity: The reduced Yang-Yang relation for $\rho = \rho_\mathrm{c}$ is

$$\frac{\widetilde{C}_\mathrm{V}}{\widetilde{T}} = \frac{d^2\widetilde{P}}{d\widetilde{T}^2} - \frac{d^2\widetilde{\mu}}{d\widetilde{T}^2}, \tag{3.117}$$

which is valid for both mean field and asymptotic critical region. From "complete scaling", the presence of a_3 term implies a so-called Yang-Yang anomaly: the divergence of the heat capacity in the two-phase region near the critical point is shared among the second derivatives of pressure and chemical potential.[19, 21] Since we have

$$a_3 \frac{d^2\widetilde{P}}{d\widetilde{T}^2} = -\frac{d^2\widetilde{\mu}}{d\widetilde{T}^2}, \tag{3.118}$$

these two second derivatives may be calculated from $\widetilde{C}_\mathrm{v}$ by the formula

$$\frac{d^2\widetilde{P}}{d\widetilde{T}^2} = \frac{1}{1+a_3}\frac{\widetilde{C}_\mathrm{v}}{\widetilde{T}}, \quad -\frac{d^2\widetilde{\mu}}{d\widetilde{T}^2} = \frac{a_3}{1+a_3}\frac{\widetilde{C}_\mathrm{v}}{\widetilde{T}}. \tag{3.119}$$

Experimental tests of the Yang-Yang anomaly are even more controversial since traces of impurities can easily mimic such an anomaly, thus making any conclusions

unreliable.[100] However, the development of a method to calculate a_3 from a classical equation of state which can be used for the critical region make this separation much more practical. For classical Van der Waals fluids, we have already shown that $a_3 = 0.25$. Thus, since we know that heat capacity jump $\Delta \widetilde{C}_v$ for Van der Waals fluids is $\Delta \widetilde{C}_v / \widetilde{T} = 3\mu_{11}^2 / \mu_{30} = 9/2$, by using Eqs. (4.2) we may obtain the contribution from pressure $d^2 \widetilde{P}/d\widetilde{T}^2 = 18/5$ and from chemical potential is $-d^2 \widetilde{\mu}/d\widetilde{T}^2 = 9/10$. Since Wyczalkowska and coworkers[99] didn't considered the existence of a_3 term, their results for $d^2\widetilde{P}/d\widetilde{T}^2$ and $d^2\widetilde{\mu}/d\widetilde{T}^2$ are not consistent with "complete scaling". By using their results for the isochoric molar heat capacity $\widetilde{C}_v$, we present a simple method to separate $d^2\widetilde{P}/d\widetilde{T}^2$ and $d^2\widetilde{\mu}/d\widetilde{T}^2$ by introducing the asymmetric coefficient a_3.

When $\Delta \widetilde{T} > 0$ and $\Delta \widetilde{\rho} = 0$, in the mean-field region, it is well known that the isochoric heat capacity recovers the ideal-gas limit $\widetilde{C}_v = 3/2$ and the second derivative of pressure vanishes $d^2\widetilde{P}/d\widetilde{T}^2 = 0$. By employing the Yang-Yang relation (3.117), the second derivative of chemical potential is

$$-\frac{d^2 \widetilde{\mu}}{d\widetilde{T}^2} = \frac{\widetilde{C}_V}{\widetilde{T}} - \frac{d^2 \widetilde{P}}{d\widetilde{T}^2} = \frac{\frac{3}{2}}{\widetilde{T}}. \tag{3.120}$$

Considering the crossover from asymptotic critical region to mean field, since $d^2\widetilde{P}/d\widetilde{T}^2 = 0$ far from the critical point and $\frac{d^2\widetilde{P}}{d\widetilde{T}^2} = \frac{1}{1+a_3}\frac{\widetilde{C}_v}{\widetilde{T}}$ in the critical region, we may construct the crossover like

$$\frac{d^2 \widetilde{P}}{d\widetilde{T}^2} = \frac{1}{1+a_3}\left(\frac{\widetilde{C}_v}{\widetilde{T}} - \frac{\frac{3}{2}}{\widetilde{T}}\right). \tag{3.121}$$

82

From Yang-Yang relation, $d^2\widetilde{\mu}/d\widetilde{T}^2$ is calculated

$$-\frac{d^2\widetilde{\mu}}{d\widetilde{T}^2} = \frac{a_3}{1+a_3}\frac{\widetilde{C}_{\rm v}}{\widetilde{T}} + \frac{1}{1+a_3}\frac{\frac{3}{2}}{\widetilde{T}} = \frac{a_3}{1+a_3}\left(\frac{\widetilde{C}_{\rm v}}{\widetilde{T}} - \frac{\frac{3}{2}}{\widetilde{T}}\right) + \frac{\frac{3}{2}}{\widetilde{T}}. \tag{3.122}$$

When $\Delta\widetilde{T} < 0$ along the coexistence curve, in the mean field area, we may construct the $d^2\widetilde{P}/d\widetilde{T}^2$ and $d^2\widetilde{\mu}/d\widetilde{T}^2$ as

$$\frac{d^2\widetilde{P}}{d\widetilde{T}^2} = \frac{18}{5} + C_1\left(\widetilde{T}-1\right), \tag{3.123}$$

$$\frac{d^2\widetilde{\mu}}{d\widetilde{T}^2} = -\frac{9}{10} + C_2\left(\widetilde{T}-1\right) - \frac{\frac{3}{2}}{\widetilde{T}}, \tag{3.124}$$

where $18/5$ and $9/10$ are their respective contributions to the heat capacity jump, and $C_1 = \left(\frac{d^3\widetilde{P}_{\rm cxc}}{d\widetilde{T}^3}\right)_{\Delta\widetilde{T}=0,\Delta\widetilde{\rho}=0}$, $C_2 = \left(\frac{d^3\widetilde{\mu}_{\rm cxc}}{d\widetilde{T}^3}\right)_{\Delta\widetilde{T}=0,\Delta\widetilde{\rho}=0}$. From the Yang-Yang relation we have

$$\frac{\widetilde{C}_{\rm V}}{\widetilde{T}} = \frac{9}{2} + (C_1 - C_2)\,\Delta\widetilde{T} + \frac{\frac{3}{2}}{\widetilde{T}}, \tag{3.125}$$

which may be transformed to

$$\widetilde{C}_{\rm V} = 6 + (4.5 + C_1 - C_2)\,\Delta\widetilde{T} + (C_1 - C_2)\,\Delta\widetilde{T}^2. \tag{3.126}$$

Since $C = \left(\frac{d\widetilde{C}_{\rm V}}{d\widetilde{T}}\right)_{\Delta\widetilde{T}=0}$, it is clear that $C = 4.5 + C_1 - C_2$. Therefore, if we know C and C_1, we may calculate C_2 easily. Considering the crossover from asymptotic critical region to mean field, since in the asymptotic critical region $\frac{d^2\widetilde{P}}{d\widetilde{T}^2} = \frac{1}{1+a_3}\frac{\widetilde{C}_{\rm v}}{\widetilde{T}}$ and

83
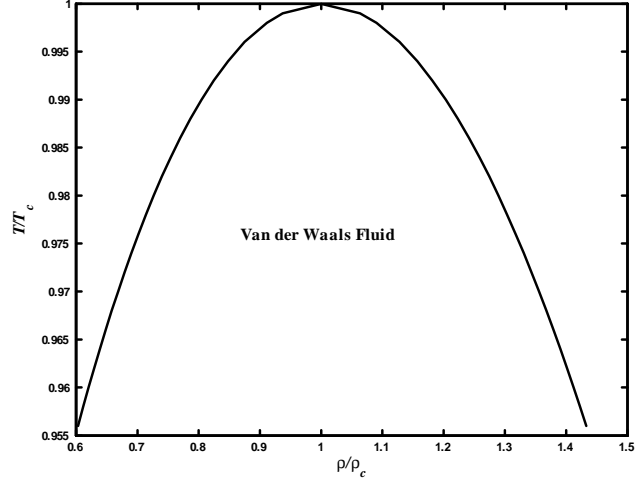
Figure 3.16: The coexistence curve of the Van der Waals fluid.[101]

far from the critical point $\frac{d^2\widetilde{P}}{d\widetilde{T}^2} \sim C_1\left(\widetilde{T}-1\right)$, we may add these two limits together:

$$\frac{d^2\widetilde{P}}{d\widetilde{T}^2} = \frac{1}{1+a_3}\frac{\widetilde{C}_{\mathrm{v}}}{\widetilde{T}} + C_1\left(\widetilde{T}-1\right). \tag{3.127}$$

In the same way we obtain the crossover formula for $d^2\widetilde{\mu}/d\widetilde{T}^2$,

$$-\frac{d^2\widetilde{\mu}}{d\widetilde{T}^2} = \frac{a_3}{1+a_3}\frac{\widetilde{C}_{\mathrm{v}}}{\widetilde{T}} - C_2\left(\widetilde{T}-1\right) + \frac{\frac{3}{2}}{\widetilde{T}}. \tag{3.128}$$

The calculated crossover heat capacity data for $c_t = 1$ is obtained from Wyczalkowska and coworkers.[99] Then we calculate the first derivative $C = \left(\frac{d\widetilde{C}_{\mathrm{v}}}{d\widetilde{T}}\right)_{\Delta\widetilde{T}=0}$ $= 14.5$ numerically. From the coexistence curve of Van der Waals model obtained by Barieau,[101] as shown in Fig (3.16), we find $C_1 = \left(\frac{d^3\widetilde{P}_{\mathrm{cxc}}}{d\widetilde{T}^3}\right)_{\Delta\widetilde{T}=0,\Delta\widetilde{\rho}=0} = 1.08$ numerically. Thus, $C_2 = 4.5 + C_1 - C = -8.92$.

Then, the heat capacity $\widetilde{C}_{\mathrm{v}}$, $d^2\widetilde{P}/d\widetilde{T}^2$ and $d^2\widetilde{\mu}/d\widetilde{T}^2$ may be plotted as func-

84
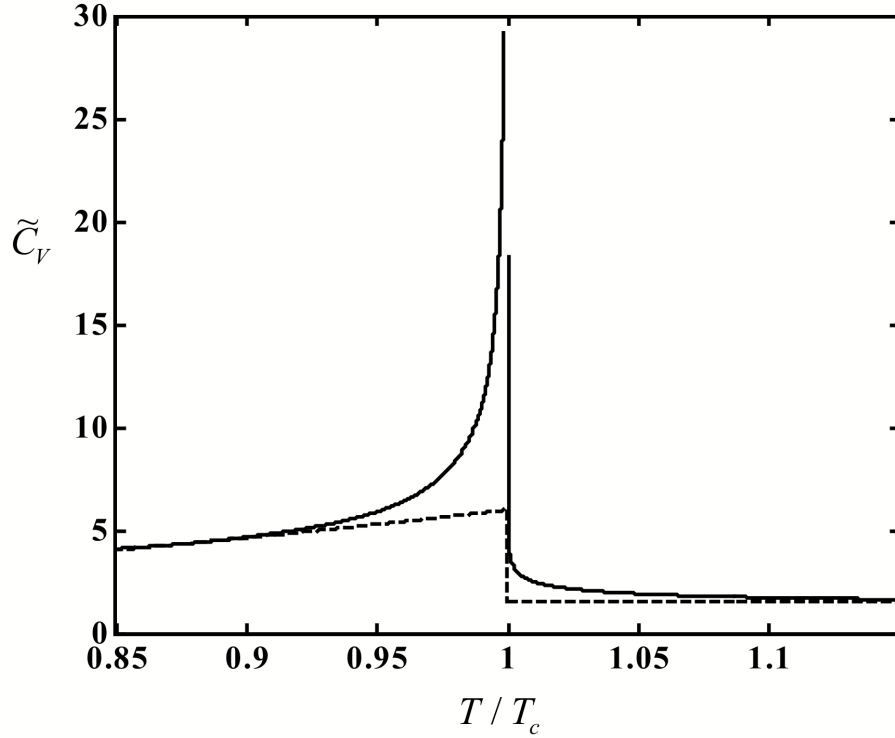
Figure 3.17: Reduced isochoric molar heat capacity $\widetilde{C}_V$ of the crossover[99] for $c_t = 1$ (solid line) and classical (dash line) Van der Waals equation along the critical isochore as a function of T/T_c.

tions of temperature.

<u>Diameter:</u> As a result of "complete scaling", the "diameter" ρ_d contains two non-analytical contributions $\left|\Delta\widetilde{T}\right|^{2\beta}$ and $\left|\Delta\widetilde{T}\right|^{1-\alpha}$, associated with the terms $a_3\Delta\widetilde{P}$ and $b_2\Delta\widetilde{\mu}$ in the scaling fields. The term $D_2\left|\Delta\widetilde{T}\right|^{2\beta}$ should dominate near the critical point since $2\beta < 1 - \alpha$. It is very challenge to verify this consequence of "complete scaling" experimentally. The nonanalytical contributions in the "diameter" are usually not large enough to be separated unambiguously.

To unambiguously separate $1 - \alpha$ term and 2β term and reliably determine the two asymmetry coefficients a_3 and b_2, we combine accurate experimental and
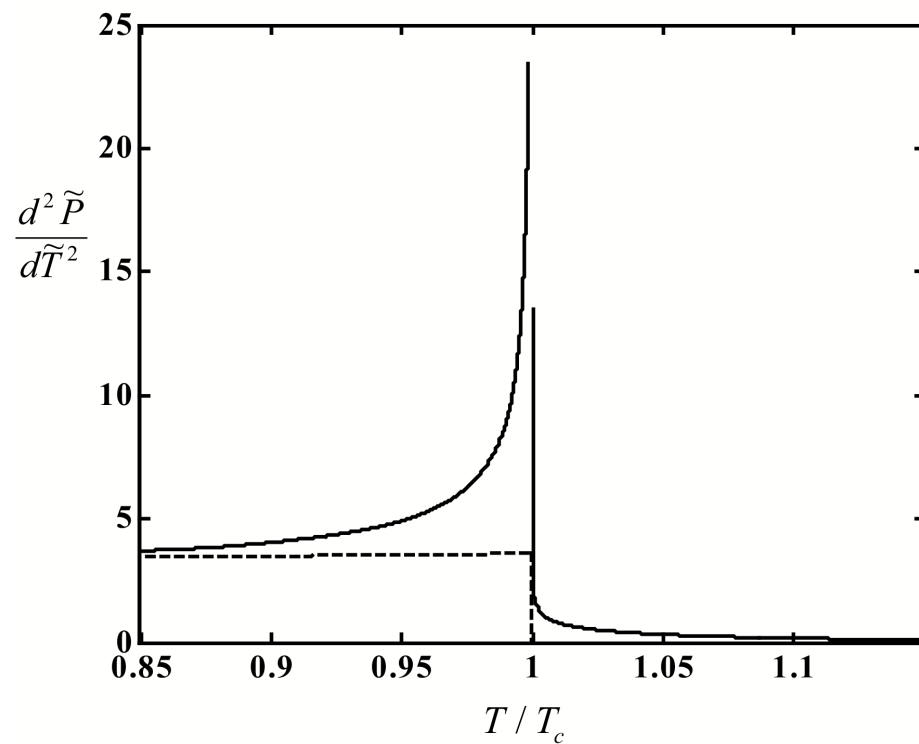
Figure 3.18: Second derivative $\left(\partial^2 \widetilde{P}/\partial \widetilde{T}^2\right)_\rho$ of the crossover[99] for $c_t = 1$ (solid line) and classical (dash line) Van der Waals equation along the critical isochore as a function of T/T_c.
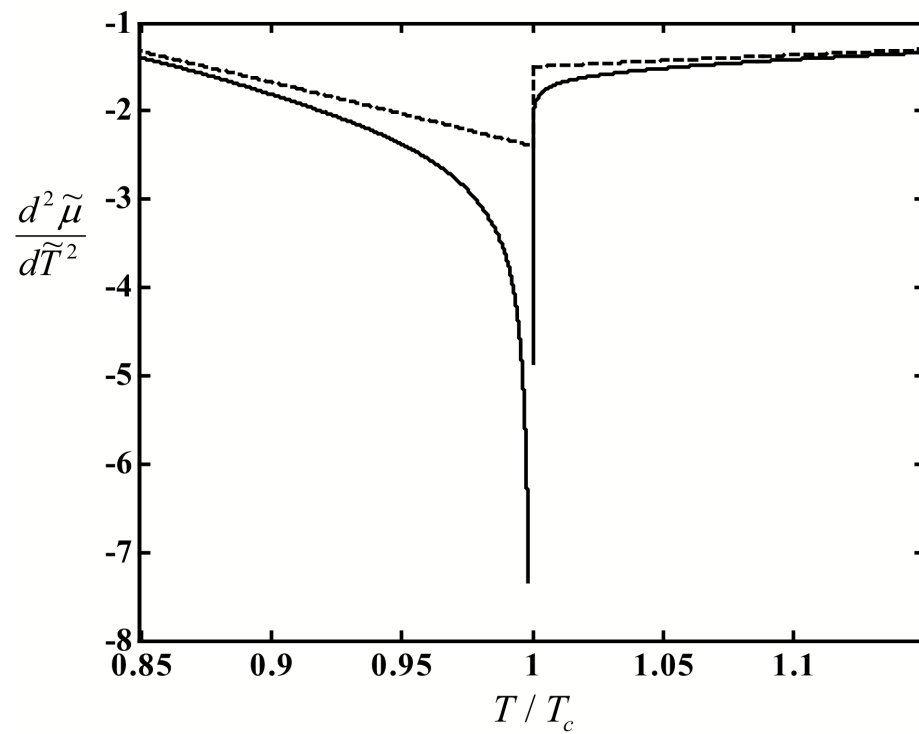
Figure 3.19: Second derivative $\left(\partial^2\widetilde{\mu}/\partial\widetilde{T}^2\right)_\rho$ of the crossover[99] for $c_t = 1$ (solid line) and classical (dash line) Van der Waals equation along the critical isochore as a function of T/T_c.

simulational vapor-liquid coexistence and heat-capacity data. We have exploited the fact that the coefficients D_1 and D_0 in Eq. (4.2) are actually not independent. By introducing the critical background B_{cr}, as shown in Eq. (4.5), which can be obtained theoretically[46] and by analyzing heat-capacity data, Eq. (??) becomes a formula with only two adjustable coefficients, D_1 and D_2. We have examined a number of systems, real fluids and simulated models, for which we could find both heat-capacity and coexistence data in the range $\left|\Delta\widetilde{T}\right| < 0.01$, which will be discussed in the next chapter. Now let us consider how to separate $1 - \alpha$ and 2β term of the calculated diameter for the crossover Van der Waals fluid.

The renormalized critical part of the Helmholtz free energy density is

$$\Delta\widetilde{A}_{\mathrm{cr}} = \frac{1}{2}tM^2\mathcal{T}\mathcal{D} + \frac{\overline{u}u^*\Lambda}{4!}M^4\mathcal{D}^2\mathcal{U} - \frac{1}{2}t^2\mathcal{K}, \tag{3.129}$$

with

$$t = c_t\Delta\widetilde{T}, \quad M = c_\rho\Delta\widetilde{\rho}, \quad u^*\overline{u}\Lambda = u_0/c_\rho^4, \tag{3.130}$$

where

$$c_t = a_0\left(\nu_0\right)^{2/3}/c_0, \quad c_\rho = c_0^{1/2}\nu_0^{-1/3}, \quad c_tc_\rho = a_0. \tag{3.131}$$

One takes approximate expressions for the rescaling functions $\mathcal{T}$, $\mathcal{D}$, $\mathcal{K}$, and $\mathcal{U}$ as:

$$\mathcal{T} = Y^{(2\nu-1)/\Delta_{\mathrm{s}}}, \quad \mathcal{D} = Y^{-\eta\nu/\Delta_{\mathrm{s}}}, \tag{3.132}$$

$$\mathcal{U} = Y^{\nu/\Delta_{\mathrm{s}}}, \quad \mathcal{K} = \frac{\nu}{\alpha\overline{u}\Lambda}\left(Y^{-\alpha/\Delta_{\mathrm{s}}} - 1\right), \tag{3.133}$$

where Y is a crossover function and is to be evaluated from the equation

$$1 - (1 - \overline{u})\, Y = \overline{u} Y^{\nu/\Delta_s} \left(1 + \frac{\Lambda^2}{\kappa^2}\right)^{1/2}, \qquad (3.134)$$

with $\kappa^2 = 2c_t \left|\Delta\widetilde{T}\right| \mathcal{T}$ for two phase region where κ is a measure of a distance from the critical point and related to the inverse correlation length. The explicit solution[45] for the rescaled order parameter M along the two phase boundary is given by

$$M^2 = (\Delta\widetilde{\rho})^2 = \frac{6 c_t t}{u^* \overline{u} \Lambda} Y^{(2\beta-1)/\Delta_s}. \qquad (3.135)$$

In principle this crossover equation contains two major parameters, namely, Λ and c_t. However, as the cutoff wave number q_{D} for the critical fluctuations is of the same order as q_0 for molecular fluids, the dimensionless $\Lambda = q_{\mathrm{D}}/q_0$ will be of order unity.[99] Therefore, just as for the lattice gas model, we can take $\Lambda = 1$. By adjusting c_t, which is related to the strength of the intermolecular interactions, the effects of the critical fluctuations is studied. The classical equation is recovered when $c_t = 0$, which corresponds to weak long-range interactions. The increase of c_t means the increasingly shorter-ranged interactions. The coupling constant $\overline{u}$ may be calculated by $\overline{u} = \frac{u_0}{a_0^2} \frac{c_t^2}{u^* \Lambda}$.

The diameter is $\widetilde{\rho}_{\mathrm{d}} - 1 = a_3 \left(1 + a_3\right) \phi_1^2 + b_2 \phi_2$ and $\phi_2 = \Delta\widetilde{s} = \partial\Delta\widetilde{A}_{\mathrm{cr}}/\partial\Delta\widetilde{T}$. Substituting Eq. (3.135) into Eq. (3.129) and taking the first derivative with respect to $\Delta\widetilde{T}$, we get the $\Delta\widetilde{s}$ for the two-phase region. For the Van der Waals fluid, $a_3 = \frac{1}{4}$ and $b_2 = \frac{4}{45}$. We can separate $1 - \alpha$ and 2β term of the calculated diameter for
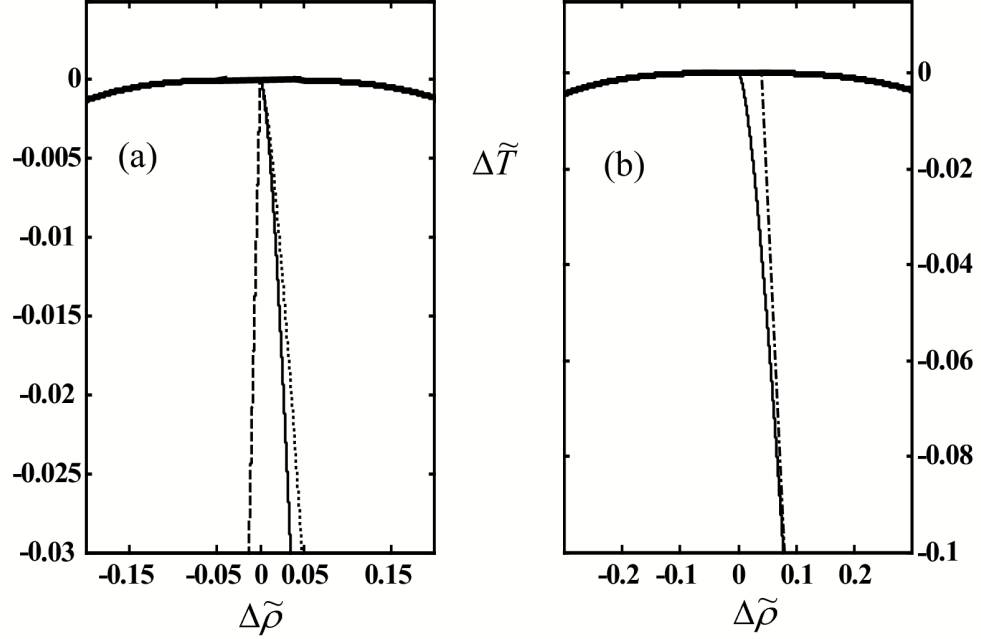
Figure 3.20: Crossover diameter in a van der Waals equation of state modified by fluctuations with a short interaction range $c_t = 0.5$. Thick solid curves are the phase boundary. (a) two contributions in the singular diameter (solid line): $1 - \alpha$ and linear term (dashed line) and 2β (dotted line); (b) Crossover between rectilinear diameter (dashed-dotted line) and singular diameter (solid line) in a broader critical region.

crossover Van der Waals fluids. In Fig. 3.20 the crossover behavior for $c_t = 0.5$ between rectilinear diameter and complete-scaling singular diameter is shown for the van der Waals equation of state renormalized by fluctuations.[99] A fluctuation shift in the van der Waals critical density is mainly controlled by the $\left|\Delta\hat{T}\right|^{2\beta}$ singularity since the van der Waals value of a_3 is relatively large $(a_3/(1 + a_3) = b_2/\hat{\mu}_{11} = 0.2)$.

CHAPTER 4

VAPOR-LIQUID ASYMMETRY IN REAL FLUIDS AND

SIMULATED MODELS

4.1 Separating the two singular sources of asymmetry in diameters

As a result of "complete scaling", the order parameter ϕ_1 in fluids is, in general, a nonlinear combination of density and entropy,

$$\phi_1 = \frac{\Delta\widetilde{\rho} + b_2\Delta\widetilde{s}}{1 + a_3\Delta\widetilde{\rho}}, \tag{4.1}$$

the weakly fluctuating scaling density ϕ_2 in first approximation is associated with the density of entropy only, $\phi_2 = \Delta\widetilde{s}$. There is an important thermodynamic conse-quence of "complete scaling" that can be checked experimentally. The "diameter" ρ_d should contain two non-analytical contributions, associated with the terms $a_3\Delta\widetilde{P}$ and $b_2\Delta\widetilde{\mu}$ in the scaling fields:

$$\widetilde{\rho}_\mathrm{d} - 1 = a_3\left(1 + a_3\right)\phi_1^2 + b_2\phi_2 + \ldots$$

$$= D_2\left|\Delta\widetilde{T}\right|^{2\beta} + D_1\left|\Delta\widetilde{T}\right|^{1-\alpha} + D_0\left|\Delta\widetilde{T}\right| + \ldots \tag{4.2}$$

where $D_2 = a_3B_0^2/(1 + a_3)$ and $D_1 = b_2A_0^-/(1 - \alpha)$ with B_0 and A_0^- being the amplitudes in the asymptotic scaling power laws for the liquid/vapor densities, $\Delta\widetilde{\rho} = \pm B_0\left|\Delta\widetilde{T}\right|^\beta + \ldots$, and isochoric heat capacity in the two-phase region, $C_\mathrm{V}/R =$

$A_0^- \left| \Delta \widetilde{T} \right|^{-\alpha} + ...(A_0^- = A_0^+/0.523)$.[43] Note, since $2\beta < 1 - \alpha$, the term $D_2 \left| \Delta \widetilde{T} \right|^{2\beta}$ should dominate near the critical point . Experimental verification of complete scaling is a very challenging task. The nonanalytical contributions in the "diameter" are usually not large enough to be separated unambiguously. Attempts to fit some experimental and simulational data to Eq. (4.2) showed very poor conversions,[21, 82] mainly because of a strong correlation between the linear and $D_1 \left| \Delta \widetilde{T} \right|^{1-\alpha}$ terms. As shown in Fig. 4.1, the fitting to only $\left| \Delta \widetilde{T} \right|^{1-\alpha}$ and linear term (dot curve) or only $\left| \Delta \widetilde{T} \right|^{2\beta}$ term (dash curve) cannot yield a good description of the experimental data since the systematic variation is very clear. However, it is clear that $\left| \Delta \widetilde{T} \right|^{2\beta}$ term plays a crucial role in describing the diameter of vapor-liquid coexistence curve in SF_6 near the critical point as the dashed curve in Fig. 4.1 qualitatively catches the singularity near the critical point, while the dot curve is almost linear. The circles in Fig. 4.1 represent the experimental data obtained by Weiner *et al.*.[79]

The power law with the first correction to scaling to describe the heat capacity is

$$C_\mathrm{V} = A_0^- \left| \Delta \widetilde{T} \right|^{-\alpha} + A_1^- \left| \Delta \widetilde{T} \right|^{-\alpha+\Delta_\mathrm{s}} + B \left| \Delta \widetilde{T} \right|, \tag{4.3}$$

where $B = (B_\mathrm{cr} + B_\mathrm{ideal})$. B_cr is the so-called "critical background" that is induced by the critical fluctuation and B_ideal is the ideal-gas background that represents the value of the specific heat far from the critical point.[86] However, since the diameter can be obtained from the equation of state in terms of P, V and T, the ideal-gas background is irrelevant. Therefore, only the fluctuation-induced modification of the background specific heat capacity B_cr needs to be considered.
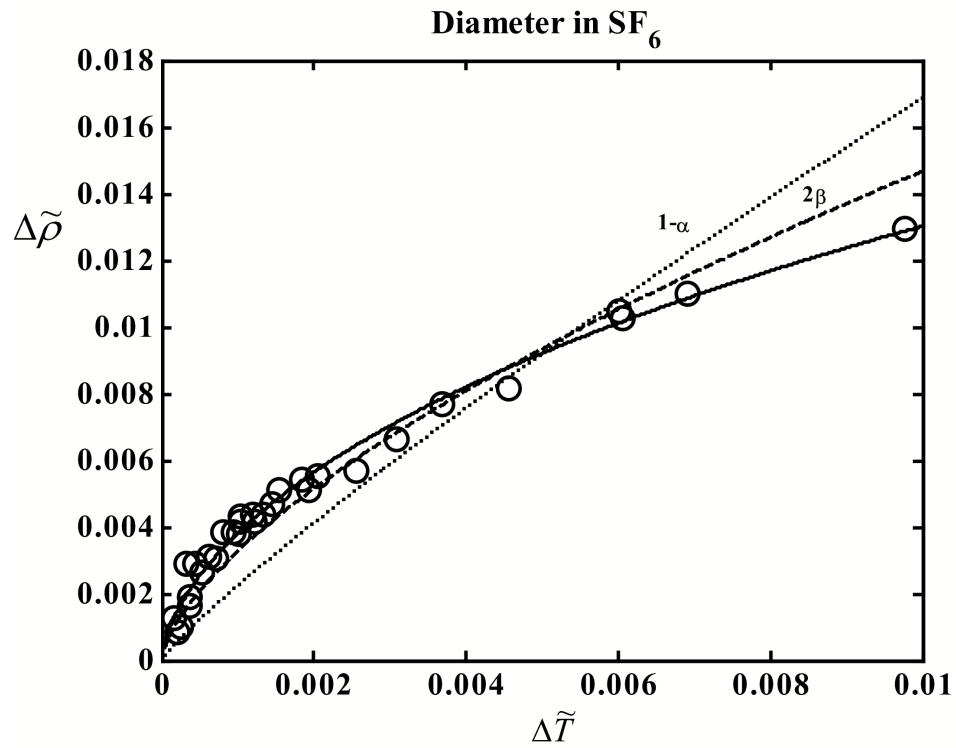
Figure 4.1: The liquid-vapor coexistence curve of SF$_6$. The circles indicate experimental data of Weiner *et al.*[79] Curves: solid - fit to Eq. (4.2), dashed - fit to only 2β term, dotted - fit to only $1 - \alpha$ and linear terms. Heat-capacity source.[89, 88]

Now we are ready to determine the two asymmetry coefficients, a_3 and b_2, and to prove conclusively the validity of "complete scaling" by combining accurate experimental and simulational vapor-liquid coexistence and heat-capacity data. We have exploited the fact that the coefficients D_1 and D_0 in Eq. (4.2) are actually not independent. The weakly fluctuation scaling density is the critical part of the entropy density. Neglecting the higher-order term $A_1^- \left|\Delta\widetilde{T}\right|^{1-\alpha+\Delta_s}$ in the two-phase region at average density $\rho = \rho_c$

$$\phi_2 = \int \frac{\Delta C_V}{RT} dT = -\frac{A_0^-}{(1-\alpha)R} \left|\Delta\widetilde{T}\right|^{1-\alpha} + \frac{B_{cr}}{R} \left|\Delta\widetilde{T}\right|, \qquad (4.4)$$

where ΔC_V is the critical part of the isochoric heat capacity, fluctuation-induced analytical part of entropy. The critical background can be obtained theoretically[46] and by analyzing heat-capacity data. If $D_0 = -B_{cr}$ is known, Eq. (4.2) becomes

$$\widetilde{\rho}_d - 1 = D_2 \left|\Delta\widetilde{T}\right|^{2\beta} + D_1 \left(-\frac{A_0^-}{(1-\alpha)R} \left|\Delta\widetilde{T}\right|^{1-\alpha} + \frac{B_{cr}}{R} \left|\Delta\widetilde{T}\right|\right), \qquad (4.5)$$

with only two adjustable coefficients, D_1 and D_2. Moreover, a_3 and b_2 may be obtained by the simple relations

$$\frac{a_3}{1+a_3} = \frac{D_2}{B_0^2}, \quad b_2 = D_1. \qquad (4.6)$$

94

4.2 Asymmetry coefficients in real fluids and simulated models

We have examined a number of systems, real fluids, including several hydrocarbons, and simulated models, such as the hard-core square-well (HCSW) fluid and the restricted primitive model electrolyte (RPM), for which we could find coexistence data in the range $\left|\Delta\widetilde{T}\right| < 0.01$. In this range the terms of higher-order than linear in Eq. (4.2) are within experimental errors. Experimental data closer than $\left|\Delta\widetilde{T}\right| < 10^{-4}$ were avoided as they might be affected by errors in ρ_c and T_c and by other factors, such as gravity, impurities, *etc.*. For all systems studied we have been able to obtain reliable values of B_cr and to conclusively separate two singular contributions to the diameter. Tables 4.1 and 4.2 list all the parameters needed in the fitting and the fitting results. Note, the HCSW fluids studied here consist of hard spheres of diameter d with attractive square wells of depth ϵ and interaction ranges $1.5d$.[97] The RPM electrolyte consists of an equal number of positive and negative ions with hard-core diameter d.[97] The ions are of charges $\pm q_0$ and interact with each other via the Coulomb potential, $\varphi\left(r\right) = \pm q_0^2/Dr$, where r is the interparticle distance and D is the dielectric constant of medium. The critical parameters listed in Tables 4.1 for HCSW and RPM have been made dimensionless by $\rho_\mathrm{c}^* = \rho_\mathrm{c}d^3$ and $T_\mathrm{c}^* = k_\mathrm{B}T_\mathrm{c}/\epsilon$ (HCSW) and $T_\mathrm{c}^* = k_\mathrm{B}T_\mathrm{c}Dd/q_0^2$ (RPM), where k_B is the Boltzmann constant.

It is very difficult to obtain the heat-capacity data within the critical region $\left|\Delta\widetilde{T}\right| < 10^{-4}$ for all the fluids we have studied. Therefore, we have tried three ways to obtain A_0^-. For methane, ethane, pentane and heptane, we use the unpublished
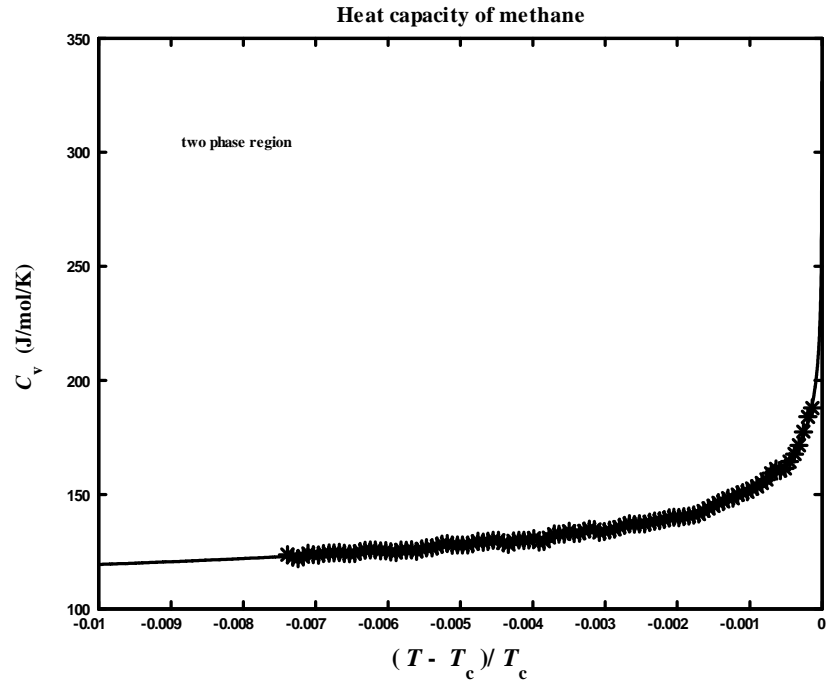
Figure 4.2: Heat-capacity data of methane in two-phase region.[98] The solid line is the fitting of Eq. (4.3).
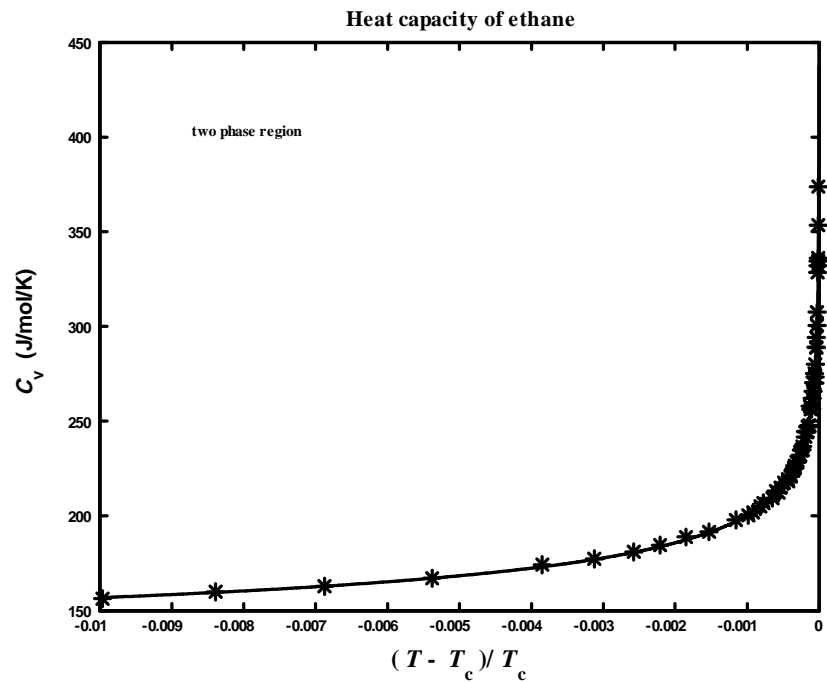
Figure 4.3: Heat-capacity data of ethane in two-phase region.[98] The solid line is the fitting of Eq. (4.3).

Fluids	T_c (K)	ρ_c $\left(\frac{\text{mol}}{\text{dm}^3}\right)$	A_0^- $\left(\frac{\text{J}}{\text{mol·K}}\right)$	A_1^- $\left(\frac{\text{J}}{\text{mol·K}}\right)$	B_{cr} $\left(\frac{\text{J}}{\text{mol·K}}\right)$	B_0	10σ
HD[17]	35.957	16.07	65.00		-30.00	1.358	0.03
neon[17]	44.479	23.97	70.00		-30.00	1.497	0.04
methane[91]	190.551	10.14	74.54	35.95	-29.62	1.551	0.05
nitrogen[17]	126.214	11.20	78.19	0	-28.63	1.565	0.03
ethene[17]	282.377	7.665	90.00		-57.70	1.642	0.05
ethane[17]	305.363	6.851	98.34	35.98	-57.70	1.649	0.04
HCSW[97]	1.218*	0.3076*	68.51	0	-51.63	1.926	0.02
RPM[97]	0.0507*	0.0760*	96.60	0	-40.98	3.635	0.01
water[95]	647.096	17.84	116.4	0	-32.00	2.035	0.04
pentane[92, 93]	469.610	3.204	157.0	406.8	-183.6	1.776	0.08
SF$_6$[79]	318.707	5.012	143.1	0	-31.16	1.733	0.03
F113[90]	486.968	3.026	165.0		-30.00	1.841	0.04
heptane[94]	539.860	2.318	187.7	97.78	-152.8	1.843	0.09

Table 4.1: Critical parameters, heat-capacity coefficients and amplitudes for various fluids. Note: * means that the data are dimensionless.

heat-capacity data from Abdulagatov and coworkers.[98] They have been fitted by Eq. (4.3) to obtain A_0^- and B. Figs. 4.2 and 4.3 show the heat-capacity data and fitting results for methane and ethane. The A_0^- and B for SF$_6$, water and nitrogen have been obtained from the literature.[89, 85, 95] By plotting A_0^- as a function of the critical density ρ_c for all A_0^- obtained from experimental data and then by interpolating, we obtain A_0^- for HD, neon, ethene and Freon113 due to the two-scale factor of universality[2] $A_0^+ \rho_c \left(\xi_0^+\right)^3 R^{-1} = 0.171$ where ξ_0^+ is treated approximately as a constant. A_0^- of HCSW and RPM are calculated from three-scale factor of universality[2] $A_0^+ \Gamma_0^+ / B_0^2 = 0.06$ where Γ_0^+ and B_0 are obtained from reference papers.[97, 96] For those fluids we have experimental data for the heat capacity, B_{cr} may be obtained by $B_{\text{cr}} = B - B_{\text{ideal}}$, where B_{ideal} may be calculated by well known formula and coefficients.[75] For most other fluids $B_{\text{cr}} = z_0 R \nu / (\alpha \overline{u} \Lambda)$ is employed to calculate the approximate value of B_{cr} by using $z_0 \simeq 0.3$, $\overline{u} = 0.5$ and $\Lambda = 1$.[44] Since

Fluids	ρ^*	D_2	D_1	a_3	b_2	$10^3\sigma$
HD[17]	0.3469	-0.0237	-0.0593	-0.0127	-0.0593	0.03
neon[17]	0.3221	-0.0404	-0.0683	-0.0177	-0.0683	0.03
methane[91]	0.3025	-0.0586	-0.0730	-0.0238	-0.0730	0.08
nitrogen[17]	0.2884	-0.0442	-0.0701	-0.0177	-0.0701	0.04
ethene[17]	0.2506	-0.0094	-0.0745	-0.0035	-0.0745	0.28
ethane[17]	0.2293	0.0038	-0.0603	0.0014	-0.0603	0.41
HCSW[97]	0.3140	0.0306	-0.0529	0.0083	-0.0529	0.77
RPM[97]	0.1479	1.5876	-0.483	0.137	-0.483	0.51
water[95]	0.1861	0.2361	-0.0482	0.0618	-0.0482	0.45
pentane[92, 93]	0.1436	0.3136	0.0207	0.110	0.0207	1.00
SF_6[79]	0.1576	0.4607	0.0351	0.181	0.0351	0.40
F113[90]	0.1367	0.6074	0.0483	0.218	0.0483	0.53
heptane[94]	0.1201	0.9156	0.0941	0.369	0.0941	1.60

Table 4.2: Asymmetry parameters for fluids

the results usually are in the range of 30 J/(mol·K)$< B_{cr} <$ 50 J/(mol·K), we just

take $B_{cr} = 30$ J/(mol·K).

The fluids we have studied may be classified into three types, (1) $a_3 < 0$

and $b_2 < 0$, (2) $a_3 > 0$ and $b_2 < 0$, and (3) $a_3 > 0$ and $b_2 > 0$. This results is

similar to our results for the Flory-Huggins model plus three-body interactions in

the previous chapter. When a_3 and b_2 are both small negative numbers, $i.e.$ $a_3 < 0$

and $b_2 < 0$, such as HD, neon, methane, nitrogen and ethene whose molecular

volume is very small, the contributions to diameters from entropy are positive while

the contributions of 2β terms are negative. As shown in Figs. 4.4, 4.5, 4.6, 4.7 and

4.8, the diameters produced by only the entropy have the same direction as that of

the actual diameters, while the diameters produced by 2β term have the opposite

direction. The compensation of the two contributions produces diameters which are

almost rectilinear. When $a_3 > 0$ and $b_2 < 0$, both of these two contributions to the

diameters have the same inclination as that of the actual diameters and their sum

constructs the full diameters. As shown in Figs. 4.9 and 4.10, in ethane and HCSW, contributions from the entropy are more important than those from 2β term. In RPM and water, the results are opposite, although the two contributions are very close, as shown in Figs. 4.11 and 4.12. For fluids with large molecular volumes, a_3 and b_2 are both positive. Notice that the values of a_3 are relatively large, in general > 0.1, while the value of b_2 are small compared to a_3, here in general < 0.1. In this case, the 2β term yields a large positive contribution to the actual diameter, while the terms from the entropy are small and negative. The net result of these two kinds of contributions is an actual diameter with an appreciable curvature near the critical point, as shown in Figs. 4.13, 4.14, 4.15 and 4.16.

From the above analysis, it is clear that there exist appreciable singularities in diameters of fluids with large molecular volumes, and that these singularities can only be described by a term proportional to $\left|\Delta\widetilde{T}\right|^{2\beta}$. This means they have relatively large and positive a_3. For fluids with relatively small molecular volumes, the diameters are almost rectilinear. The contributions from the entropy play a crucial role in describing them, which means b_2 must be negative and a_3 should also be less than zero but with a small absolute value. There exists a transition region in which neither of these two contributions is dominant.

The quality of the fits[74] is assessed by the chi-square χ_ν^2

$$\chi_\nu^2 = \frac{1}{N-M}\frac{\sum\left(y_i - \widehat{y_i}\right)^2}{\overline{z}^2},\tag{4.7}$$

where the y_i are the experimental data, $\widehat{y_i}$ are values of calculation, N is the number

99
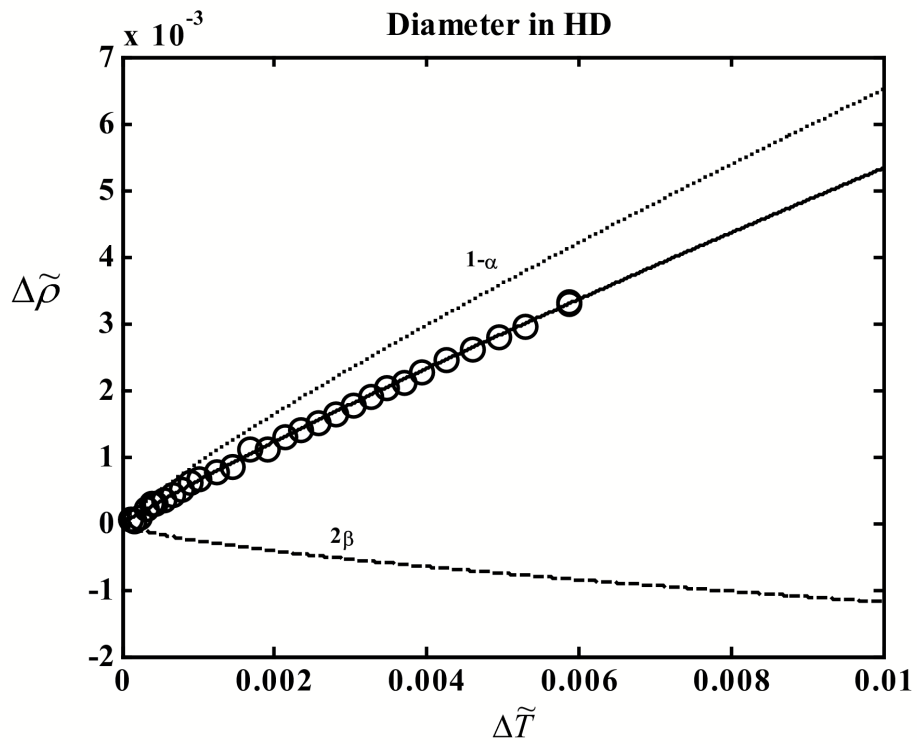
Figure 4.4: The liquid-vapor coexistence curve of HD. The circles indicate experimental data of Pestak *et al.*[17] Curves: solid - fit to Eq. (4.2), dashed -2β term, dotted - $1 - \alpha$ and linear terms. Heat-capacity coefficients are from interplation.
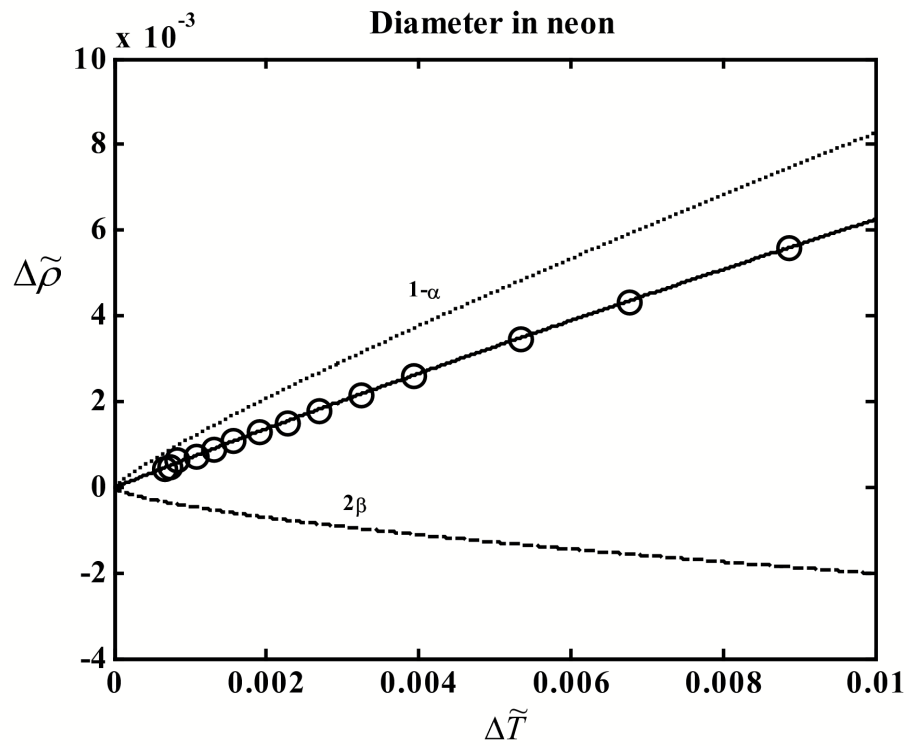
Figure 4.5: The liquid-vapor coexistence curve of neon. The circles indicate experimental data of Pestak *et al.*[17] Curves: solid - fit to Eq. (4.2), dashed -2β term, dotted - $1 - \alpha$ and linear terms. Heat-capacity coefficients are from interplation.
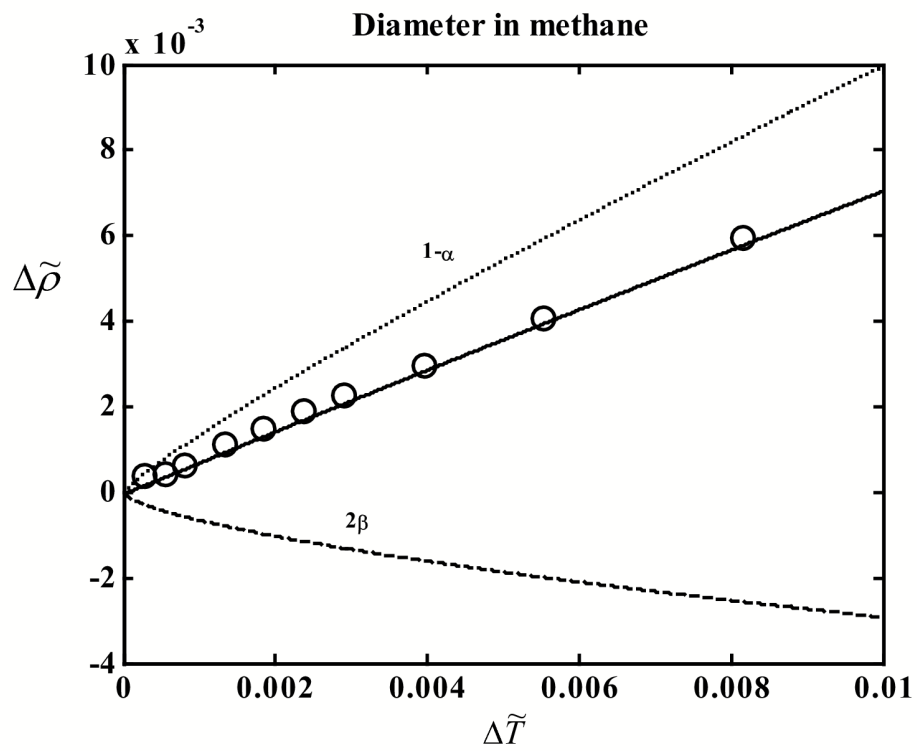
Figure 4.6: The liquid-vapor coexistence curve of methane. The circles indicate experimental data.[91] Curves: solid - fit to Eq. (4.2), dashed -2β term, dotted - $1-\alpha$ and linear terms. Heat-capacity source.[98]
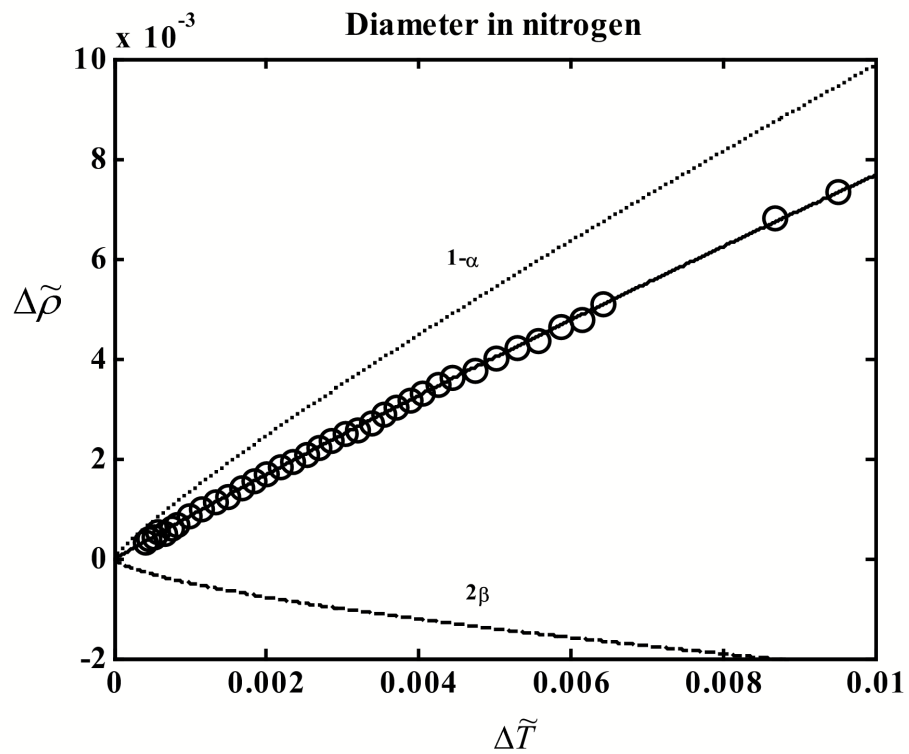
Figure 4.7: The liquid-vapor coexistence curve of nitrogen. The circles indicate experimental data of Pestak *et al.*[17] Curves: solid - fit to Eq. (4.2), dashed -2β term, dotted - $1 - \alpha$ and linear terms. Heat-capacity source.[85]
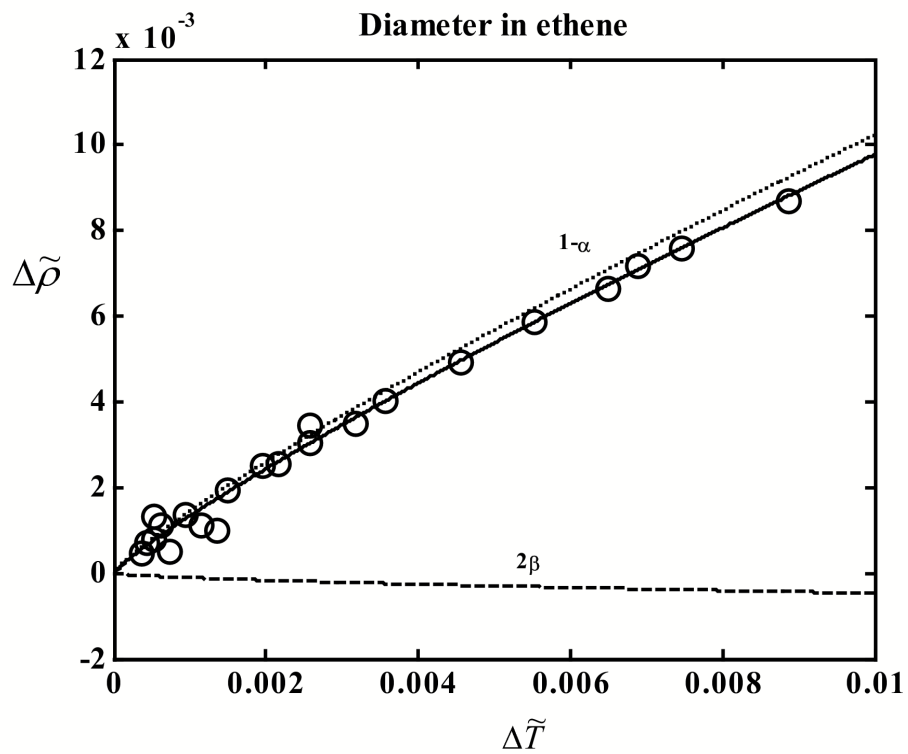
Figure 4.8: The liquid-vapor coexistence curve of ethene. The circles indicate experimental data of Pestak *et al.*[17] Curves: solid - fit to Eq. (4.2), dashed -2β term, dotted - $1 - \alpha$ and linear terms. Heat-capacity coefficients are from interplation.

Diameter in ethane
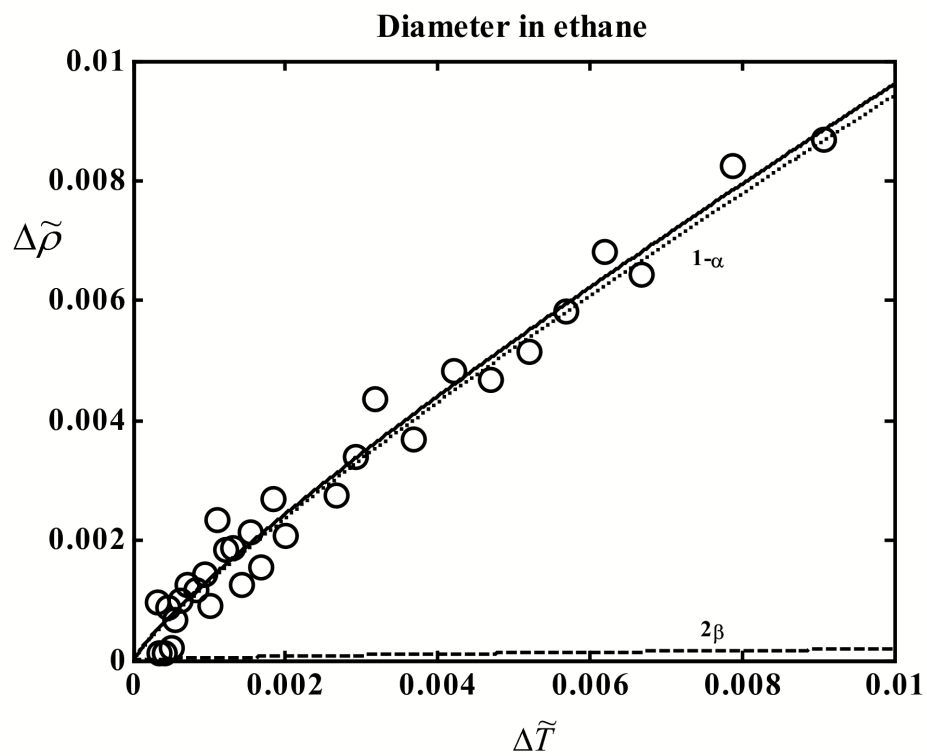
Figure 4.9: The liquid-vapor coexistence curve of ethane. The circles indicate experimental data of Pestak *et al.*[17] Curves: solid - fit to Eq. (4.2), dashed -2β term, dotted - 1 − α and linear terms. Heat-capacity source.[98]
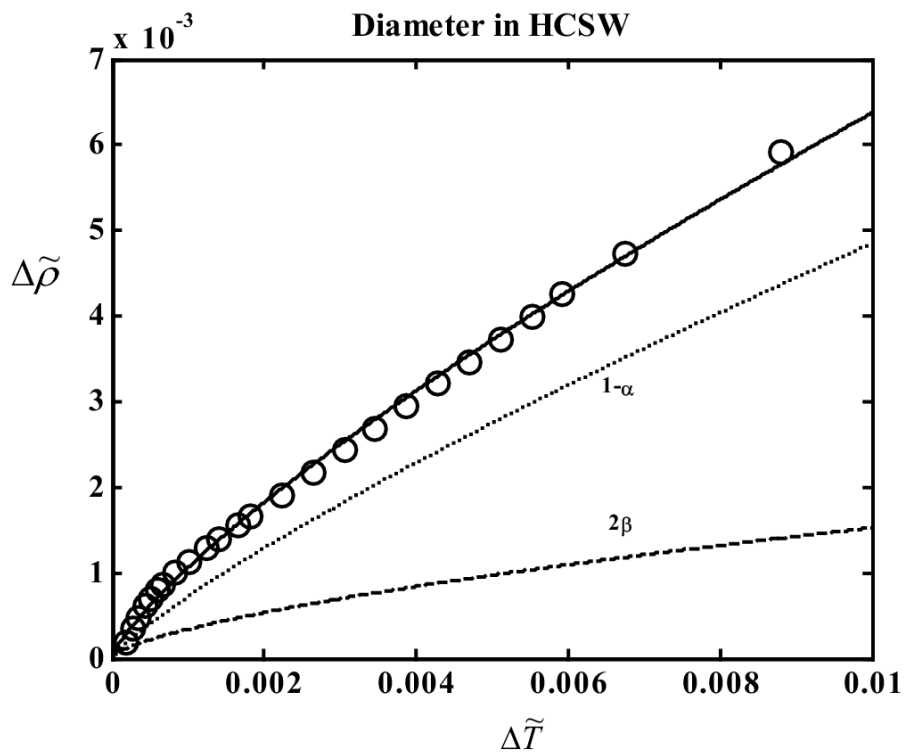
Figure 4.10: The liquid-vapor coexistence curve of HCSW. The circles indicate experimental data.[97] Curves: solid - fit to Eq. (4.2), dashed -2β term, dotted - $1-\alpha$ and linear terms. Heat-capacity source.[97]

106
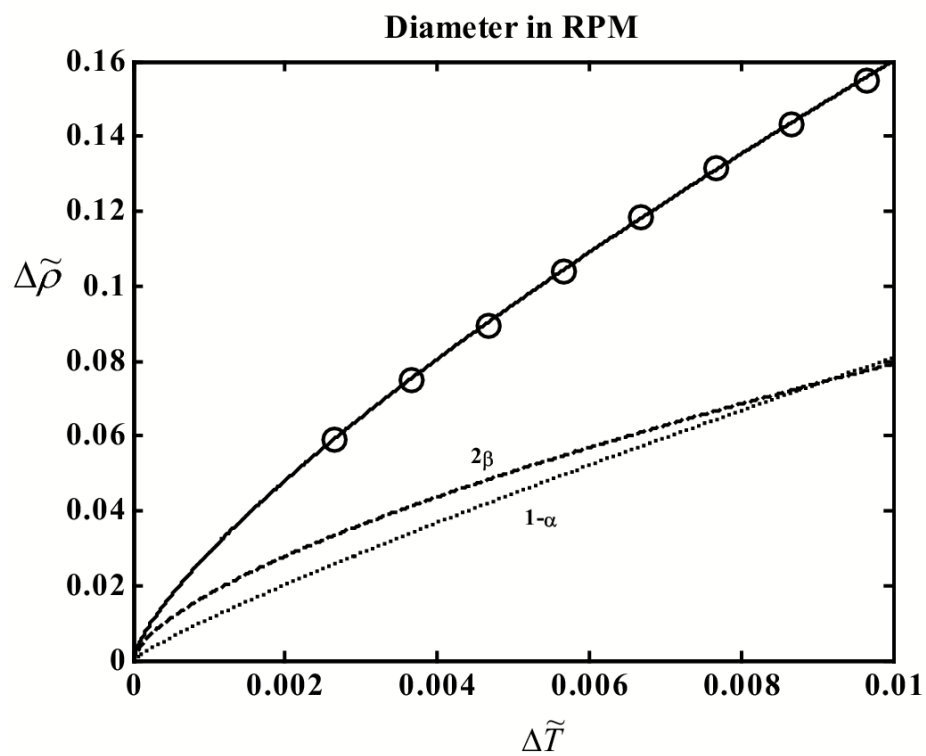
Figure 4.11: The liquid-vapor coexistence curve of RPM. The circles indicate experimental data.[97] Curves: solid - fit to Eq. (4.2), dashed -2β term, dotted - $1 - \alpha$ and linear terms. Heat-capacity source.[96]
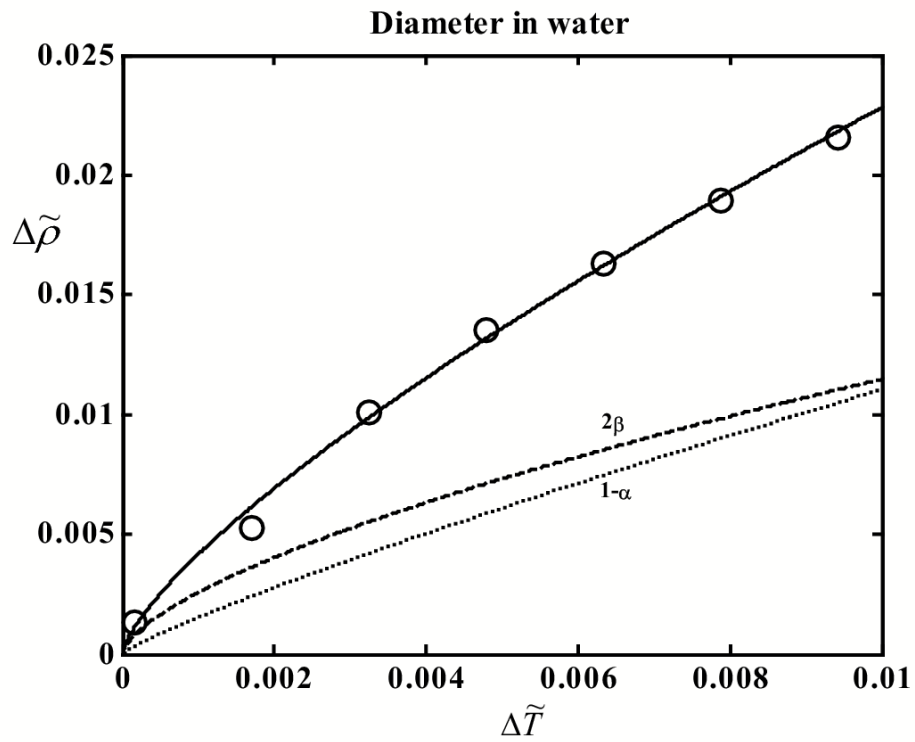
Figure 4.12: The liquid-vapor coexistence curve of water. The circles indicate experimental data.[95] Curves: solid - fit to Eq. (4.2), dashed -2β term, dotted - $1 - \alpha$ and linear terms. Heat-capacity source.[95]
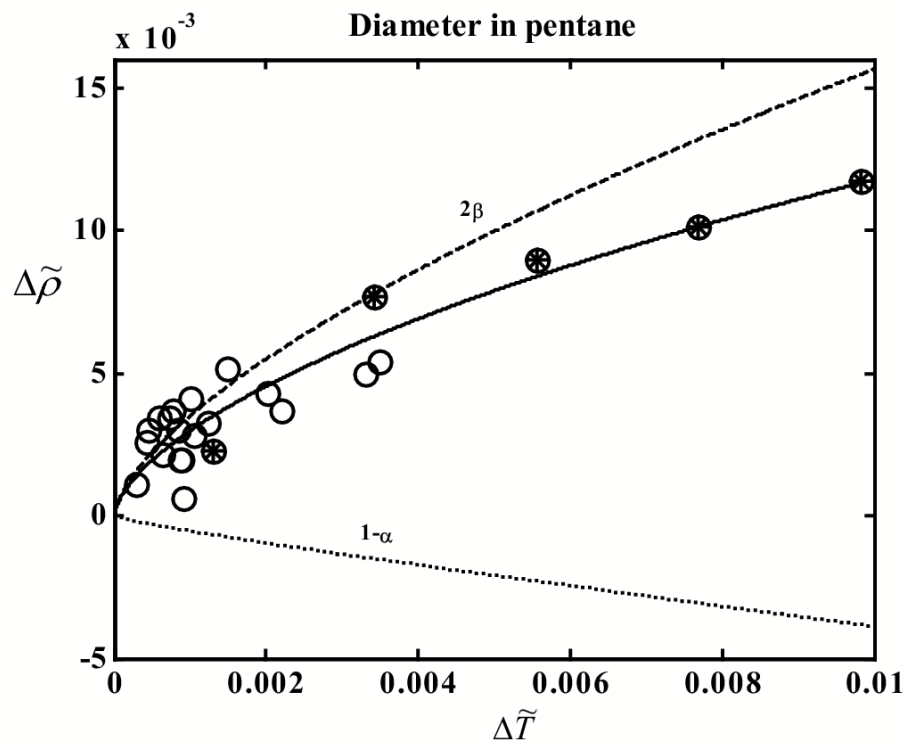
Figure 4.13: The liquid-vapor coexistence curve of pentane. The circles indicate experimental data.[92, 93] Curves: solid - fit to Eq. (4.2), dashed -2β term, dotted - $1 - \alpha$ and linear terms. Heat-capacity source.[98]
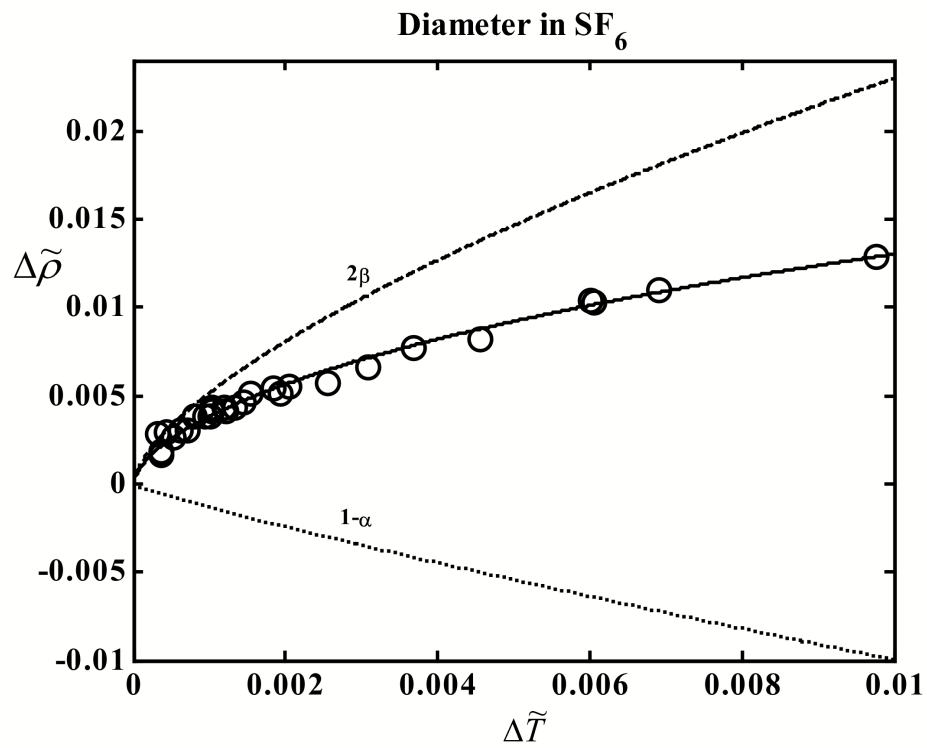
Figure 4.14: The liquid-vapor coexistence curve of SF_6. The circles indicate experimental data of Weiner *et al.*[79] Curves: solid - fit to Eq. (4.2), dashed -2β term, dotted - $1 - \alpha$ and linear terms. Heat-capacity source.[89, 88]

Diameter in Freon113
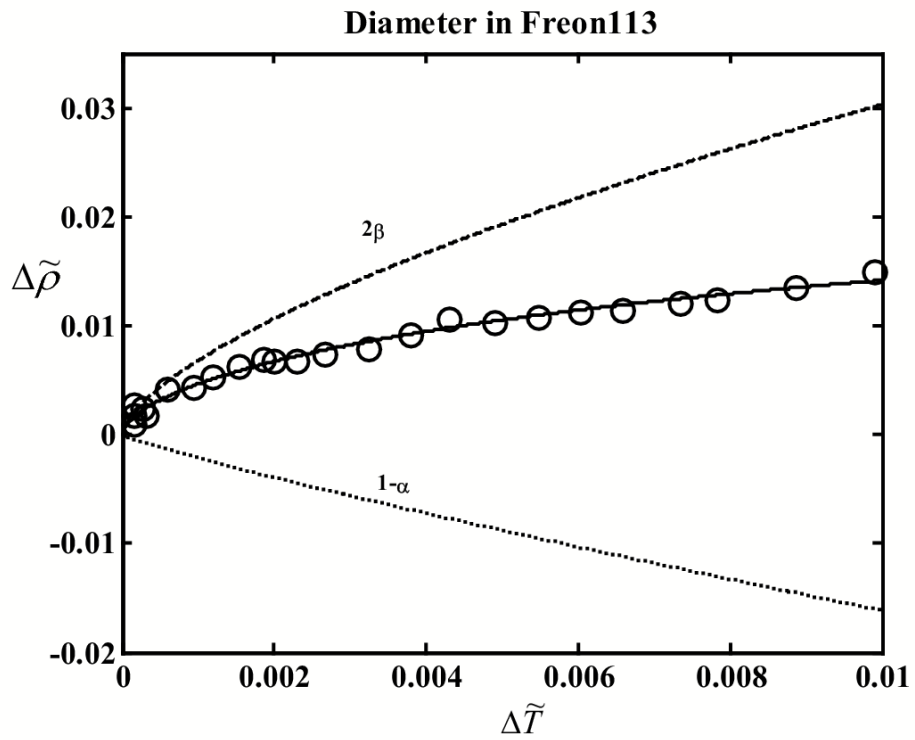
Figure 4.15: The liquid-vapor coexistence curve of Freon113. The circles indicate experimental data.[90] Curves: solid - fit to Eq. (4.2), dashed -2β term, dotted - $1-\alpha$ and linear terms. Heat-capacity coefficients are from interplation.

111
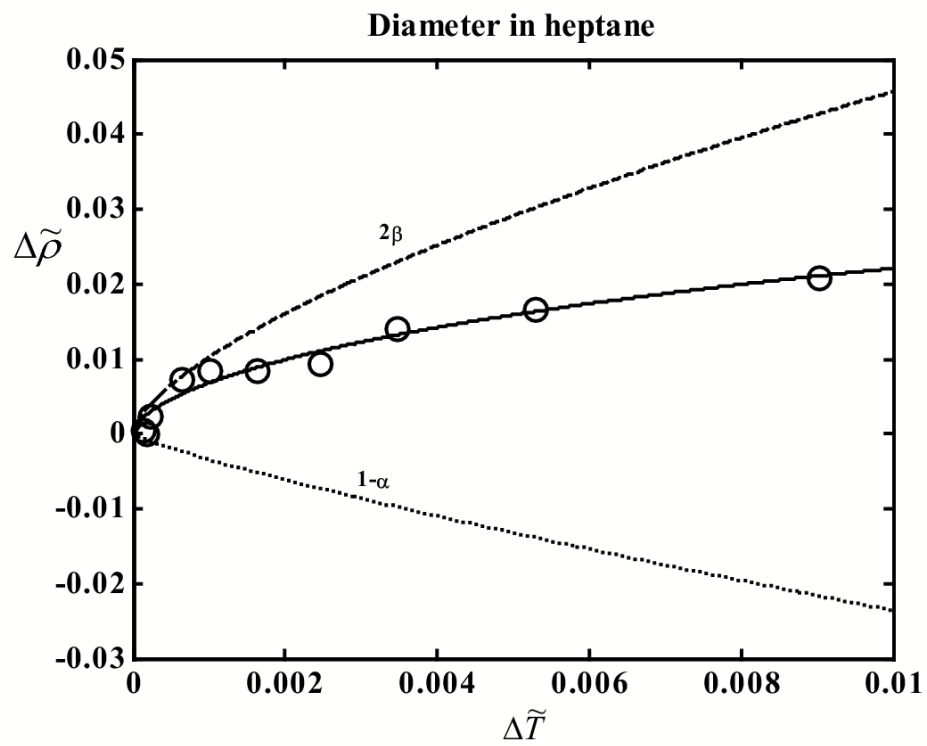
Figure 4.16: The liquid-vapor coexistence curve of heptane. The circles indicate experimental data.[94] Curves: solid - fit to Eq. (4.2), dashed -2β term, dotted - $1-\alpha$ and linear terms. Heat-capacity source.[98]

of experimental data, M is the number of fitted parameters, and $\bar{z}$ is the average standard deviation of the experimental values. If the fitting function is a good approximation to the parent function, the value of χ_ν^2 should be approximately unity. If the fitting function is not appropriate for describing the data, one has $\chi_\nu^2 > 1$. Since it is difficult to find $\bar{z}$ in the original paper, we just assume $\bar{z} = 1$. σ is used to measure the accuracy of our fit.

$$\sigma^2 = \frac{1}{N - M} \sum (y_i - \widehat{y}_i)^2 , \tag{4.8}$$

Fig. 4.17 shows the residual plots from fits of the diameters of (a) HD and (b) Freon113. The fitting function is Eq. (4.5).

4.3   Discussion

As early as in 1930's Eyring[80, 81] essentially explained the existence of the law of rectilinear diameter and discussed the origination of the slight inclination in the vapor-liquid diameter. In his picture Eyring treated the cell walls in the lattice-gas model as physical walls made up of other molecules. Since the lattice produced by the molecular structure has its own thermal-expansion coefficient, it will thermally expand as the temperature increases. Therefore, the higher the temperature, the lower the average density of the coexisting phases, which results in a slight inclination in the right direction like that in the real fluids.

In 1972 Widom[16] gave a comprehensive review of vapor-liquid asymmetry and the nature of the critical point. By introducing the penetrable-sphere model,
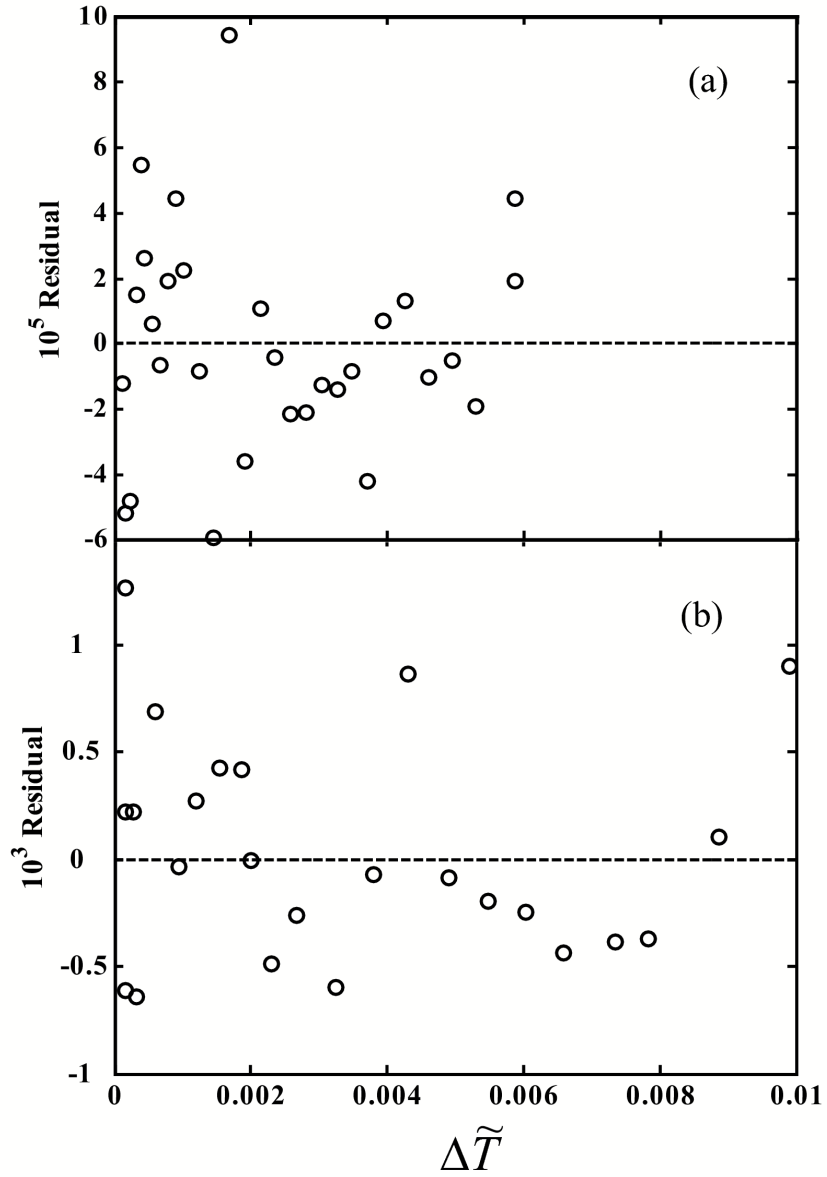
Figure 4.17: Residual plots from fits of the diameters of (a) HD and (b) Freon113. The fitting function is Eq. (4.5).

he proved that the law of rectilinear diameter is to be violated and a singular term $\propto \left| \Delta \widetilde{T} \right|^{1-\alpha}$, which is related to the entropy, must appear. Pestak *et al.*[17] studied the experimental coexistence-curve diameters near the critical point of SF_6, C_2H_6, C_2H_4, N_2 and Ne in 1987. They found that the slope of the diameter far from the critical point, the amplitude of singular deviation from the law of rectilinear diameter within the critical region, and order-parameter amplitude, all increase systematically with T_c and are all proportional to the critical polarizability product, which is a dimensionless measure of the relative importance of three- versus two-body interactions. They also have suggested that three-body interactions play an important role in those properties relevant to the vapor-liquid asymmetry of pure fluids. In their work the possibility of incorporating the effects of three-body interactions into an effective pair potential is explored, in the critical region which is equivalent to the thermal scaling field with a mixing of physical variables temperature and chemical potential.[17] Ultimately it leads to a breakdown in the classical law of the rectilinear diameter. Furthermore, the magnitude of the field mixing and the diameter anomaly scales with the product of the particle polarizability and the critical number density.[17] However, after studying the amplitude of the rectilinear diameter for a large number of normal fluids in 1990, Singh and Pitzer[18] found that the diameter slope shows a linear dependence on the acentric factor and conclude that the shape of the pair potential is the primary factor in determining the slope of the diameter rather than the relative strength of three-body interactions. They also mentioned that close to the critical point the shape of the two-body potential has the equally logical effect on the increase of the amplitude D_1 of $1 - \alpha$ term. A new

term $\propto \left|\Delta\widetilde{T}\right|^{2\beta}$ is found in the expression of diameters recently as a result of the "complete scaling" developed by Fisher and Orkoulas,[19, 21] The new singular term actually dominates the earlier $\left|\Delta\widetilde{T}\right|^{1-\alpha}$ term near the critical point since $2\beta < 1-\alpha$. It will be an interesting task to explore the origin of these two singular terms.

We have studied a number of fluids in this chapter. In the diameters of some fluids, such as SF_6, $C_2F_3Cl_3$, $n\text{-}C_5H_{12}$ and $n\text{-}C_7H_{16}$, the $\left|\Delta\widetilde{T}\right|^{2\beta}$ term dominates (a_3 is relatively large and positive) while in many other fluids, such as HD, Ne, N_2, and CH_4, the two singular contributions in diameter largely compensate each other (a_3 is small and negative), creating an illusion of rectilinear diameter even close to the critical point. In Fig. 4.18 the two asymmetry coefficients are plotted against the dimensionless density ρ^* defined as $\rho^* = \rho_c(8\xi_0^3)$, where ξ_0 is the amplitude of the correlation length (representing the range of interactions) obtained from the heat-capacity amplitude A_0^+ through the two-scale factor of universality, $A_0^+ \rho_c \xi_0^3 = 0.171.$[43] A general trend in the two sources of asymmetry is clear: the $\left|\Delta\widetilde{T}\right|^{2\beta}$ singularity, predicted by complete scaling, is a dominant contribution into the singular diameter if the molecular size/interaction-range ratio is large. Apparently, ξ_0 does not change much with increase of molecular volume. Thus, we hypothesize that when the molecular size is large, the $\left|\Delta\widetilde{T}\right|^{2\beta}$ singularity may be dominant.

According to "complete scaling", asymmetry in fluid criticality originates from the coupling between density and entropy fluctuations which produces $1-\alpha$ term in coexistence-curve diameter and from the nonlinear coupling between density and volume fluctuations which produces 2β term in diameter. From Fig. 4.18, it

116
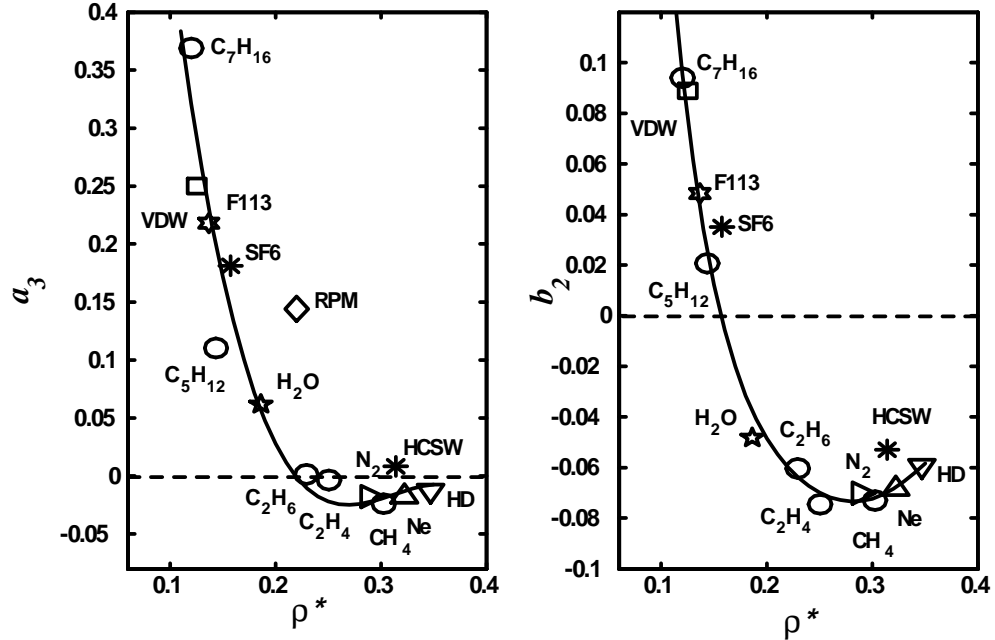
Figure 4.18: Complete-scaling asymmetry coefficients a_3 (a) and b_2 (b) *versus* reduced critical density $\rho^* = \rho_c(8\xi_0^3)$. VDW is a modified-by-fluctuations van der Waals fluid[99] with a short interaction range ($R = (\rho^*)^{1/3} = 0.5$). HCSW is a simulated hard core square-well model.[82] For a simulated restrictive primitive model (RPM)[82] $a_3 = 0.14$ and $b_2 = -0.48$ with $\rho^* \simeq 0.22$. The solid curves are given as a guidance.

is clear that both 2β and $1 - \alpha$ terms depend strongly on the molecular volume.

Eyring's idea[80, 81] may give us some insight into this problem although it can not

be proved up to now. We may consider that the volume of lattice cells is the sum

of the molecular volume and the space between molecules. It is guessed that the

asymmetry from a_3 depends on the molecular volume, but that from b_2 depends

on the distance between molecules which is strongly related to the intermolecular

interactions (three-body or two-body).

CHAPTER 5

ASYMMETRY OF LIQUID-LIQUID PHASE EQUILIBRIA

Liquid-liquid phase equilibria in fluid mixtures are fascinating phenomena in thermodynamics that are also of great practical interest.[111, 112] As discussed in the previous chapter, Fisher and co-workers have shown that the most general formulation of such linear mixing for one-component fluids ("complete scaling") should also include a contribution from the pressure[19, 21]

$$h_1 = a_1 \Delta \widetilde{\mu} + a_2 \Delta \widetilde{T} + a_3 \Delta \widetilde{P}, \tag{5.1}$$

$$h_2 = b_1 \Delta \widetilde{T} + b_2 \Delta \widetilde{\mu} + b_3 \Delta \widetilde{P}. \tag{5.2}$$

The mixing of the physical fields into scaling fields in the form of Eqs. (5.1) and (5.2) means that all three physical fields are mixed into two independent scaling fields. The appropriate field-dependent thermodynamic potential $\Psi(h_1, h_2)$ is thus associated neither with the molar Gibbs energy μ nor with the density of the grand potential $-P$, but rather with a linear combination of both. As a result, the order parameter in one-component fluids is, in general, a nonlinear combination of density and entropy. The "diameter" of the vapor-liquid coexistence curve, which characterizes its asymmetry, contains two non-analytical contributions, associated with the terms $a_3 \Delta \widetilde{P}$ and $b_2 \Delta \widetilde{\mu}$ in the scaling fields

$$\widetilde{\rho}_{\mathrm{d}} = \frac{\rho_{\mathrm{l}} + \rho_{\mathrm{g}}}{2\rho_{\mathrm{c}}} = 1 + D_2 \left| \Delta \widetilde{T} \right|^{2\beta} + D_1 \left| \Delta \widetilde{T} \right|^{1-\alpha} + D_0 \left| \Delta \widetilde{T} \right|. \tag{5.3}$$

118

The leading $(2\beta < 1 - \alpha)$ nonanalytical term $D_2 \left| \Delta \widetilde{T} \right|^{2\beta}$ is absent in the conventional scaling formulation.

The generalization of "complete scaling" to binary fluids has been initially done by Cerdeiriña *et al.*[30] In this chapter we will analyze it further. A controversial issue of the proper definition of the order parameter in binary fluids will be clarified. A straightforward analogy between "incompressible" binary liquids mixtures and one-component fluids enables us to unambiguously confirm the validity of "complete scaling" by analyzing the coexisting curves of liquid solutions of nitrobenzene in various hydrocarbons (from n-pentane to n-hexadecane). Another consequence of "complete scaling" for binary mixtures, an effect that is analogous to the Yang-Yang anomaly in one-component fluids, is also elucidated.

5.1   Liquid-liquid critical phenomena

Let us consider the conventional scaling to study liquid-liquid critical phenomena first. To understand the thermodynamic behavior of fluids and fluid mixtures near critical points, one needs to distinguish between fields that are intensive thermodynamic properties and densities that are thermodynamic properties conjugate to the fields.[117, 62] Fields remain uniform in the two-phase region, while densities differ along the two sides of the phase boundary. The asymptotic critical behavior of the thermodynamic properties can be completely characterized in terms of two independent scaling fields, h_1 and h_2, that are analytic functions of the physical fields, such that at the critical point $h_1 = h_2 = 0$. The principle of isomorphic critical behavior asserts that $\Psi_{\mathrm{cr}}(h_1, h_2)$ is the same singular function for all fluids and fluid

mixtures. The variety of actual critical phase behavior, observed experimentally, is determined by the relation between the scaling fields h_1 and h_2 and the physical fields.[23, 4]

In one-component real fluids the physical fields are the pressure P, the temperature T and the chemical potential μ. The three fields are not independent but satisfy the differential relation

$$dP = sdT + \rho d\mu. \tag{5.4}$$

As we discussed in chapter 2, in traditional scaling the fields h_1 and h_2 are functions of the physical fields and in linear approximation[23, 4]

$$h_1 = a_1 \Delta\widetilde{\mu} + a_2 \Delta\widetilde{T}, \quad h_2 = b_1 \Delta\widetilde{T} + b_2 \Delta\widetilde{\mu}. \tag{5.5}$$

Thus, we have that $\Delta\widetilde{\rho}$ along the coexistence boundary will asymptotically vary as

$$\Delta\widetilde{\rho} = \phi_1 + b_2\phi_2 = \pm B_0 \left|\Delta\widetilde{T}\right|^{\beta} + B_a \left|\Delta\widetilde{T}\right|^{1-\alpha}, \tag{5.6}$$

Equation (5.6) contains the first asymptotic term of a so-called Wegner expansion.[6] The leading confluent singularity in the expansion is proportional to $|\Delta\widetilde{T}|^{\Delta_s}$, where Δ_s is a universal correction-to-scaling exponent.[57] In addition, there is a contribution from the regular analytic part of P^r in accordance with Eq. (2.26), yielding in first approximation a term in Eq. (5.6) that is proportional to $\Delta\widetilde{T}$. Thus in the next

120

approximation the expansion for $\Delta\widetilde{\rho}$ becomes[57, 118]

$$\Delta\widetilde{\rho} = \pm B_0 \left|\Delta\widetilde{T}\right|^{\beta} \left[1 + B_1 \left|\Delta\widetilde{T}\right|^{\Delta_s}\right] + B_a \left|\Delta\widetilde{T}\right|^{1-\alpha} + d_1\Delta\widetilde{T}. \tag{5.7}$$

where B_0, B_1, B_a, and d_1 are system-dependent coefficients.

For a binary liquid mixture we can identify the physical fields with the pressure P, the temperature T, the chemical potential μ_1 of the solvent and the difference $\mu_{\Delta 21} = \mu_2 - \mu_1$ between the chemical potential μ_2 of the solute and the chemical potential μ_1 of the solvent. These fields satisfy the differential relation,

$$d\mu_1 = -S_{\mathrm{m}} dT + V_{\mathrm{m}} dP - x_2 d\mu_{\Delta 21}. \tag{5.8}$$

For nearly incompressible liquid mixtures near a consolute point, we take P, T, and μ as the independent fields and μ_1 as the field-dependent potential. In the linear approximation, the scaling fields are

$$h_1 = a_0\Delta\widetilde{P} + a_1\Delta\widetilde{\mu}_{\Delta 21} + a_2\Delta\widetilde{T}, \quad h_2 = b_0\Delta\widetilde{P} + b_1\Delta\widetilde{T} + b_2\Delta\widetilde{\mu}_{\Delta 21}. \tag{5.9}$$

In this and in the subsequent section we consider liquid-liquid separation at a constant pressure P, so that $dP= 0$. Then the scaling fields reduce to

$$h_1 = a_1\Delta\widetilde{\mu}_{\Delta 21} + a_2\Delta\widetilde{T} , \quad h_2 = b_1\Delta\widetilde{T} + b_2\Delta\widetilde{\mu}_{\Delta 21}. \tag{5.10}$$

while at constant pressure

$$d\mu_1 = -S_\mathrm{m} dT - x_2 d\mu_{\Delta 21}. \tag{5.11}$$

Note that in binary liquids there exists a locus of critical consolute points as a function of the pressure. Hence, μ_c and T_c, as well as the coefficients a_1, a_2, b_1, b_2, will depend on the actual pressure P.

On comparing Eq. (5.11) with Eq. (5.4) and Eq. (5.10) with Eq. (5.5) we may conclude that μ_1 is analogous to the pressure P in a one-component fluid, that $\mu_{\Delta 21}$ is analogous to the molar Gibbs energy μ, and that the mole fraction $x_2 = -(\partial \mu_1/\partial \mu)_{T,P}$ is analogous to the density $\rho = (\partial P/\partial \mu)_T$ in a one-component fluid. If there is no confusion, to simplify we will take $x = x_2$. Hence, $\Delta x = x - x_\mathrm{c}$ has the same expansion, Eq. (5.7), along the liquid-liquid phase boundary of a binary liquid mixture (at constant pressure) as $\Delta \widetilde{\rho}$ along the vapor-liquid phase boundary in a one-component fluid

$$x = x_\mathrm{c} \pm B_0 \left| \Delta \widetilde{T} \right|^\beta \left[1 + B_1 \left| \Delta \widetilde{T} \right|^{\Delta_\mathrm{s}} \right] + B_\mathrm{a} \left| \Delta \widetilde{T} \right|^{1-\alpha} + d_1 \Delta \widetilde{T}. \tag{5.12}$$

There exists some ambiguity in the precise definition of the order parameter which we have here asymptotically identified with the mole fraction x. The choice of order parameter is affected by symmetry considerations. For instance, if in the case of one-component fluids we had selected T and P as the independent fields and the molar Gibbs energy μ as the field-dependent potential, we would have obtained the

122

molar volume as the asymptotic order parameter. While the volume does satisfy the same asymptotic power laws as the density, vapor-liquid symmetry considerations, confirmed by the lattice gas, clearly indicate that the density is the preferred order parameter.[43] Similarly, if one adopts in the case of binary mixtures μ_1, T and μ as the independent fields and the pressure P as the field-dependent potential and then takes the limit of nearly incompressible liquid mixtures, one finds the partial density ρx as the asymptotic order parameter.[23] Other possibilities are mass fraction or volume fraction. For the coexistence curves to be considered in the present chapter, we found that it made little difference whether the concentration is expressed in mass fractions or mole fractions.[28]

With known experimental values for the critical temperature T_c and the critical concentration x_c, Eq. (5.12) contains four system-dependent coefficients. Starting with the work of Greer,[119] the validity of Eq. (5.12) for the representation of coexistence curves of liquid mixtures, either with an UCST or a LCST, has been well established.[120, 121, 122, 123] As examples we show in Figs. (5.1) and (5.2) the coexistence curves of 3-methylpentane+nitroethane and of n-heptane+acetic anhydride, respectively. The values of the coefficients in Eq. (5.12) resulting from fits to the experimental data,[71, 72, 73] together with the standard deviations σ,[74] are listed in Table 5.1. The coefficients of the last two terms of Eq. (5.12) are strongly correlated, so that retaining only three terms in the expansion may be adequate in practice. However, since these terms have different physical origins (the term proportional to $|\Delta\widetilde{T}|^{1-\alpha}$ arising from the singular critical part of the order parameter and the term proportional $\Delta\widetilde{T}$ from the analytic background), it is conceptually

system	$T_{\mathrm{u}}(K)$	x_{u}	B_0	B_1	B_{a}	d_1	10σ
3-methylpentane + nitroethane[71, 72]	299.607	0.497	0.95	-0.25	0.51	-0.32	0.04
n-heptane + Acetic anhydride[73]	341.672	0.486	0.93	-0.52	1.05	-1.15	0.09

Table 5.1: Parameters for phase equilibrium in systems with an UCST

important to retain both terms in the subsequent extension of the theory to closed solubility loops in chapter 6. Equation (5.12) is an expansion around the critical point and has only a limited range of validity, but Figs. (5.1) and (5.2) indicate that the equation is adequate in the temperature range of the experimental data. If one wants to represent coexistence curves over much larger ranges of temperature, one needs to extend Eq. (5.12) into an equation that accounts for the crossover from fluctuation-induced singular behavior near the critical point to analytic behavior far away from the critical point, which will not be considered here. The two systems we examine here have relatively symmetric coexistence curves which may be described very well by Eq. (5.12). However, if strongly asymmetric systems are studied, they may require the "complete scaling" in order to characterize the large singularity of the diameters near the critical point.

5.2   "Complete scaling" and order parameter for binary fluids

Generalization of critical-point universality to binary fluids is known as the isomorphism principle.[2, 23, 24] This principle assumes that a variety of critical phenomena in binary fluids can be described in a universal way with two independent scaling fields, namely an "ordering" field h_1 and a "thermal" field h_2, and with a field-dependent thermodynamic potential, given by Eq. (2.27), just as in a one-
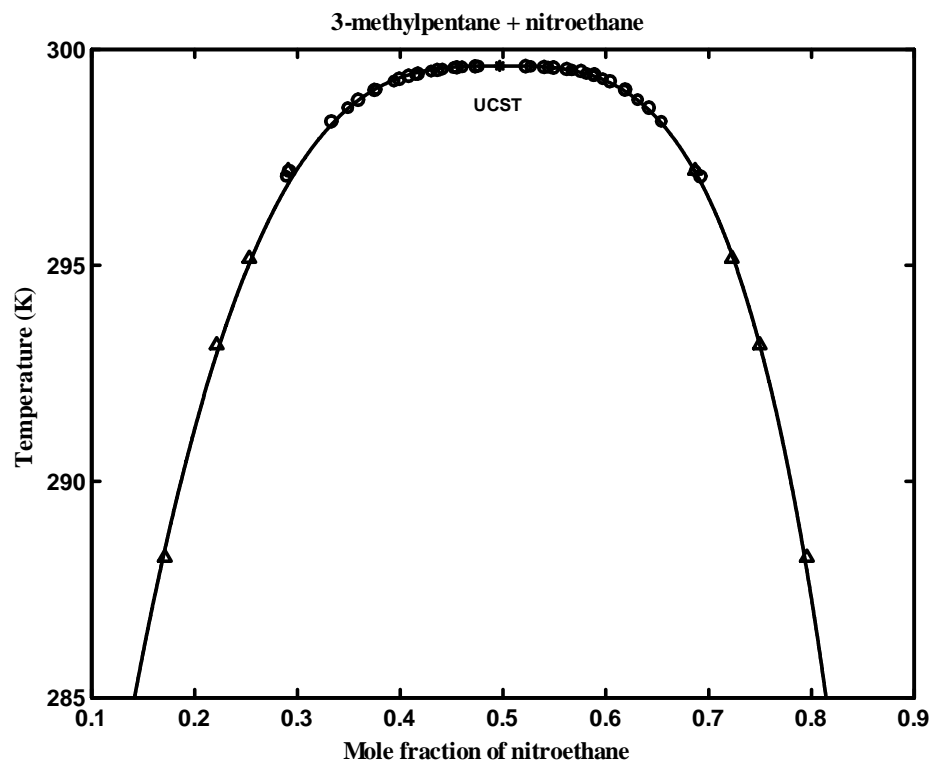
Figure 5.1: The coexistence curve of 3-methylpentane + nitroethane system. The circles and stars indicate experimental data of Wims *et al.*[71] and Khosla and Widom.[72] The solid curve is a fit to Eq. (5.12).
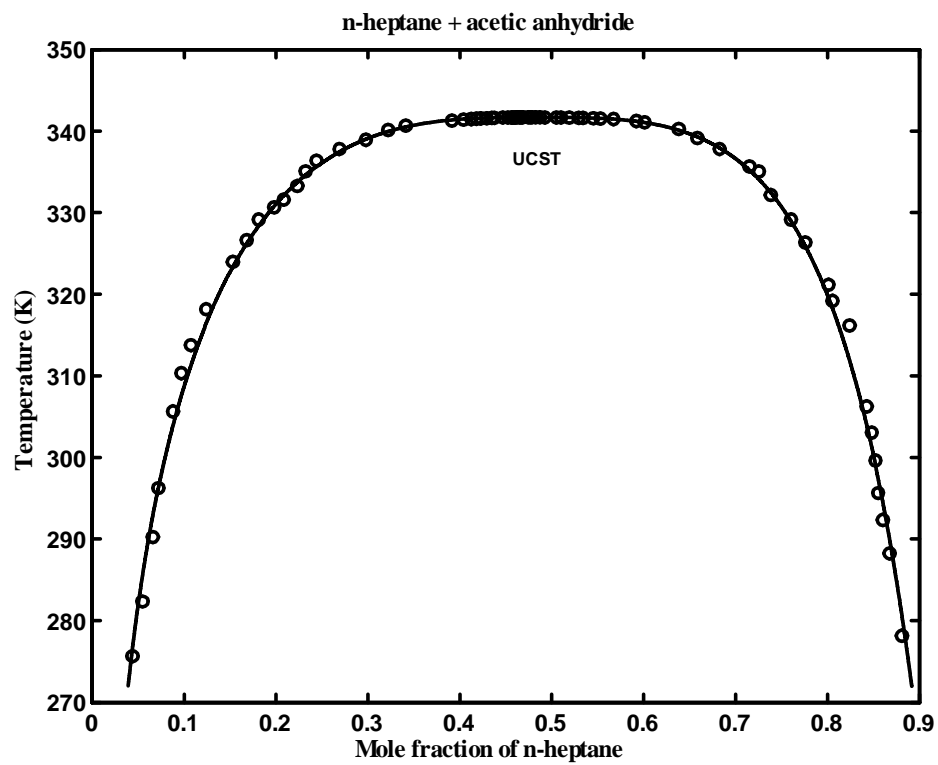
Figure 5.2: The coexistence curve of n-heptane + acetic anhydride system. The circles indicate experimental data of Nagarajan *et al.*.[73] The solid curve is a fit to Eq. (5.12).

component fluid. The actual variety of experimentally observed critical behavior in binary fluids is hidden in the relations between the scaling fields and physical fields. The concept of "complete scaling" implies that all physical fields, independent and dependent, are to be mixed into the scaling fields. Thus, for a more complete treatment the scaling fields for binary fluids in linear approximation are no longer given by Eq. (5.9), but should read

$$h_1 \; = \; a_0 \Delta \widetilde{P} + a_1 \Delta \widetilde{\mu}_{\Delta 21} + a_2 \Delta \widetilde{T} + a_3 \Delta \widetilde{\mu}_1, \tag{5.13}$$

$$h_2 \; = \; b_0 \Delta \widetilde{P} + b_1 \Delta \widetilde{T} + b_2 \Delta \widetilde{\mu}_{\Delta 21} + b_3 \Delta \widetilde{\mu}_1. \tag{5.14}$$

where $\Delta \widetilde{\mu}_1 = \frac{\mu_1 - \mu_{1c}}{RT_c}$ (with the chemical potential of solvent μ_1 conjugate to molar density ρ) and $\Delta \widetilde{\mu}_{\Delta 21} = \frac{\mu_{\Delta 21} - \mu_{\Delta 21c}}{RT_c}$ (with the solute/solvent chemical potential difference $\mu_{\Delta 21}$ conjugate to mole fraction x). The singular part Ψ_{cr} of field-dependent thermodynamic potential Ψ is now a linear combination of the chemical potentials, temperature, and pressure,

$$\Psi_{\mathrm{cr}} = \Delta \widetilde{P} - x_c \Delta \widetilde{\mu}_{\Delta 21} - \Delta \widetilde{\mu}_1 - \widetilde{S}_c \Delta \widetilde{T}, \tag{5.15}$$

where x_c is the critical mole fraction of solute and $\widetilde{S}_c = S_c / R$. Noting that $\phi_1 = -\partial \left(\Psi_{\mathrm{cr}} \right) / \partial h_1$, $\phi_2 = -\partial \left(\Psi_{\mathrm{cr}} \right) / \partial h_2$, $\widetilde{x} = -\partial \mu_1 / \partial \mu_{\Delta 21}$, $\widetilde{S} = -\partial \mu_1 / \partial \widetilde{T}$ and $\widetilde{\rho} =$

$\partial \widetilde{P}/\partial \widetilde{\mu}_1$, we obtain from Eqs. (5.13), (5.14) and (5.15)

$$\widetilde{x} = \frac{1 + a_1\phi_1 + b_2\phi_2}{1 - a_3\phi_1 - b_3\phi_2}, \tag{5.16}$$

$$\widetilde{S} = \frac{1 + \left(a_2/\widetilde{S}_c\right)\phi_1 + \left(1/\widetilde{S}_c\right)\phi_2}{1 - a_3\phi_1 - b_3\phi_2}. \tag{5.17}$$

$$\widetilde{\rho} = \frac{1 - a_3\phi_1 - b_3\phi_2}{1 + a_0\phi_1 + b_0\phi_2}, \tag{5.18}$$

Thus, the mole fraction, entropy, and density appear to be nonlinear combinations of the scaling densities ϕ_1 and ϕ_2.

In the incompressible liquid-mixture limit the pressure-containing terms in the scaling fields vanish and Eqs. (5.13) and (5.14) reduce to

$$h_1 = a_1\Delta\widetilde{\mu}_{\Delta 21} + a_2\Delta\widetilde{T} + a_3\Delta\widetilde{\mu}_1, \tag{5.19}$$

$$h_2 = b_1\Delta\widetilde{T} + b_2\Delta\widetilde{\mu}_{\Delta 21} + b_3\Delta\widetilde{\mu}_1. \tag{5.20}$$

while Eq. (5.18) becomes linear,

$$\widetilde{\rho} = 1 - a_3\phi_1 - b_3\phi_2. \tag{5.21}$$

Equations (5.19) and (5.20) are analogous to Eqs. (5.1) and (5.2) with $\Delta\widetilde{\mu}_{\Delta 21}$ serving the same role as $\Delta\widetilde{\mu}$ and with $\Delta\widetilde{\mu}_1$ serving the same role as $\Delta\widetilde{P}$. As experiments on liquid-liquid equilibria are usually conducted at essentially constant (in practice, saturation) pressure, the terms $\Delta\widetilde{P}$ in Eqs. (5.13), (5.14) and (5.15) containing can also be neglected for weakly compressible liquid mixtures. In a completely

128

symmetric incompressible binary liquid mixture (fully equivalent to the lattice-gas model) $h_1 = a_1 \Delta \tilde{\mu}_{\Delta 21}$, while the order parameter is solely associated with the mole fraction x, $\phi_1 = a_1 \Delta \tilde{x}$. Similarly, the thermal scaling field $h_2 = b_1 \Delta \tilde{T}$, and the second scaling density $\phi_2 = b_1 \Delta \tilde{S}$, while Ψ_{cr} is simply equal to the critical part of $\tilde{\mu}_1$.[2, 23, 24] Most binary liquids are asymmetric even when their compressibility is negligible. Hence, the order parameter of binary liquids cannot in general be represented in terms of concentration only.

Since two system-dependent amplitudes are incorporated into the scaling function $f^{\pm}\left(\frac{h_1}{h_2^{\beta+\gamma}}\right)$, one can adopt $a_1 = 1$ and $b_1 = 1$. Moreover, in an incompressible binary liquid a suitable choice of the critical-entropy (arbitrary) value imposes constrains on other coefficients in the scaling fields.[23, 24] With the choice $\tilde{S}_c = \left(\frac{\partial \tilde{\mu}_1}{\partial \tilde{T}}\right)_{h_1=0,c}$, $a_2 - \tilde{S}_c a_3 = 0$ and $b_3 = 0$, such that the entropy can be associated with the weakly-fluctuating second scaling density only, $\phi_2 = \Delta \tilde{S}$, and $h_2 = \Delta \tilde{T}$ (at $h_1 = 0$), while the mole fraction can be expanded as

$$\tilde{x} = 1 + (1 + a_3)\phi_1 + a_3(1 + a_3)\phi_1^2 + b_2\phi_2 + \ldots. \tag{5.22}$$

or in terms of $h_2 = \Delta \tilde{T}$:

$$\tilde{x} = 1 \pm B_0 \left|\Delta \tilde{T}\right|^{\beta} + D_2 \left|\Delta \tilde{T}\right|^{2\beta} + D_1 \left|\Delta \tilde{T}\right|^{1-\alpha} + \ldots. \tag{5.23}$$

where $B_0 = \lim_{\Delta \tilde{T} \to 0} (1 + a_3) \phi_1 |h_2|^{-\beta}$, $D_2 = B_0^2 a_3/(1+a_3)$, and $D_1 = b_2 A_0^-/(1-\alpha)R$. In Eq. (5.23) B_0 is the asymptotic amplitude of the liquid-liquid coexistence curve

and A_0^- is the asymptotic amplitude of the isobaric heat capacity, $C_{P,x} = A_0^- \left|\Delta\widetilde{T}\right|^{-\alpha} +$ ..., in the two-phase region.

From Eq. (5.23), in the exact analogy with Eq. (5.3), it follows that the "singular diameter" of concentrations x' and x'' of the coexisting phases in a weakly compressible binary liquid has the form

$$\widetilde{x}_d = \frac{x' + x''}{2x_c} = 1 + D_2 \left|\Delta\widetilde{T}\right|^{2\beta} + D_1 \left|\Delta\widetilde{T}\right|^{1-\alpha} + \ldots, \qquad (5.24)$$

while the dimensional difference of the concentrations

$$\frac{x' - x''}{2x_c} = B_0 \left|\Delta\widetilde{T}\right|^{\beta} + \ldots. \qquad (5.25)$$

Eq. (5.24) may be expressed in the form that the entropy is employed just as we did for the vapor-liquid diameter,

$$\widetilde{x}_d - 1 = D_2 \left|\Delta\widetilde{T}\right|^{2\beta} + D_1 \left(-\frac{A_0^-}{(1-\alpha)R} \left|\Delta\widetilde{T}\right|^{1-\alpha} + \frac{B_{cr}}{R} \left|\Delta\widetilde{T}\right|\right). \qquad (5.26)$$

Whereas the Ising-like order parameter ϕ_1 in fluids as a function of $h_2 = \Delta\widetilde{T}$ is symmetric with respect to a change of its sign, one can see from Eqs. (5.16) and (5.23) that the molar concentrations of the coexisting phases as a function of temperature may exhibit asymmetry. This asymmetry originates from two different sources. One source, a correlation between entropy and concentration that generates

130

a $b_2\phi_2 = b_2\Delta\widetilde{S} \propto \left|\Delta\widetilde{T}\right|^{1-\alpha}$ term, has been extensively discussed in the literature. However, as $2\beta < 1 - \alpha$, the leading asymmetric term is $a_3(1 + a_3)\phi_1^2 \propto \left|\Delta\widetilde{T}\right|^{2\beta}$. This term originates from the mixing of $\Delta\widetilde{\mu}_1$ into h_1 and is a direct consequence of "complete scaling".

In fact, experimental data on "diameters" of liquid-liquid coexistence systematically have called for the presence of the $\left|\Delta\widetilde{T}\right|^{2\beta}$ term.[28, 29, 102] In the past, this contribution was attributed to the choice of the composition variable. Specifically, any concentration variable X can be transformed into a certain new concentration variable Y through a non-linear relation $Y = X/\left[X + (1 - X)\,p\right]$, where p is a parameter characterizing the transformation.[29, 102] As an example, mole fraction is transformed into mass fraction with $p = M_2/M_1$, where M_1 and M_2 are the solute and solvent molecular masses, respectively. It is easy to demonstrate that, if X is the variable for which the XT coexistence curve is symmetric, the "diameter" of the YT coexistence curve exhibits a $\left|\Delta\widetilde{T}\right|^{2\beta}$ singularity. This is why $\left|\Delta\widetilde{T}\right|^{2\beta}$ term was commonly regarded as a spurious effect arising from a "wrong" choice of the composition variable in the data analysis.[28] The theory presented here shows that the $\left|\Delta\widetilde{T}\right|^{2\beta}$ singularity cannot be completely eliminated for any conventional choice of the concentration, expressed through molar, volume, or mass fractions. This singular term is a fundamental consequence of "complete scaling". However, it is interesting that in the incompressible limit, as follows from Eqs. (5.16) and (5.21), a product of the mole fraction and molar density, the "partial density" ρx, is a linear combination of the scaling densities, being $\widetilde{\rho x} = 1 + a_1\phi_1 + b_2\phi_2$, in which the $\left|\Delta\widetilde{T}\right|^{2\beta}$

131

singularity is eliminated. Taking the difference of these products for two coexisting liquid phases, in first approximation one obtains the true Ising-like order parameter in the incompressible limit.

5.3 Experimental evidence for "complete scaling" in binary liquid solutions

Experimental evidence for "complete scaling" in liquid mixtures has recently been presented by Cerdeiriña *et al.*[30] For a systematic study of the nature of asymmetry in liquid-liquid equilibria, we have followed Cerdeiriña *et al.* by further analyzing experimental coexistence-curve data for nitrobenzene+n-alkane mixtures.[103, 104, 105, 106, 107, 108, 109, 110] The reason for this choice is that for these mixtures the asymmetry of liquid-liquid coexistence can be tuned by the number of carbon atoms in n-alkane molecules, while the quality of the available experimental data is relatively high. The mole fractions of the two coexisting liquid phases have been analyzed within the range $3 \cdot 10^{-4} \leq \left| \Delta \widetilde{T} \right| \leq 1 \cdot 10^{-2}$ to exclude data affected by uncertainties in the critical parameters (very close to the critical point) and data affected by higher-order contributions (far away from the critical point). The critical parameters (adopted from the literature[103, 104, 105, 106, 107, 108, 109, 110]), the n-alkane/nitrobenzene molecular-volume ratios, $\nu_{\mathrm{alk}}/\nu_{\mathrm{NB}}$ (calculated), and the asymptotic amplitudes B_0 (obtained from fits of the mole fractions to $(x' - x'')/2x_{\mathrm{c}} = B_0 \left| \Delta \widetilde{T} \right|^{\beta}$, for the systems studied are presented in Table 5.2. One can see that with increase of the molecular-volume ratio, the critical mole fraction of n-alkane (regarded as the solute) significantly decreases while the amplitude B_0 increases, as shown in Fig. 5.3.

system	x_c (alkane)	T_c (K)	ν_{alk}/ν_{NB}	B_0	10σ
NB+C$_5$[105]	0.610	297.10	1.12	1.14	0.02
NB+C$_6$[103]	0.572	293.13	1.28	1.32	0.03
NB+C$_7$[103]	0.529	291.94	1.44	1.47	0.02
NB+C$_8$[104]	0.495	293.05	1.59	1.58	0.02
NB+C$_{10}$[105]	0.425	295.96	1.91	1.84	0.03
NB+C$_{11}$[106]	0.395	298.01	2.07	2.02	0.03
NB+C$_{12}$[107]	0.369	300.37	2.22	2.07	0.04
NB+C$_{13}$[108]	0.357	303.00	2.38	2.14	0.04
NB+C$_{14}$[109]	0.324	304.94	2.54	2.22	0.05
NB+C$_{16}$[110]	0.284	309.69	2.86	2.39	0.06

Table 5.2: Critical parameters and critical amplitudes for various binary liquid mixtures
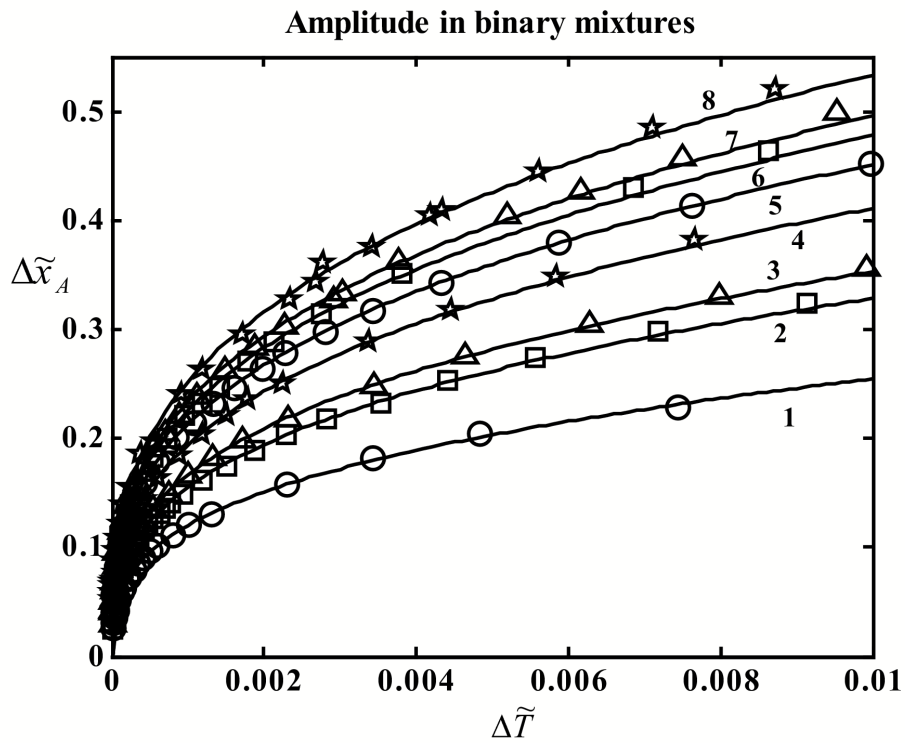
Figure 5.3: Mole fraction difference $\Delta\widetilde{x}_A = (x' - x'')/2x_c$ of the liquid-liquid coexistence curve for nitrobenzene+n-pentane (1), n-heptane (2), n-octane (3), n-decane (4), n-undecane (5), n-tridecane (6), n-tetradecane (7), and n-hexadecane (8) as a function of $\Delta\widetilde{T}$. The solid curves represent $B_0 \left|\Delta\widetilde{T}\right|^{\beta}$ for $\Delta\widetilde{x}_A$.

The results of fitting the liquid-liquid coexistence-curve data to Eq. (5.26) for all the systems are presented in Table 5.3, where we take $A_0^- = 42.9$ J/(mol·K)^2 and $B_{cr} = 22.4$ J/(mol·K)^{44} which is for Nitroethane-isooctane for all systems as an approximation.

The $D_2 \left| \Delta \widetilde{T} \right|^{2\beta}$ term can be clearly observed in all systems analyzed, except for nitrobenzene+n-pentane, as shown in Fig. 5.4. With understandable exceptions for the mixtures with n-hexane and n-heptane, both exhibiting small $D_2 \left| \Delta \widetilde{T} \right|^{2\beta}$ contributions. For the mixtures with n-hexane and n-heptane, which both have low asymmetry, D_1 and D_2 are strongly correlated and thus less reliable. Nevertheless, the overall trend is clear: the contribution of the $\left| \Delta \widetilde{T} \right|^{2\beta}$ singularity significantly increases with increase of the number of carbon atoms in n-alkane molecules, as shown in table 5.3. The slopes increase dramatically with increase of the number of carbon atoms in n-alkane molecules or, equivalently, with increase of the solute/solvent molecular-volume ratio. Figure 5.5 shows the mole fraction "diameter" $\Delta \widetilde{x}_d = (x' + x'') / 2x_c$ for the mixture nitrobenzene+n-hexadecane, the most asymmetric system among studied. A strong deviation from the rectilinear diameter in this mixture is evident. The solid curves in Fig. 5.5 represents a fit of $(x' + x'') / 2x_c$ to Eq. (5.26). Obviously, the contribution from $D_2 \left| \Delta \widetilde{T} \right|^{2\beta}$ term (dash line) provides a crucial description of the "singular diameter" for nitrobenzene+n-hexadecane, proving that this term is dominant. Fig. 5.6 is the residual plot from fit of the diameter of nitrobenzene+n-hexadecane by fitting Eq. (5.26).

system	D_2	D_1	a_3	b_2	10σ
NB+C$_5$[105]	0.086	0.073	0.071	0.073	0.01
NB+C$_6$[103]	0.180	0.043	0.115	0.053	0.01
NB+C$_7$[103]	0.220	0.042	0.113	0.042	0.01
NB+C$_8$[104]	0.285	0.029	0.129	0.029	0.01
NB+C$_{10}$[105]	0.730	0.019	0.275	0.019	0.02
NB+C$_{11}$[106]	0.978	0.014	0.315	0.014	0.03
NB+C$_{12}$[107]	0.990	0.024	0.300	0.024	0.06
NB+C$_{13}$[108]	1.16	-0.080	0.337	-0.080	0.02
NB+C$_{14}$[109]	1.36	-0.072	0.383	-0.072	0.01
NB+C$_{16}$[110]	1.85	-0.007	0.479	-0.007	0.02

Table 5.3: Asymmetry parameters for various binary liquid mixtures
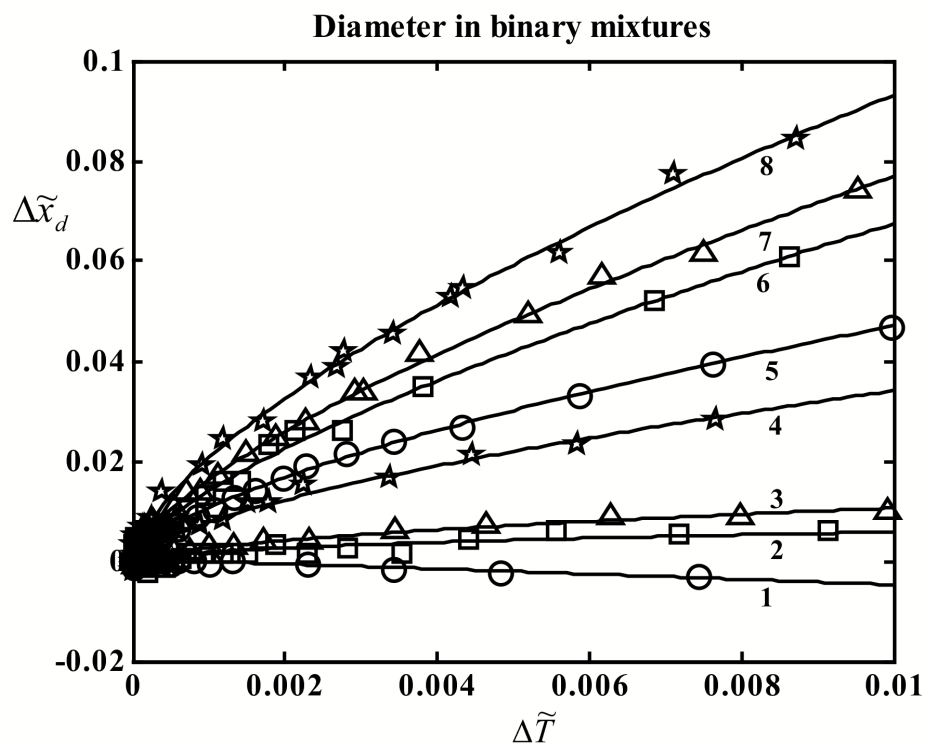
Figure 5.4: Mole fraction reduced diameter $\Delta\widetilde{x}_{\mathrm{d}} = (x' + x'')/2x_{\mathrm{c}} - 1$ of the liquid-liquid coexistence curve for nitrobenzene+n-pentane (1), n-heptane (2) , n-octane (3), n-decane (4), n-undecane (5), n-tridecane (6), n-tetradecane (7), and n-hexadecane (8) as a function of $\Delta\widetilde{T}$. The solid curves represent Eq. (5.26) for $\Delta\widetilde{x}_{\mathrm{d}}$.
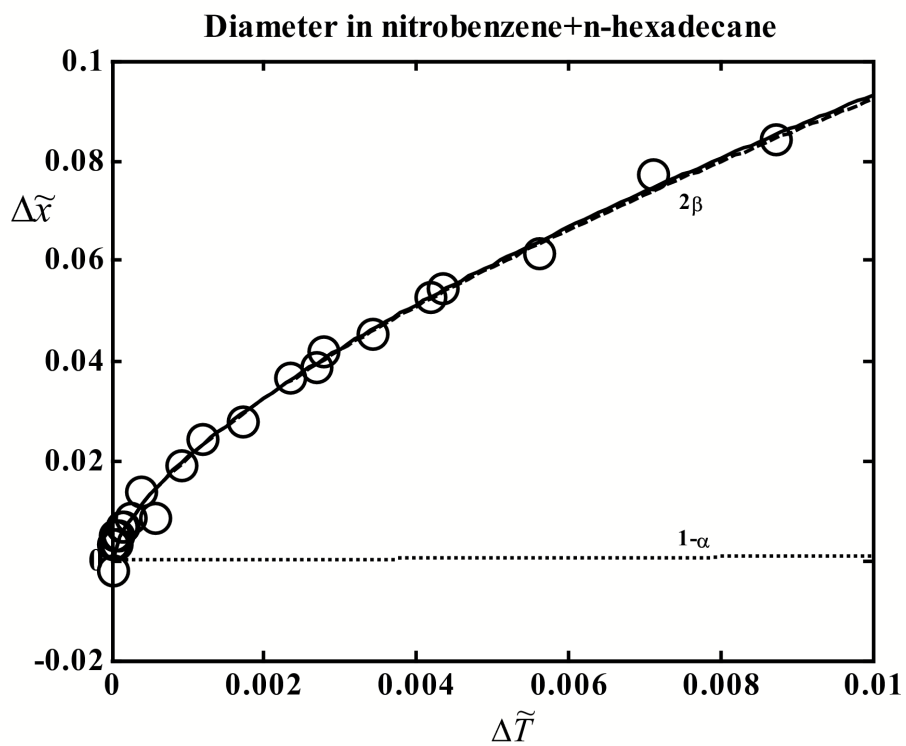
Figure 5.5: The liquid-liquid coexistence curve of nitrobenzene+n-hexadecane. The circles indicate experimental data of An *et al.*[110] Curves: solid - fit to Eq. (5.26), dashed -2β term, dotted - $1 - \alpha$ and linear terms.
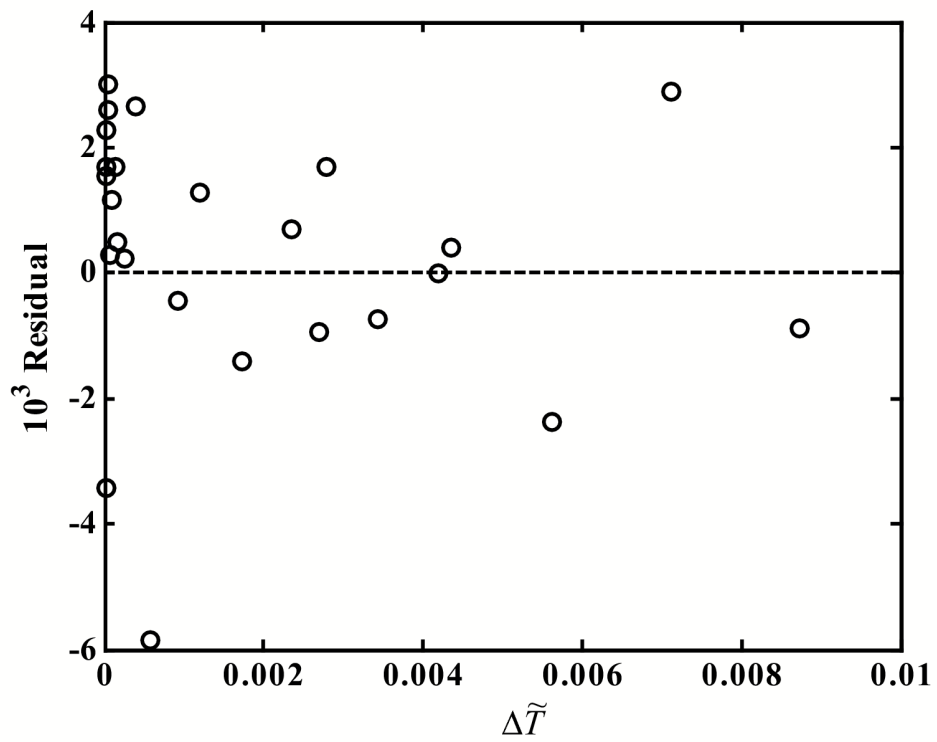
Figure 5.6: Residual plot from fit of the diameter of nitrobenzene+n-hexadecane. The fitting function is Eq. (5.26).

5.4   The nature of asymmetry of liquid-liquid equilibria

The behavior of the coefficient D_2 is basically controlled by the coefficient a_3 originating from "complete scaling", since $D_2 = B_0^2 a_3/(1 + a_3)$. As follows from Eqs. (5.21) and (5.22), in lowest approximation $\Delta\widetilde{\rho}/\Delta\widetilde{x} = -a_3/a_1(1 + a_3)$, where $a_1 = 1$. Physically, it means that while the $D_1\left|\Delta\widetilde{T}\right|^{1-\alpha}$ term originates from a correlation between entropy and concentration, the $D_2\left|\Delta\widetilde{T}\right|^{2\beta}$ term originates from a correlation between molar concentration and molar density. Estimating $\Delta\widetilde{\rho}/\Delta\widetilde{x}$ as

$$\frac{\Delta\widetilde{\rho}}{\Delta\widetilde{x}} \approx \frac{x_{\mathrm{c}}}{\rho_{\mathrm{c}}}\left(\rho_{\mathrm{alk}} - \rho_{\mathrm{NB}}\right) \approx k\left(1 - \frac{\nu_{\mathrm{alk}}}{\nu_{\mathrm{NB}}}\right) \equiv \delta. \tag{5.27}$$

where $x_{\mathrm{c}}/\rho_{\mathrm{c}}\nu_{\mathrm{alk}}$ is approximated as a constant k, one obtains $D_2/B_0^2 = a_3/(1+a_3) \approx -\delta$. Figure 5.7 illustrates that such a rough estimate is in reasonable agreement with experiment. From Fig 5.8 (a), it is clear that the a_3 increases when $\nu_{\mathrm{alk}}/\nu_{\mathrm{NB}}$ increases, which means the ratio of molecular volumes of two components plays a crucial role in the asymmetry of liquid-liquid phase equilibrium. From Fig 5.8 (b), it is clear that the b_2 decreases when $\nu_{\mathrm{alk}}/\nu_{\mathrm{NB}}$ increases. The data of b_2 are scattered, which may be because we don't have exact A_0^- and B_{cr} for each binary liquid mixture.

Another consequence of "complete scaling" in binary fluids is an analogue of the so-called Yang-Yang anomaly. For one-component fluids there is a thermodynamic relation between the isochoric molar heat capacity C_{V} in the two-phase
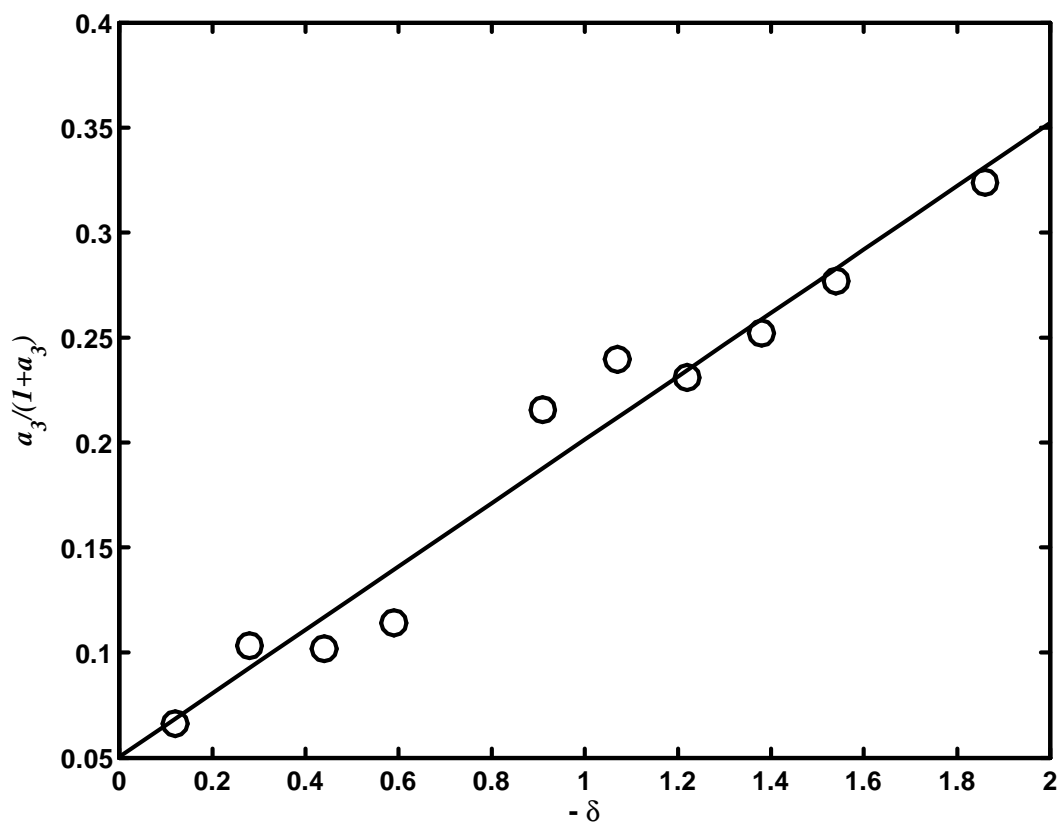
Figure 5.7: D_2/B_0^2 as a function of $-\delta$ for nitrobenzene+n-alkane mixtures.
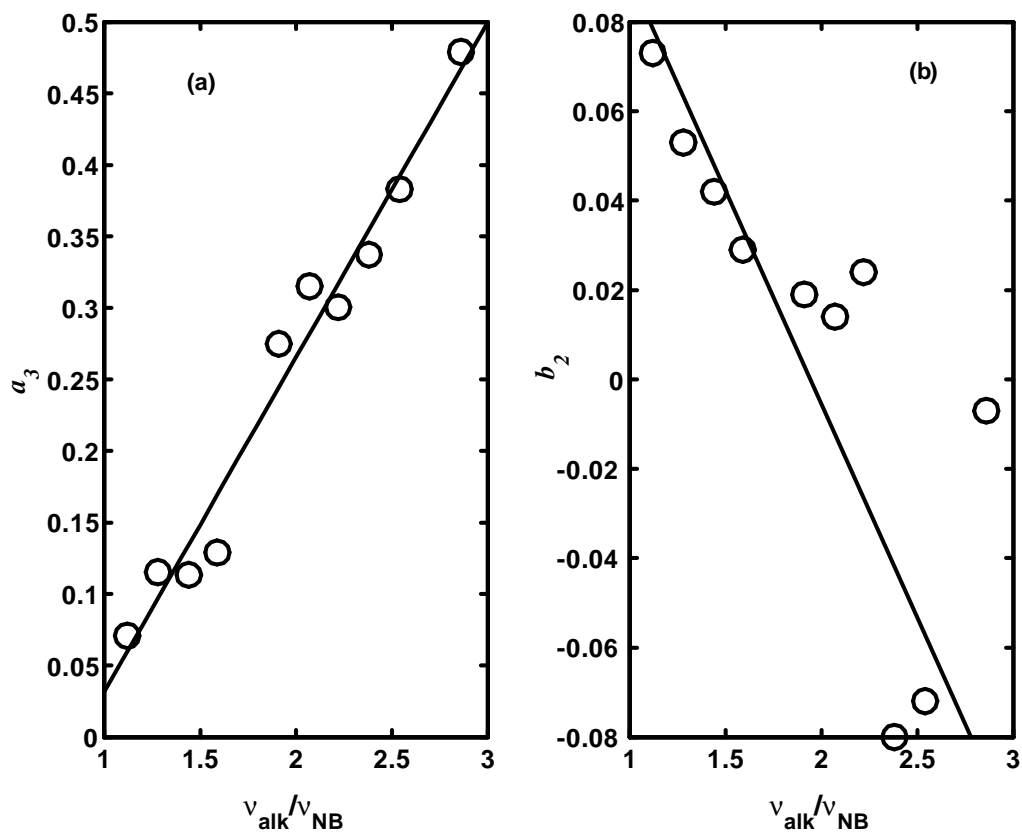
Figure 5.8: (a) a_3 as a function of $\nu_{\mathrm{alk}}/\nu_{\mathrm{NB}}$ for nitrobenzene+n-alkane mixtures. (b) b_2 as a function of $\nu_{\mathrm{alk}}/\nu_{\mathrm{NB}}$ for nitrobenzene+n-alkane mixtures.

region and the second derivatives of chemical potential and pressure[22]

$$\frac{C_{\mathrm{V}}}{T} = \frac{1}{\rho}\left(\frac{d^2 P}{dT^2}\right)_{\mathrm{cxc}} - \left(\frac{d^2 \mu}{dT^2}\right)_{\mathrm{cxc}}, \tag{5.28}$$

The presence of the $a_3 \Delta \widetilde{P}$ term in Eq. (5.1) implies that both the pressure and chemical potential derivatives diverge as $\left|\Delta \widetilde{T}\right|^{-\alpha}$. A chemical-potential share in the heat-capacity divergence is proportional to a_3.[19, 21] The analogue of Eq. (5.28) for binary fluids follows from thermodynamics and reads

$$\frac{C_{\mathrm{P,x}}}{T} = -x\left(\frac{d^2 \mu_{\Delta 21}}{dT^2}\right)_{P,\mathrm{cxc}} - \left(\frac{d^2 \mu_1}{dT^2}\right)_{P,\mathrm{cxc}}, \tag{5.29}$$

where, as follows from Eq. (5.19),

$$\left(\frac{d^2 \mu_{\Delta 21}}{dT^2}\right)_{P,\mathrm{cxc}} = -\frac{a_3}{a_1}\left(\frac{d^2 \mu_1}{dT^2}\right)_{P,\mathrm{cxc}}, \tag{5.30}$$

By measuring $\frac{C_{\mathrm{P,x}}}{T}$ in the two-phase region at different overall compositions x and plotting the data as a linear function of x, one can obtain $-\frac{d^2 \mu_{\Delta 21}}{dT^2}$ from the slope and $-\frac{d^2 \mu_1}{dT^2}$ from the intercept at $x = 0$, with both values diverging at the critical point. In a symmetric binary liquid ($a_3 = 0$) the contribution from $\frac{d^2 \mu_{\Delta 21}}{dT^2}$ should vanish.

We conclude that the asymmetry of liquid-liquid coexistence in weakly compressible binary mixtures is a consequence of "complete scaling". It originates from two physically different sources: a correlation between concentration and entropy

141

and a correlation between concentration and density. We have also resolved a controversial issue regarding the nature of the order parameter for liquid-liquid transitions.

CHAPTER 6

CLOSED SOLUBILITY LOOPS IN LIQUID MIXTURES

Partially miscible liquid mixtures may either possess an upper critical solution temperature (UCST) above which the two liquid components are completely miscible at any concentration or a lower critical solution temperature (LCST) below which the two liquids are miscible at any concentration. In addition, there are interesting mixtures that possess both a LCST and an UCST separated by a miscibility gap inside a closed-loop phase boundary. Inside this phase boundary, also referred to as (closed) solubility loop, the system consists of two liquid phases with different compositions; outside this phase boundary the two liquid components are completely miscible. A liquid mixture with a closed-loop phase boundary is an example of a system that exhibits a re-entrant phase transition, i.e., the system can pass through two liquid-liquid phase transitions as a function of temperature at a constant overall concentration.[32] In some systems with a miscibility gap inside a closed-loop coexistence curve, the miscibility gap may shrink as a function of an external variable such as pressure or upon a change of the overall concentration of a third component so that the LCST and the UCST approach each other until they converge into a double critical point.[113, 114]

In an early paper on the subject, Hirschfelder *et al.*[115] proposed that re-entrant miscibility is related to the presence of directional short-ranged interactions associated with hydrogen bonding between unlike molecules. Attempts have been made to incorporate this idea into various lattice models for re-entrant miscibility.

143

While lattice models may provide a qualitative picture of the origin of miscibility gaps, they are not suitable for obtaining a realistic representation for the location in a temperature-concentration diagram of closed-loop phase boundaries of actual liquid mixtures.[116] For the latter purpose one needs to ensure that the known singular thermodynamic critical behavior near both the LCST and the UCST is recovered. Starting from the concept of isomorphic critical behavior in fluid mixtures,[55, 2] as systematically formulated by Anisimov *et al.*,[23] we derive an equation for closed-loop phase boundaries that both has a sound theoretical basis and is simple to use in practical engineering calculations. The quality of the simple equation will be tested by comparisons with experimental data for a variety of liquid mixtures. The interesting phase-equilibrium behavior observed upon the approach to a double critical point will also be elucidated. Fisher and coworkers[19, 21] have argued that one should also include in the definition (5.5) of the scaling fields a term proportional to ΔP, which affects the asymptotic singular behavior of the coexistence-curve diameter. We do not consider this complication here, since its effect in practice is well within the resolution of the experimental data considered in this chapter.[100]

6.1 Non-linear mixing of scaling fields

In the critical line (CL) of binary liquid mixtures, a different special point is encountered when $(dP/dT)_{\mathrm{CL}} = 0$.[23] As shown in Fig. (6.1), in general this special point is called a re-entrant critical point (RCP) such as the so-called double critical point which is a point where a line of lower critical points and a line of upper critical points merge.

144
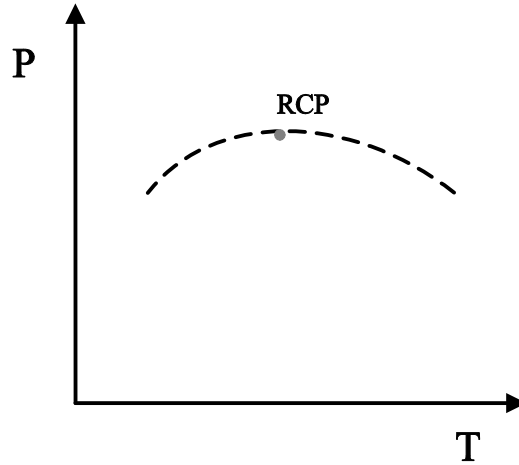
Figure 6.1: Illustration of re-entrant critical point (RCP).

Let 's consider the conventional linear mixing scaling Eqs. (5.9), when $h_1 = 0$, and $h_2 = 0$, we have the critical line in terms of reduced temperature and pressure

$$\Delta \widetilde{T} = \left(\frac{a_1 b_0 - a_0 b_2}{a_2 b_2 - a_1 b_1} \right) \Delta \widetilde{P}. \tag{6.1}$$

As we know when the critical entropy density is properly selected, $a_2 = 0$ and the normalization will make $a_1 = b_1 = 1$. Thus, $(dP/dT)_{\mathrm{CL}} = 1/(a_0 b_2 - b_0)$ may not vanish. Therefore, it is necessary to include the nonlinear terms in Eqs. (5.9) in order to characterize critical lines with a special point where $(dP/dT)_{\mathrm{CL}} = 0$.

6.2 Liquid mixtures with closed-loop phase boundaries

As shown in Fig. (6.2), a mixture of 2,4-lutidine and water is an example of a liquid mixture that possesses both a LCST and an UCST separated by a closed-loop phase boundary. In principle Eq. (5.12) could represent the phase boundary

145

in the vicinity of the LCST with $T_c = T_L, x_c = x_L$ and with appropriate amplitudes B_0, B_1, B_a, and d_1.[124] Similarly, Eq. (5.12) could be used to represent the phase boundary in the vicinity of the UCST with $T_c = T_U, x_c = x_U$ and with another set of amplitudes. The question we want to address in this section is whether theory can provide us with a single unified equation for the entire closed-loop phase boundary.

From Eq. (5.10) we note again that the scaling fields (at constant pressure) are functions of the chemical-potential difference $\mu_{\Delta 21}$ and the temperature T. We now expand the scaling fields in a Taylor series around the values μ_L and T_L at the lower critical solution point

$$ h_1 = a_1 \Delta \mu_{\Delta 21} + a_2 \Delta T + a_4 \left(\Delta T \right)^2, \qquad h_2 = b_1 \Delta T + b_2 \Delta \mu_{\Delta 21} + b_4 \left(\Delta T \right)^2. \qquad (6.2) $$

It is necessary to point out that the "complete scaling" for liquid-liquid equilibrium of binary fluid mixtures is not considered here since we now concentrate on the effect of the nonlinear terms. Adding of $a_3 \Delta \widetilde{\mu}_1$ and $b_3 \Delta \widetilde{\mu}_1$ to Eq. (6.2) would complicate the derivation very much.

We need to emphasize that in this section the symbol Δ designates the difference between the actual value of the thermodynamic property and its value at the LCST to be indicated by a subscript L. Thus in Eq. (6.2) $\Delta \mu_{\Delta 21} = \mu_{\Delta 21} - \mu_{\Delta 21L}$ and $\Delta T = T - T_L$. We want to describe miscibility gaps with a variety of temperature differences $T_U - T_L$. As we shall see in the subsequent section, in the limit $T_U - T_L \longrightarrow 0$ the terms in Eq. (6.2) proportional to ΔT will vanish. For this reason we need to add in Eq. (6.2) terms proportional to $(\Delta T)^2$ to accommodate closed

solubility loops with arbitrary values of $T_U - T_L$.

Along the phase boundary the strong scaling field h_1 is zero, so that $\Delta\mu_{\Delta 21} = -a_2 a_1^{-1}\Delta T - a_4 a_1^{-1}(\Delta T)^2$, which can be substituted into the expansion for the weak scaling field h_2 in Eq. (6.2). Thus along the phase boundary, h_2 will depend on temperature as

$$h_2 = (b_1 - b_2 a_2 a_1^{-1})\Delta T + (b_4 - b_2 a_4 a_1^{-1})(\Delta T)^2. \tag{6.3}$$

At a critical point both scaling fields h_1 and h_2 must vanish. Thus the right-hand side of Eq. (6.3) must be zero not only for $T = T_L$, but also for $T = T_U$. It thus follows that Eq. (6.3) can be rewritten as

$$h_2 = a(T - T_U)(T - T_L), \tag{6.4}$$

with $a = b_4 - b_2 a_4 a_1^{-1}$. To retain consistency with the notation in the previous section we normalize the scaling field h_2 by taking $a = 1/T_U T_L$, so that

$$h_2 = \tau_{UL} = \frac{(T - T_U)(T - T_L)}{T_U T_L}. \tag{6.5}$$

As explained in the previous section, the chemical potential μ_1 of the solvent plays the role of the field-dependent potential Ψ in Eq. (2.26). Its singular part depends on the scaling fields h_1 and h_2 such that

$$d(\Delta\mu_1) = \phi_1 dh_1 + \phi_2 dh_2. \tag{6.6}$$

Substitution of the expansion (6.2) for the scaling fields into Eq. (6.6) yields

$$d\left(\Delta\mu_1\right) = \left[\left(a_2 + 2a_4\right)\phi_1 + \left(b_1 + 2b_4\right)\phi_2\right]d\left(\Delta T\right) + \left(a_1\phi_1 + b_2\phi_2\right)d\left(\Delta\mu_{\Delta 21}\right). \quad (6.7)$$

On the other hand Eq. (5.11) implies that (at constant pressure)

$$d\left(\Delta\mu_1\right) = -S_{\mathrm{m}}d\left(\Delta T\right) - \Delta x d\left(\Delta\mu_{\Delta 21}\right). \quad (6.8)$$

From Eqs. (6.7) and (6.8) we note that

$$\Delta x = x - x_{\mathrm{L}} = -(a_1\phi_1 + b_2\phi_2). \quad (6.9)$$

On comparing Eqs. (5.4), (6.5) and (6.9) we conclude that Δx has the same asymptotic expansion as Eq. (5.6) for $\Delta\widetilde{\rho}$ but with $\Delta\widetilde{T}$ replaced by $h_2 = \tau_{\mathrm{UL}}$. Adding the correction proportional to $|h_2|^{1-\alpha}$ as in Eq. (5.7), as well as a regular background contribution that now will be proportional to $\Delta T = T - T_{\mathrm{L}}$, we obtain

$$x = x_{\mathrm{L}} \pm B_0\left|\tau_{\mathrm{UL}}\right|^\beta\left[1 + B_1\left|\tau_{\mathrm{UL}}\right|^{\Delta_s}\right] + B_{\mathrm{a}}\left|\tau_{\mathrm{UL}}\right|^{1-\alpha} + d_1\left(\frac{T}{T_{\mathrm{L}}} - 1\right). \quad (6.10)$$

Since $x = x_{\mathrm{U}}$ at the UCST, it follows that the coefficient d_1 must satisfy the condition

$$d_1 = \left(x_{\mathrm{U}} - x_{\mathrm{L}}\right)T_{\mathrm{L}}/\left(T_{\mathrm{U}} - T_{\mathrm{L}}\right). \quad (6.11)$$

Equation (6.11) for a closed solubility loop is obtained from Eq. (5.12) for the

coexistence curve of liquid mixtures when one replaces $\Delta T = (T - T_c)/T_c$ in the singular part of the expansion by τ_{UL} defined in Eq. (6.5). This redefinition of the temperature variable for dealing with closed solubility loops is not new, but has been adopted by several previous investigators.[33, 34, 32] Here we have shown how this procedure follows from the principle of isomorphism of critical behavior in fluid mixtures. Our approach on the basis of isomorphism of critical behavior is similar to the approach of Malomuzh and Veitsman[35, 36] for dealing with phase equilibria in systems in the vicinity of double critical points, a topic that we shall address in the subsequent section. With known experimental values for the temperature and concentration of both the lower critical consolute point and the upper critical consolute point, Eq. (6.10) can be used to described closed solubility loops with only three adjustable parameters, namely the coefficients B_0, B_1, and B_a, with d_1 being fixed by Eq. (6.11).

We have checked the validity of Eq. (6.10) for closed-loop phase boundaries by comparing with experimental data for 2,4-lutidine+water, 2,5-lutidine+water and 2,6-lutidine+water obtained by Andon and Cox,[39] with experimental data for tetrahydrofurane+water (THF+H_2O) and tetrahydrofurane+heavy water (THF+D_2O) obtained by Matous and coworkers[40, 41] and by Oleinikova and Weingärtner.[67] The results are shown in Fig. 6.2 - Fig. 6.8 . The corresponding system-dependent constants in Eq. (6.10), together with the standard deviation σ of the fits are presented in Table 6.1. For THF+H_2O and THF+D_2O experimental have been obtained by two different research groups. Since the actual location of the critical consolute points and, hence, the location of the phase boundary, is very sensitive

to small impurities, data of different laboratories have been analyzed separately. The measurements of Oleinikova and Weingärtner only cover a limited temperature range above the LCST, so that we cannot estimate the corresponding values of T_U and x_U from the experimental data directly, so that they had to be included as adjustable constants in the fitting process. The presence of an UCST in THF+H_2O and in THF+D_2O does explain the upward curvature of the data of Oleinikova and Weingärtner at the higher temperatures in Figs. 6.7 and 6.8.

Equation (6.10) represents an asymptotic expansion for the coexistence curves of liquid mixtures around critical consolute points. It is possible to represent the closed solubility loops on the basis of a more extensive theory of crossover critical behavior.[8] However, we have found that an equally good description is obtained with Eq. (6.10) that is much simpler and convenient for practical calculations. While the expansion (6.10) for coexistence curves becomes less accurate farther away from the critical temperature, in the case of Eq. (6.10) this drawback is compensated by the feature that on moving away from the LCST one approaches the UCST where the equation becomes correct again. As a consequence, the simple equation (6.10) is capable of representing solubility loops in a temperature range as large as 200 K, as can be seen from Fig. 6.4.

6.3   Liquid mixtures with a double critical point

In the previous section we considered closed solubility loops in liquid mixtures at atmospheric pressure. Liquid-liquid separation phenomena become even more interesting when the pressure is added as a variable.[113, 114, 125] As an example we

system	$T_U(K)$	x_U	$T_L(K)$	x_L	d_1	B_0	B_1	B_a	σ
2,4-lutidine + water[39]	461.85	0.630	296.55	0.745	-0.21	0.80	0.95	1.07	0.02
2,5-lutidine + water[39]	480.05	0.630	286.25	0.720	-0.13	0.96	-0.30	1.04	0.03
2,6-lutidine + water[39]	503.85	0.605	307.15	0.688	-0.13	1.06	-0.46	1.07	0.03
THF + water[40]	410.25	0.480	344.95	0.530	-0.26	1.08	0.85	0.23	0.02
THF + heavy water[41]	416.71	0.458	336.88	0.518	-0.25	1.22	-1.08	0.21	0.02
THF + water[67]	408.75	0.484	343.45	0.534	-0.26	1.13	0.46	-0.16	0.01
THF + heavy water[67]	414.93	0.464	335.10	0.509	-0.19	1.23	-0.51	0.25	0.01

Table 6.1: Parameters for phase equilibrium in systems with an UCST and a LCST.
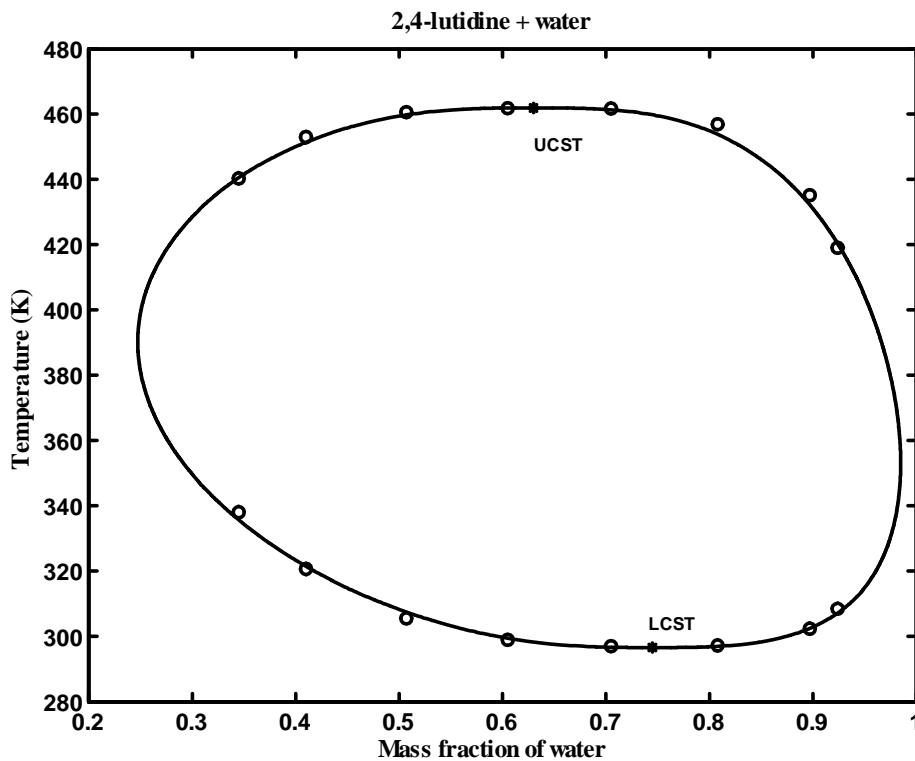
Figure 6.2: The coexistence curve of 2,4-lutidine + water system. The circles indicate experimental data of Andon and Cox.[39] The solid curve is a fit to Eq. (6.10).
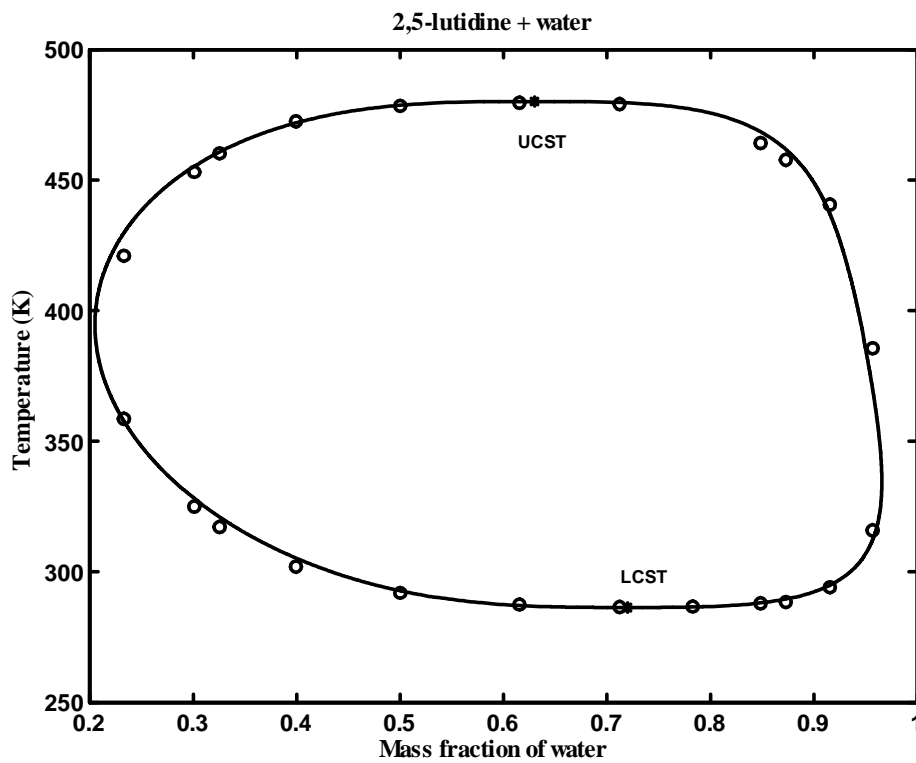
Figure 6.3: The coexistence curve of 2,5-lutidine + water system. The circles indicate experimental data of Andon and Cox.[39] The solid curve is a fit to Eq. (6.10).
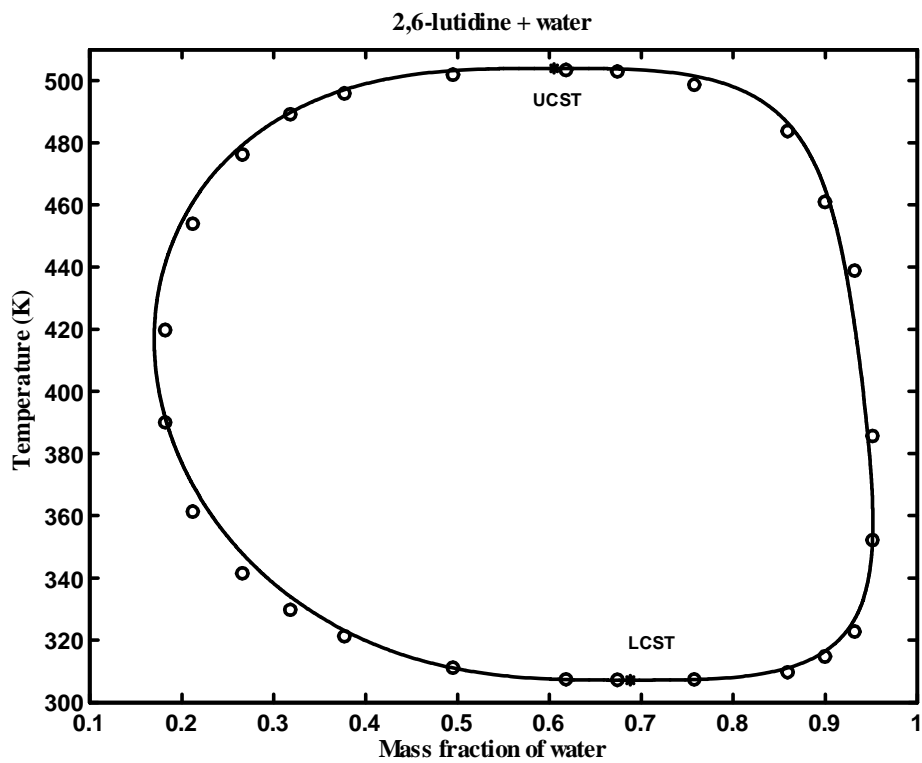
Figure 6.4: The coexistence curve of 2,6-lutidine + water system. The circles indicate experimental data of Andon and Cox.[39] The solid curve is a fit to Eq. (6.10).
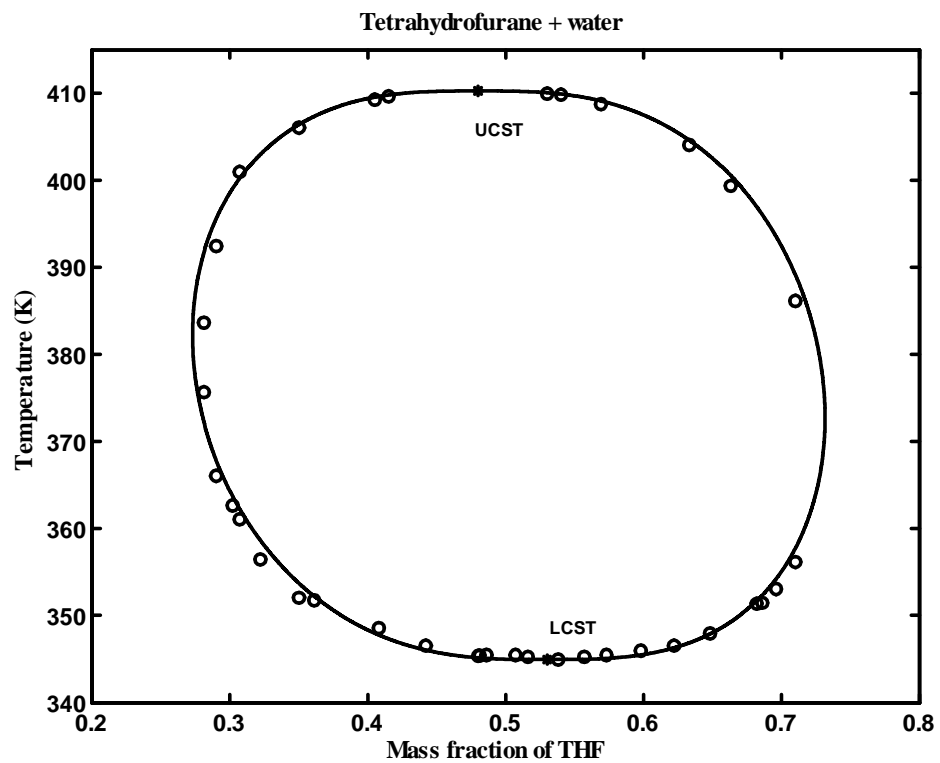
Figure 6.5: The coexistence curve of THF + water system. The circles indicate experimental data of Matous *et al.*[40] The solid curve is a fit to Eq. (6.10).
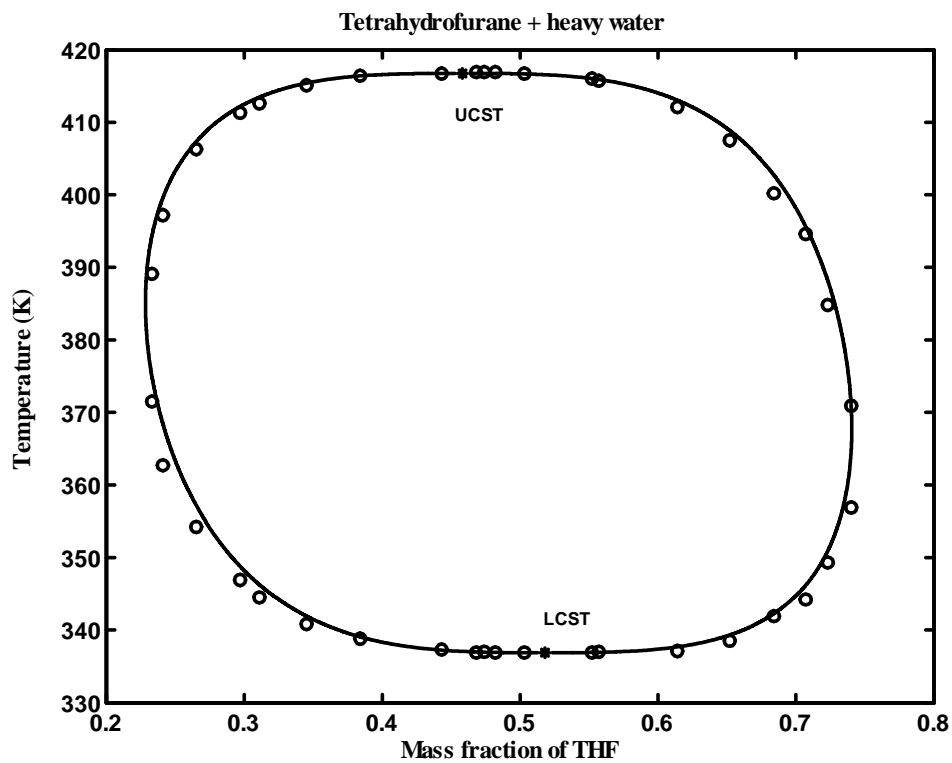
Figure 6.6: The coexistence curve of THF + heavy water system. The circles indicate experimental data of Lejcek *et al.*[41] The solid curve is a fit to Eq. (6.10).
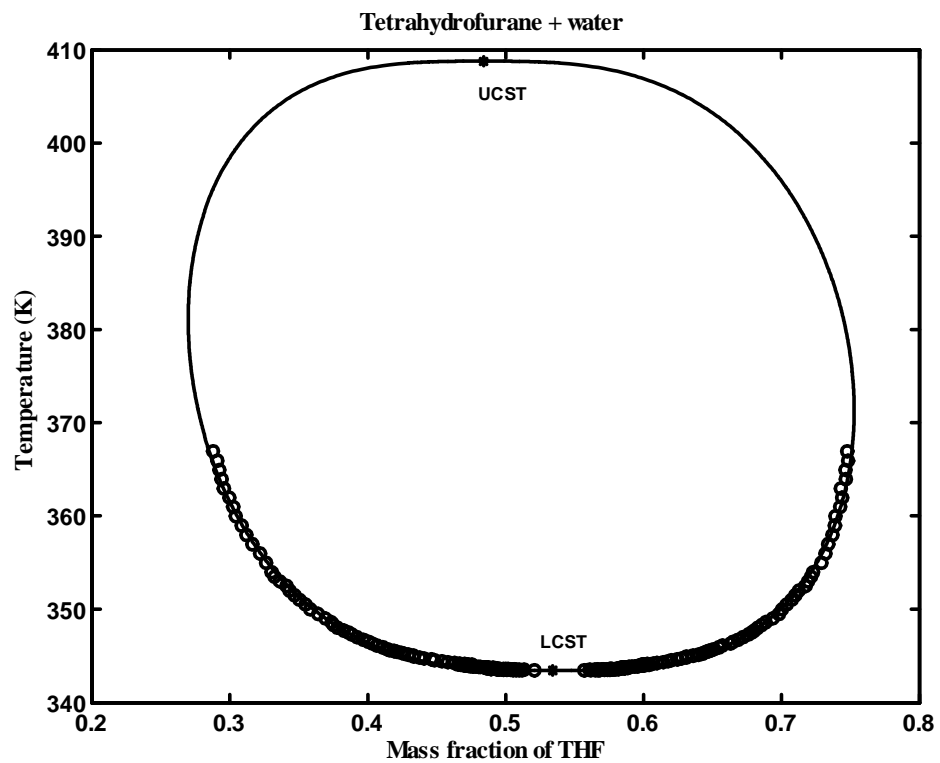
Figure 6.7: The coexistence curve of THF + water system. The circles indicate experimental data of Oleinikova *et al.*[67] The solid curve is a fit to Eq. (6.10).
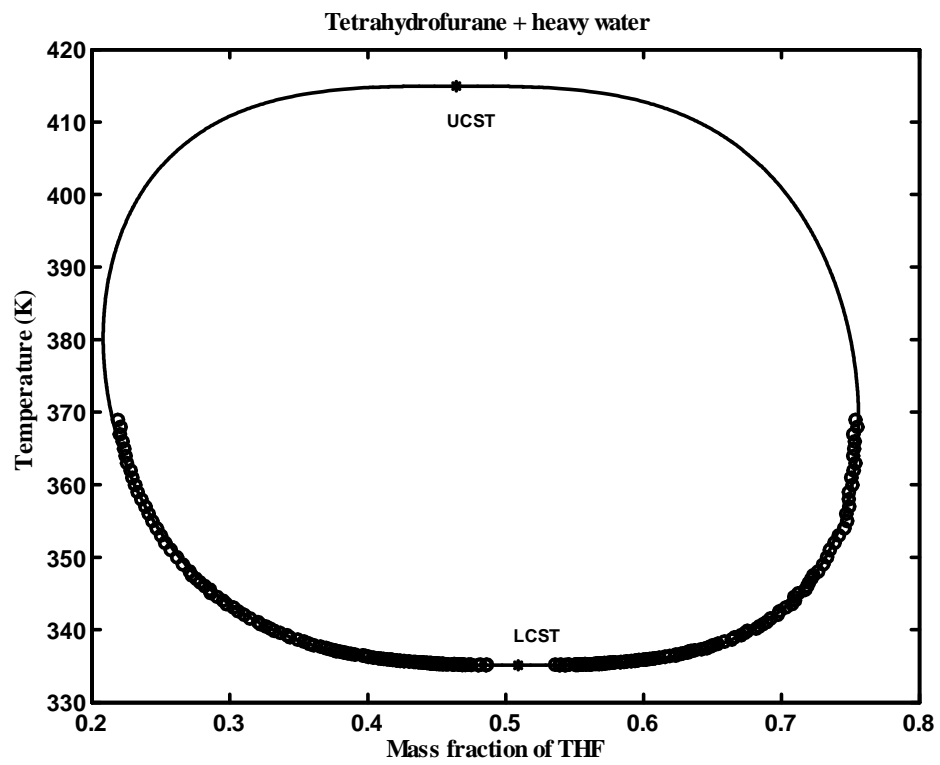
Figure 6.8: The coexistence curve of THF + heavy water system. The circles indicate experimental data of Oleinikova *et al.*[67] The solid curve is a fit to Eq. (6.10).

pressure (atm)	$T_U(K)$	x_U	$T_L(K)$	x_L	d_1	B_0	B_1	B_a	10σ
200	380.45	0.374	288.35	0.404	-0.092	0.62	3.3	-0.23	0.07
300	373.45	0.376	297.05	0.399	-0.089	0.75	2.5	-0.35	0.07
400	369.35	0.378	302.45	0.394	-0.077	0.81	2.1	-0.44	0.10
500	365.55	0.378	309.15	0.390	-0.063	0.90	1.5	-0.40	0.10
600	360.95	0.379	314.95	0.386	-0.045	0.80	4.4	-0.14	0.08
700	355.45	0.380	322.05	0.383	-0.031	0.97	1.0	0.33	0.12
800	350.15	0.380	330.65	0.380	0	0.77	5.6	2.58	0.04

Table 6.2: Parameters for phase equilibria in the 2-butanol + water system

shown in Fig. 6.9 solubility data for 2-butanol+water obtained by Moriyoshi *et al.*[42] at pressures ranging from 200 to 800 atm. The size of the miscibility gaps inside the closed solubility loops decreases with increasing pressures until it shrinks into what is called a hypercritical or double critical point (DCP) at $P_D = (845 \pm 5)$ atm, $T_D = (340.0 \pm 1.5)$ K and $x_D = (0.131 \pm 0.002)$ mole fraction of 2-butanol. In binary liquids there exists a one-dimensional locus of critical consolute points in $P - T - x$ space to which we refer as critical line (CL).[117] At each pressure Eq. (6.10) can still be used to represent these solubility loops as shown in Fig. 6.9, but with system-dependent constants that now depend on pressure as shown in Table 6.2.

Closed solubility loops have also been observed in many ternary mixtures.[113, 114, 125] As an example we shown in Fig. 6.10 some solubility data obtained by the research group of Schneider for a mixture of hexadecane+1-dodecanol in carbon dioxide with a constant CO_2 mass fraction of 0.63.[125, 126, 127] The phase behavior in this ternary mixture is interesting, since it is an example of systems that display a miscibility window instead of a miscibility gap.[114] That is, the solubility loops in Fig. 6.10

158
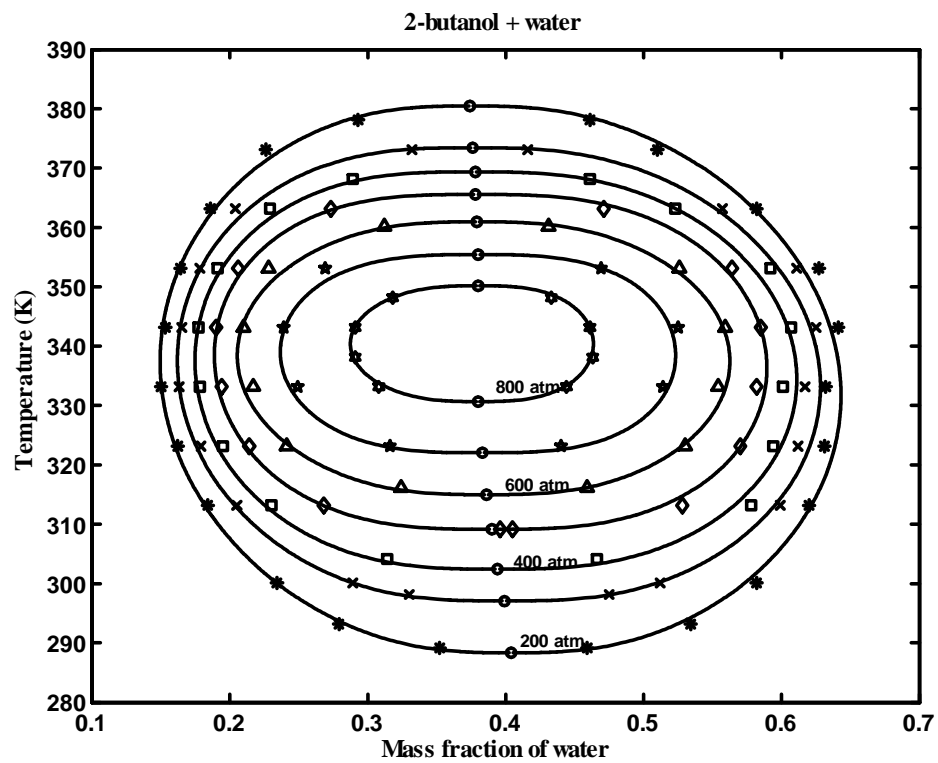
Figure 6.9: Pressure dependence of 2-butanol + water system. The stars are experimental data obtained by Moriyoshi *et al.*[42] The solid curves are fits to Eqs (6.10). The circles are the critical points.

pressure (MPa)	$T_U(K)$	x_U	$T_L(K)$	x_L	d_1	B_0	B_1	B_a	σ
15	325.00	0.820	300.00	0.820	0.000	0.865	8.3	11.6	0.02
16	330.00	0.800	297.00	0.810	-0.090	0.914	6.9	6.2	0.02
25	397.10	0.590	292.90	0.790	-0.562	0.603	17.5	-1.7	0.06

Table 6.3: System-dependent constants and standard deviations as a function of pressure for hexadecane+1-dodecanol+carbon dioxide with a 0.63 mass fraction of carbon dioxide.

enclose a region where the system is completely miscible, while it is only partially miscible outside these solubility loops. Thus now the system is homogeneous at temperatures below the UCST and at temperatures above the LCST. Equation (6.10) with system-dependent constants listed in Table 6.3 can also be used to characterize solubility loops that enclose a miscibility window, although in this case an accurate representation is hampered by a considerable spread of the experimental data at the individual pressures.

Returning to the miscibility gaps displayed in Fig. 6.9, we want to address the question whether the theory of critical phenomena enables one to derive an equation for the solubility loops as a function of pressure. For this purpose we need an equation for $T_{U,L}$ and $x_{U,L}$ as a function of pressure, where $T_{U,L}$ stands for T_U or T_L and $x_{U,L}$ for x_U or x_L. Following Malomuzh and Veitsman[35, 36] we now expand the scaling fields h_1 and h_2 around the double critical point (DCP):

$$h_1 = a_0 \Delta P + a_1 \Delta \mu_{\Delta 21} + a_2 \Delta T + a_4 (\Delta T)^2 + a_5 (\Delta T)^3 ,$$

$$h_2 = b_0 \Delta P + b_1 \Delta T + b_2 \Delta \mu_{\Delta 21} + b_4 (\Delta T)^2 + b_5 (\Delta T)^3 . \qquad (6.12)$$

We emphasize that in this section the symbol Δ designates the difference between
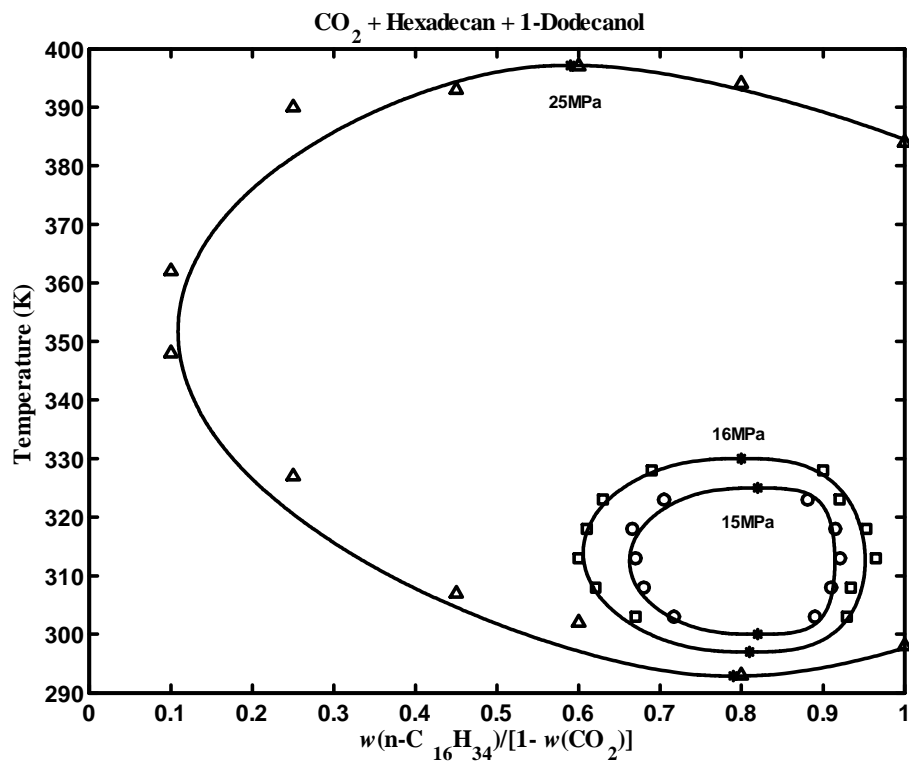
Figure 6.10: Solubility loops in hexadecane+1-dodecanol+carbon dioxide at a fixed CO_2 mass fraction of 0.63. The symbols indicate experimental data obtained by the research group of Schneider.[125, 126, 127] The curves represent values calculated from Eq. (6.10).

the actual value of the thermodynamic property and its value at the DCP indicated by a subscript D. Thus in Eq. (6.12) $\Delta P = P - P_\mathrm{D}$, $\Delta\mu_{\Delta 21} = \mu_{\Delta 21} - (\mu_{\Delta 21})_\mathrm{D}$, and $\Delta T = T - T_\mathrm{D}$. In Fig. 6.11 we have plotted the critical pressures as a function of temperature for 2-butanol+water. The right branch represents the locus of upper critical consolute points and the left branch the locus of lower critical consolute points. The two branches meet at the DCP. The DCP is a special critical point where $(dP_\mathrm{c}/dT)_\mathrm{CL} = 0$.[23, 113] Hence, near the DCP ΔP will vary asymptotically as $\pm(\Delta T)^2$. Since along the critical locus $(\Delta T)^2$ is of the same order of magnitude as ΔP, one can readily verify that the terms in Eq. (6.2) with coefficients a_2 and b_1 must vanish when h_1 and h_2 are expanded around the DCP. Instead we have added terms proportional to $(\Delta T)^3$ to account for asymmetries that will become evident shortly. At the critical locus $h_1 = 0$ and $h_2 = 0$. Solving Eq. (6.12) with $h_1 = h_2 = 0$ for $\Delta T_\mathrm{U,L} = T_\mathrm{U,L} - T_\mathrm{D}$ and $\Delta\left(\mu_{\Delta 21}\right)_\mathrm{U,L} = \left(\mu_{\Delta 21}\right)_\mathrm{U,L} - \left(\mu_{\Delta 21}\right)_\mathrm{D}$ by iteration we obtain

$$\Delta T_\mathrm{U,L} = \pm a_T \left|\Delta P\right|^{1/2} + b_T \left|\Delta P\right|, \tag{6.13}$$

$$\left(\Delta\mu_{\Delta 21}\right)_\mathrm{U,L} = a_x \left|\Delta P\right| \pm b_x \left|\Delta P\right|^{3/2}, \tag{6.14}$$

where the coefficients a_T, b_T, a_x, b_x are related to the coefficients in the expansion (6.12) for the scaling fields by:

$$a_T = \left(\frac{a_0 b_2 - a_1 b_0}{a_1 b_4 - a_4 b_2}\right)^{1/2}, \quad a_x = -a_4 a_1^{-1} a_T^2 - a_0 a_1^{-1} \tag{6.15}$$

$$b_T = a_T^2 \left(\frac{a_1 b_5 - a_5 b_2}{a_1 b_4 - a_4 b_2}\right), \quad b_x = -a_1^{-1} a_T^3 \left[a_5 + 2\left(\frac{a_1 b_5 - a_5 b_2}{a_1 b_4 - a_4 b_2}\right)\right] \tag{6.16}$$

162

It is important to note from Eq. (6.16) that $a_5 = b_5 = 0$ implies $b_T = b_x = 0$. Thus in the absence of terms proportional to $(\Delta T)^3$ in Eq. (6.12) we recover the symmetric asymptotic parabolic dependence of the critical pressure on ΔT, while $(\mu_{\Delta 21})_U$ would be equal to $(\mu_{\Delta 21})_L$ at all pressures. Hence, the cubic terms in Eq. (6.12) yield a first-order correction for asymmetric behavior of $\Delta T_{U,L}$ and $\Delta (\mu_{\Delta 21})_{U,L}$ as a function of ΔP.

We prefer to introduce dimensionless variables $\Delta \widetilde{T}_{U,L} = \Delta T_{U,L}/T_D$, $\Delta \widetilde{P} = \Delta P/P_D$, and $\Delta (\widetilde{\mu}_{\Delta 21})_{U,L} = \Delta (\mu_{\Delta 21})_{U,L}/RT_D$, so that Eqs. (6.15) and (6.16) can be rewritten as:

$$\Delta \widetilde{T}_{U,L} = \pm a_T^* \left| \Delta \widetilde{P} \right|^{1/2} + b_T^* \left| \Delta \widetilde{P} \right|, \qquad (6.17)$$

$$(\Delta \widetilde{\mu}_{\Delta 21})_{U,L} = a_x^* \left| \Delta \widetilde{P} \right| \pm b_x^* \left| \Delta \widetilde{P} \right|^{3/2}, \qquad (6.18)$$

with dimensionless coefficients a_T^*, a_x^*, b_T^*, and b_x^*. The solid curve in Fig. 6.11 represents the values for the critical pressure as a function of temperature calculated from Eq. (6.17) with coefficients given in Table 6.4. The expansions (6.17) and (6.18) become less accurate further away from the DCP and at 200 atm the deviations become substantial. Hence, the critical temperatures at 200 atm and below have not been included in the fit of Eq. (6.17) to the experimental data. To extend the representation of the critical locus till atmospheric pressure, one would have to add additional terms to the expansion (6.12). We have not done so, since we want here to concentrate on the mathematical behavior of the liquid-liquid phase-separation phenomenon in the vicinity of the DCP as implied by the principle of isomorphic critical behavior.

P_{D} (atm)	T_{D} (K)	x_{D}	a_T^*	b_T^*	a_x^*	b_x^*	B_0
845	340.0	0.380	0.133	-0.0239	0.0470	-0.0935	0.95

Table 6.4: Parameters for phase equilibrium in three dimensions for the 2-butanol + water system
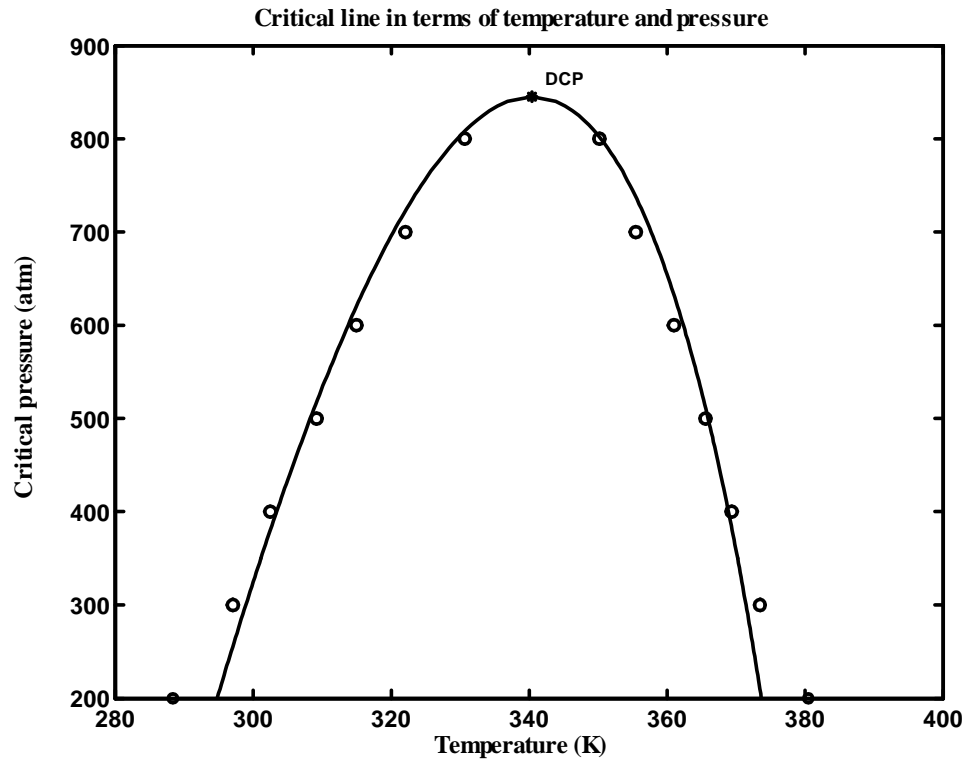
Figure 6.11: Critical line in terms of temperature and pressure. The circles are the critical temperatures and the solid curve represents Eq. (6.17).

To determine the relationship between the critical concentrations and the pressure we first transform the field variable $\mu_{\Delta 21}$ into another variable ζ such that

$$\widetilde{\mu}_{\Delta 21} = \frac{\mu_{\Delta 21}}{RT_{\mathrm{D}}} \cong \frac{\mu_{\Delta 21}}{RT} = \ln \frac{\zeta}{1-\zeta}, \tag{6.19}$$

The field variable ζ has the advantage that it varies from 0 to 1 as the concentration x of the solvent varies from 0 to 1.[128] The definition of the field variable ζ is not unique, since it depends on the zero values of energy and entropy of the two components. In practice one tries to use this freedom to impose the condition that ζ becomes equal to the concentration x on the critical locus, referred to as critical-line condition (CLC).[65] While the transformation (6.19) is a bit too simple for the CLC to be imposed rigorously,[65] Eq. (6.19) together with the CLC has been used successfully in many applications and appears to be a good approximation. From Eqs. (6.18) and (6.19) together with the CLC it follows that

$$\ln \left(\frac{x_{\mathrm{U,L}}}{1 - x_{\mathrm{U,L}}} \right) - \ln \left(\frac{x_{\mathrm{D}}}{1 - x_{\mathrm{D}}} \right) = a_x^* \left| \Delta \widetilde{P} \right| \pm b_x^* \left| \Delta \widetilde{P} \right|^{3/2}, \tag{6.20}$$

Figure 6.12 shows the critical pressure for 2-butanol+water as a function of the concentration of 2-butanol. The solid curves represent the values calculated from Eq. (6.20) with coefficients given in Table 6.4. Equation (6.20) predicts that the upper and lower critical consolute branches meet in the DCP with a common tangent $(dP_{\mathrm{c}}/dx)_{\mathrm{CL}} = -P_{\mathrm{D}}/a_x^* x_{\mathrm{D}}(1 - x_{\mathrm{D}})$ in agreement with the experimental observation.

Finally, to represent the solubility loops as a function of pressure, we need
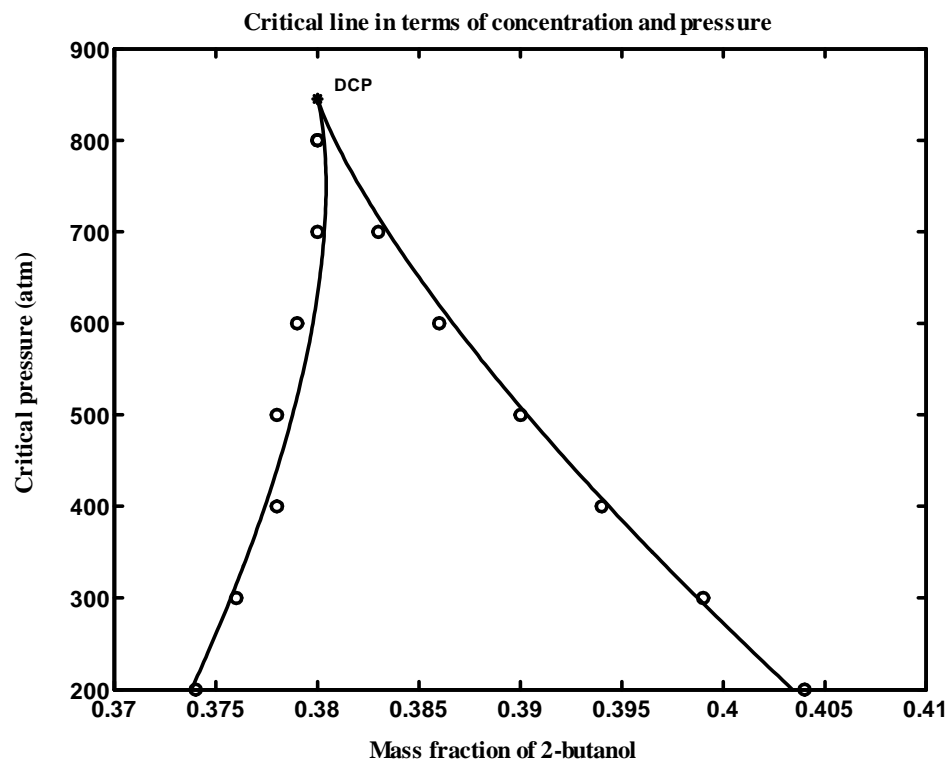
Figure 6.12: Critical line in terms of concentration and pressure. The circles are the critical mass concentrations and the solid curve represents Eq. (6.20).

also to specify the pressure dependence of the amplitudes B_0, B_1, and B_a in Eq. (6.12). An inspection of Table 6.2 shows that the dependence of the coefficients on pressure is erratic, because of the strong correlation between the coefficients. This suggests that, even with the coefficient d_1 fixed, one should be able to reduce the number of terms in the expansion to represent the rather symmetric solubility loops for the 2-butanol+water system. For a simplified description of the solubility loops we retain only the leading singular power law in Eq. (6.10), so that

$$x = x_\mathrm{L} \pm B_0 \left| \tau_\mathrm{UL} \right|^\beta + d_1 \left(\frac{T - T_\mathrm{L}}{T_\mathrm{L}} \right), \qquad (6.21)$$

with d_1 again given by Eq. (6.11). The effective amplitude B_0 is a constant of order unity and only weakly dependent on pressure. Taking $B_0 = 0.95$ independent of the pressure in Eq. (6.21) and adopting Eqs. (6.17) and (6.20) with the values of the coefficients given in Table 6.4 for the critical locus at pressures above 200 atm, we obtain for 2-butanol+water the liquid-liquid phase-separation diagram shown in Fig.6.13.

Starting from the principle of isomorphic critical behavior of fluid mixtures we have derived a simple equation for closed solubility loops in liquid mixtures at constant pressure. The simple equation is able to represent closed solubility loops at atmospheric pressure and at elevated pressures including solubility loops that span a temperature range as large as 200 K. We have also elucidated the liquid-liquid phase-separation behavior in the vicinity of a double critical point. Specifically, the
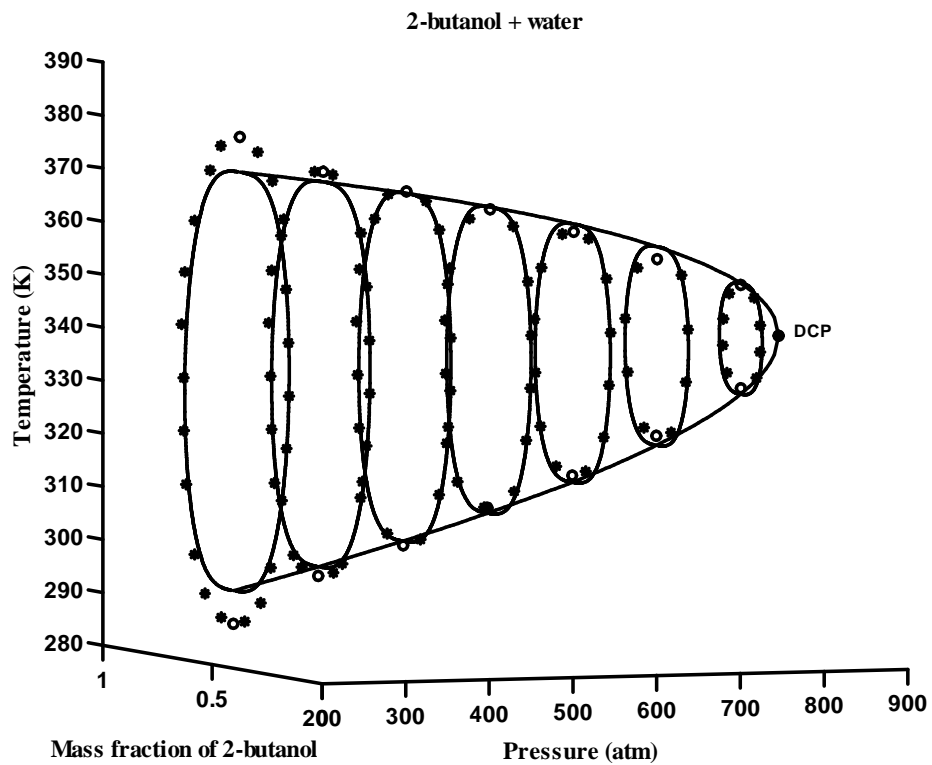
Figure 6.13: Phase equilibrium of 2-butanol + water system. The stars are experimental data obtained by Moriyoshi *et al.*[42] The solid curves represent Eqs (6.17),(6.20) and (6.21).

critical pressure exhibits an asymptotic parabolic dependence on temperature near a double critical point, while the upper and lower critical consolute branches of the critical pressure as a function of concentration meet at the double critical point with a common tangent. We have shown how an equation for solubility loops as a function of pressure can be developed from an expansion around a double critical point.

CHAPTER 7

SUMMARY

The nature of asymmetry in fluid criticality, especially for vapor-liquid equilibria of one-component fluids and liquid-liquid equilibria in binary fluid mixtures, has been investigated. To clarify the nature of vapor-liquid asymmetry, we have simplified the "complete scaling" by a proper choice of the critical entropy density $s_c = (\partial P/\partial T)_{h_1=0,c}$ to a form with only two independent mixing coefficients a_3 and b_2. We have also developed a method to obtain these two scaling-field coefficients $\frac{a_3}{1+a_3} = \frac{2}{3}\frac{\mu_{21}}{\mu_{11}} - \frac{1}{5}\frac{\mu_{40}}{\mu_{30}}$ and $b_2 = \frac{1}{\mu_{11}}\left(\frac{\mu_{21}}{\mu_{11}} - \frac{1}{5}\frac{\mu_{40}}{\mu_{30}}\right)$, responsible for two different sources of the asymmetry, from mean-field equations of state. By analyzing some classical equations of state we have found that the vapor-liquid asymmetry in classical fluids near the critical point can be controlled by molecular parameters, such as the degree of association N and the relative strength of three-body interactions c. By combining accurate vapor-liquid coexistence and heat-capacity data, we have unambiguously proved the experimental and simulation evidence of "complete scaling". A number of systems, real fluids and simulated models, such as hard-core square-well (HCSW) fluid and restricted primitive model (RPM) electrolyte, have been analyzed. The asymmetry in fluid criticality originates from coupling between density and entropy fluctuations which produces a $\left|\Delta\widetilde{T}\right|^{1-\alpha}$ term and from coupling between density and volume fluctuations which produces a $\left|\Delta\widetilde{T}\right|^{2\beta}$ term in the coexistence-curve diameter. The molecular volumes appears to play a crucial role in the asymmetry of fluids. We have demonstrated how the mean-field

170

rectilinear diameter splits up in the critical region into two "singular diameters" associated with two different sources of asymmetry. Since near-critical vapor-liquid asymmetry is completely determined by Ising critical exponents, there is no need for a special renormalization-group theoretical treatment of the asymmetric fluid criticality. Furthermore, we have examined experimental consequences of "complete scaling" when extended to liquid-liquid coexistence in binary mixtures. The procedure for extending "complete scaling" from one-component fluids to binary fluids mixtures rigorously follows from the isomorphism theory. We have shown that the "singular" diameters of liquid-liquid coexistence curves originate from two different sources, one is associated with a correlation between concentration and entropy and another one is a correlation between concentration and molar density. Finally we studied special phase equilibria that can be only described by non-linear mixing of physical fields into the scaling fields. Based on the scaling theory and isomorphism, an approach to describe the closed-loop curves is presented in which the reduced temperature $\Delta\widetilde{T} = |(T - T_{\mathrm{c}})/T_{\mathrm{c}}|$ is replaced by $\tau_{\mathrm{UL}} = |(T - T_{\mathrm{L}})(T - T_{\mathrm{U}})/(T_{\mathrm{L}}T_{\mathrm{U}})|$. The expressions to describe the critical lines near a double critical point (DCP) are derived from the isomorphism theory.

REFERENCES

1. C. Domb, *The Critical Point,* Taylor & Francis Ltd, London (1996).

2. M. A. Anisimov, *Critical Phenomena in Liquids and Liquid Crystals*, Gordon and Breach , Philadelphia (1991).

3. H. E. Stanley, *Introduction to Phase Transitions and Critical Phenomena,* Oxford University Press, New York (1971).

4. M. A. Anisimov and J. V. Sengers, in *Equations of State for Fluids and Fluid Mixtures,* J. V. Sengers, R. F. Kayser, C. J. Peters, and H. J. White, Jr. (Eds.), Elsevier, Amsterdam (2000), p. 381.

5. C. Domb and M. S. Green, eds., *Phase Transitions and Critical Phenomena,* Vol 6, Academic Press, New York (1976).

6. F. J. Wegner, *Phys. Rev. B* **5**, 4529 (1972).

7. J. M. H. Levelt Sengers, *Physica* **73**, 73 (1974).

8. T. A. Edison, *Thermophysical properties of fluids and fluid mixtures: Including critical fluctuation effects,* (Dissertation), UMCP (1998).

9. J. F. Nicoll and J. K. Bhattacharjee, *Phys. Rev. B* **23**, 389 (1981).

10. J. F. Nicoll and P. C. Albright, *Phys. Rev. B* **31**, 4576 (1985).

11. Z. Y. Chen, P. C. Albright, and J. V. Sengers, *Phys. Rev. A* **41**, 3161 (1990).

12. Z. Y. Chen, A. Abbaci, S. Tang, and J. V. Sengers, *Phys. Rev. A* **42**, 4470 (1990).

13. L. Cailletet and E. C. Mathias, *C. R. Acad. Sci.* **102**, 1202 (1886); **104**, 1563 (1887).

14. N. D. Mermin, *Phys. Rev. Lett.* **26**, 957 (1971).

15. B. Widom and J. S. Rowlinson, *J. Chem. Phys.* **52**, 1670 (1970).

16. B. Widom, *The Robert A. Welch Foundation Conferences on Chemical Research XVI. Theoretical Chemistry*, Houston (1972), p. 161.

17. M. W. Pestak, M. H. W. Chan, J. R. de Bruyn, and D. A. Balzarini, Phys. Rev. B **36**, 599 (1987).

18. R. R. Singh and K. S. Pitzer, *J. Chem. Phys.* **92**, 3096 (1990).

19. M. E. Fisher and G. Orkoulas, *Phys. Rev. Lett.* **85**, 696 (2000).

20. G. Orkoulas, M. E. Fisher, and C. Üstün, *J. Chem. Phys.* **113**, 7530 (2000).

21. Y. C. Kim, M. E. Fisher, and G. Orkoulas, *Phys. Rev. E* **67**, 061506 (2003).

22. C. N. Yang and C. P. Yang, *Phys. Rev. Lett.* **13**, 303 (1964).

23. M. A. Anisimov, E. E. Gorodetskii, V. D. Kulikov, and J. V. Sengers, *Phys. Rev. E* **51**, 1199 (1995).

24. M. A. Anisimov, E. E. Gorodetskii, V. D. Kulikov, A. A. Povodyrev, and J. V. Sengers, *Physica A* **220**, 277 (1995).

25. S. C. Greer, *Phys. Rev. A* **14**, 1770 (1976).

26. M. Ley-Koo and M. S. Green, *Phys. Rev. A* **16**, 2483 (1977).

27. A. Kumar, H. R. Krishnamurthy, and E. S. R. Gopal, *Physics Reports* **98,** 48 (1983).

28. S. C. Greer, B. K. Das, A. Kumar, and E. S. R. Gopal, *J. Chem. Phys.* **79,** 4545 (1983).

29. P. Damay and F. Leclercq, *J. Chem. Phys.* **95,** 590 (1991).

30. C. A. Cerdeiriña, M. A. Anisimov, and J. V. Sengers, *Chem. Phys. Letts.* **424**, 414 (2006).

31. J. T. Wang, M. A. Anisimov, and J. V. Sengers, *Z. Phys. Chem.* **219**, 1273 (2005).

32. T. Narayanan and A. Kumar, *Physics Reports* **249***,* 135 (1994).

33. L. A. Davidovich and I. I. Shinder, *Sov. Phys. JETP* **68**, 743 (1989).

34. L. A. Davidovich, I. I. Shinder, and E. K. Kanaki, *Phys. Rev. A* **43**, 1813 (1991).

35. N. P. Malomuzh and B. A. Veitsman, *Phys. Lett. A* **136**, 239 (1989).

36. N. P. Malomuzh and B. A. Veitsman, *Physica A* **168**, 833 (1990).

37. Y. C. Kim, M. A. Anisimov, J. V. Sengers, and E. Luijten, *J. Stat. Phys.* **110**, 591 (2003).

38. J. S. Hager, M. A. Anisimov, J. V. Sengers, and E. E. Gorodetskii, *J. Chem. Phys.* **117,** 5940 (2002).

39. R. J. L. Andon and J. D. Cox, *J. Chem. Soc.* 4601 (1952).

40. J. Matous, J. P. Novak, and J. Pick, *Collect. Czech. Chem. Commun.* **37**, 2653 (1972).

41. P. Lejcek, J. Matous, J. P. Novak, and J. Pick, *J. Chem. Thermodyn.* **7**, 927 (1975).

42. T. Moriyoshi, S. Kaneshina, K. Aihara, and K. Yabumoto, *J. Chem. Thermodyn.* **7**, 537 (1975).

43. J. V. Sengers and J. M. H. Levelt Sengers, in *Progress in Liquid Physics*, C. A. Croxton (ed.), Wiley, Chichester, U. K., (1978), p. 103.

44. V. A. Agayan, *Crossover Critical Phenomena in Simple and Complex Fluids (Dissertation),* UMCP, College Park (2000).

45. K. Gutkowski, M. A. Anisimov, and J. V. Sengers, *J. Chem. Phys.* **114,** 3133 (2001).

46. M. A. Anisimov, S. B. Kiselev, J. V. Sengers, and S. Tang, *Physica A* **188**, 487 (1992).

47. V. L. Ginzburg, *Sov. Phys. Solid State* **2**, 1824 (1960).

48. S. Tang, J. V. Sengers, and Z. Y. Chen, *Physica A* **179**, 344 (1991).

49. M. E. Fisher, *Rep. Prog. Phys.* **30**, 615 (1967).

50. G. A. Baker, B. G. Nickel and D. I. Meiron, *Phys. Rev. B* **17**, 1365 (1978).

51. J. C. Guillou and J. Zinn-Justin, *Phys. Rev. B* **21**, 3976 (1980).

52. A. J. Liu and M. E. Fisher, *Physica A* **156**, 35 (1989).

53. M. E. Fisher and S. Y. Zinn, *J. Phys. A: Math. Gen.* **31**, L629 (1998).

54. M. E. Fisher, in *Critical Phenomena*, edited by F. J. W. Hahne, Lecture Notes in Physics Vol. 186, Springer, Berlin (1982), p. 1.

55. M. A. Anisimov, A. V. Voronel and E. E. Gorodetskii, *Sov. Phys. JETP* **33**, 605 (1971).

56. J. M. H. Levelt Sengers and J. V. Sengers, in: *Perspectives in Statistical Physics*, H. J. Raveche ed., Amsterdam, North Holland (1981).

57. M. Ley-Koo and M. S. Green, *Phys. Rev. A* **23**, 2650 (1981).

58. S.-Y. Zinn and M. E. Fisher, *Physica A* **226**, 168 (1996).

59. R. Guida and J. Zinn-Justin, *J. Phys. A: Mathe . Gen.* **31**, 8103 (1998).

60. C. Bagnuls and C. Bervillier, *Phys. Rev. B* **32**, 7209 (1985).

61. C. Bagnuls, C. Bervillier, D. I. Meiron, and B. G. Nickel, *Phys. Rev. B* **35**, 3585 (1987).

62. M. E. Fisher, in *Critical Phenomena*, Proceedings of the International School of Physice "Enrico Fermi", Course LI, Varenna (1970), edited by M. S. Green (Academic, New York, 1971), p. 1.

63. A. Z. Patashinskii and V. L. Pokrovskii, *Fluctuation Theory of Phase Transitions*, Pergamon, Oxford (1979).

64. N. D. Mermin and J. J. Rehr, *Phys. Rev. Lett.* **26**, 1155 (1971).

65. M. A. Anisimov and J. V. Sengers, *Phys. Letts. A* **172**, 114 (1992).

66. F. Monroy, A. G. Casielles, A. G. Aizpiri, R. G. Rubio, and F. Ortega, *Phys. Rev. B* **47**, 630 (1993).

67. A. Oleinikova and H. Weingärtner, *Phys. Chem. Chem. Phys.* **4**, 955 (2002).

68. R. Brout, *Phase Transitions,* W. A. Benjamin Inc., New York, (1965).

69. E. M. Lifshitz and L. P. Pitaevskii, in *Statistical Physics*, 3rd Edition, Part 1, Oxford (1980), p. 277

70. A. Anderko, in *Equations of State for Fluids and Fluid Mixtures,* J. V. Sengers, R. F. Kayser, C. J. Peters, and H. J. White, Jr. (Eds.), Elsevier, Amsterdam (2000), p. 75.

71. A. M. Wims, D. McIntyre, and F. Hynne, *J. Chem. Phys.* **50**, 616 (1969).

72. M. P. Khosla and B. Widom, J. *Colloid Interface Sci.* **76**, 375 (1980).

73. N. Nagarajan, A. Kumar, E. S. R. Gopal, and S. C. Greer, *J. Chem. Phys.* **84**, 2883 (1980).

74. P. R. Bevington, *Data Reduction and Error Analysis for the Physical Sciences*, McGraw-Hill, New York (1969).

75. J. M. Smith, H. C. Van Ness, and M. M. Abbott, *Introduction to Chemical Engineering Thermodynamics*, McGraw-Hill, New York (2001).

76. L. A. Weber, *Phys. Rev. A* **2**, 2379 (1970).

77. U. Närger and D. A. Balzarini, *Phys. Rev. B* **42**, 6651 (1990).

78. I. Hahn, M. Weilert, F. Zhong, and M. Barmatz, *J. Low Temp. Phys.* **137**, 579 (2004).

79. J. Weiner, K. H. Langley, and N. C. Ford, Jr, *Phys. Rev. Lett.* **32**, 879 (1974).

80. H. Eyring, *J. Chem. Phys.* **4**, 283 (1936).

81. H. Eyring, D. Henderson, B. J. Stover, and E. M. Eyring, *Statistical Mechanics and Dynamics,* Wiley, New York (1964), p. 354.

82. Y. C. Kim and M. E. Fisher, *Chem. Phys. Letts.* **414**, 185 (2005).

83. M. I. Bagatskii, A. V. voronel', and V. G. Gusak, *Sov. Phys. JETP* **16**, 517 (1963).

84. Yu. R. Chashkin, V. G. Gorbunova, and A. V. Voronel', *Sov. Phys. JETP* **22**, 304 (1966).

85. A. V. Voronel V. G. Gorbunova, V. A. Smirnov, N. G. Shmakov, and V. V. Shekochikhina, *Sov. Phys. JETP* **63**, 965 (1972).

86. J. F. Nicoll and P. C. Albright, *Phys. Rev. B* **34**, 1991 (1986).

87. S. Moghaddam, Y. C. Kim, and M. E. Fisher, *J. Chem. Phys. B* **109**, 6824 (2005).

88. A. Haupt and J. Straub, *Phys. Rev. E* **59**, 1795 (1999).

89. M. Barmatz, F. Zhong, and A. Shih, *Int. J. Thermophy.* **25**, 1667 (2004).

90. E. T. Shimanskaya, I. V. Bezruchko, V. I. Basok, and Yu. I. Shimanskiĭ, *Sov. Phys. JETP* **53**, 139 (1981).

91. R. Kleinrahm and W. Wagner, *J. Chem. Thermodyn.* **18**, 739 (1986).

92. L. M. Artyukhovskaya, E. T. Shimanskaya, and Yu. I. Shimanskiĭ, *Sov. Phys. JETP* **32**, 375 (1971).

93. T. R. Das, C. O. Reed, Jr, and P. T. Eubank, *J. Chem. Eng. Data* **22**, 3 (1977).

94. L. M. Artyukhovskaya, E. T. Shimanskaya, and Yu. I. Shimanskiĭ, *Sov. Phys. JETP* **36**, 1140 (1973).

95. W. Wagner and A. Pruß, *J. Phys. Chem. Refer. Data* **31**, 387 (2002).

96. G. Orkoulas, M. E. Fisher, and A. Z. Panagiotopoulos, *Phys. Rev. E* **63**, 051507 (2001).

97. Y. C. Kim, *Phys. Rev. E* **71**, 051501 (2005).

98. I. M. Abdulagatov, E. E. Gorodetskiĭ, and V. P. Voronov, unpublished heat-capacity data for hydrocarbons

99. A. K. Wyczalkowska, J. V. Sengers, and M. A. Anisimov, *Physica A* **334**, 482 (2004).

100. A. K. Wyczalkowska, M. A. Anisimov, J. V. Sengers, and Y. C. Kim, *J. Chem. Phys.* **116**, 4202 (2002).

101. R. E. Barieau, *Thermodynamic Properties of a Van der Waals Fluid in the Two-phase Region*, U. S. Dept. of the Int. Library, Washington (1967).

102. A. Oleinikova and H.Weingärtner, *Chem, Phys. Lett.* **319,** 119 (2000).

103. K. Tang, C. Zhou, X. An, and W. Shen, *J. Chem. Thermodyn.* **31,** 943 (1999).

104. X. An, F. Jiang, H. Zhao, C. Chen, and W. Shen, *J. Chem. Thermodyn.* **30,** 751 (1998).

105. X. An, P. Li, H. Zhao, and W. Shen, *J. Chem. Thermodyn.* **30,** 1049 (1998).

106. X. An, F. Jiang, H. Zhao, and W. Shen, *J. Chem. Thermodyn.* **30,** 1181 (1998).

107. X. An, H. Zhao, F. Jiang, and W. Shen, *J. Chem. Thermodyn.* **30,** 21 (1998).

108. C. Zhou, X. An, F. Jiang, H. Zhao, and W. Shen, *J. Chem. Thermodyn.* **31,** 615 (1999).

109. X. An, H. Zhao, F. Jiang, C. Mao, and W. Shen, *J. Chem. Thermodyn.* **29,** 1047 (1997).

110. X. An, F. Jiang, H. Zhao, and W. Shen, *Acta Chimica Sinica* **50** 141 (1998).

111. J. S. Rowlinson and F. L. Swinton, *Liquids and Liquid Mixtures, Butterworth Scientific*, London (1982).

112. J. Levelt Sengers. *How Fluids Unmix*, Edita KNAW, Amsterdam (2002).

113. A. Wallbruch and G. M. Schneider, *J. Chem. Thermodyn.* **27**, 377 (1995); **29**, 929 (1997).

114. G. M. Schneider, *Phys. Chem. Chem. Phys.* **4**, 845 (2002); **6**, 2285 (2004).

115. J. O. Hirschfelder, D. Stevenson, and H. Eyring, *J. Chem. Phys.* **5**, 896 (1937).

116. A. G. Aizpiri, P. Chazarra, R. G. Rubio, and M. Díaz Peña, *Chem. Phys.* **146**, 39 (1990).

117. R. B. Griffiths and J. C. Wheeler, *Phys. Rev. A* **2**, 1047 (1970).

118. S. C. Greer and M. R. Moldover, *Ann. Rev. Phys. Chem.* **32**, 233 (1981).

119. S. C. Greer, *Phys. Rev. A* **14,** 1770 (1976).

120. N. Nagarajan, A. Kumar, E.S.R. Gopal, and S.C. Greer, *J. Phys. Chem.* **84,** 2883 (1980).

121. M. P. Khosla and B. Widom, *J. Colloid Interface Sci.* **76**, 375 (1980).

122. A. G. Aizpiri, R. G. Rubio, and M. Díaz Peňa, *J. Chem. Phys.* **88,** 1934 (1988).

123. M. Kleemeier, S. Wiegand, W. Schröer, and H. Weingärtner, *J. Chem. Phys.* **110,** 3085 (1999).

124. A. G. Aizpiri, F. Monroy, C. del Campo, R. G. Rubio, and M. Díaz Peňa, *Chemical Physics* **165**, 31 (1992).

125. G. M. Schneider, *J. Chem. Thermodyn.* **23,** 301 (1991).

126. M. Spree and G. M. Schneider, *High Pressure Res.* **5,** 675, (1990); *Fluid Phase Equilib.* **65,** 263 (1991).

127. A. Kordikowsky, *Fluid phase equilibria of ternary and quaternary mixtures of low-volatile organic substances with supercritical carbon dioxide at temperatures between 298 K and 393 K and pressures between 10 MPa and 100 MPA (in German)*, Ph.D. Thesis, Ruhr-Universität Bochum (1992).

128. S. S. Leung and R. B. Griffiths, *Phys. Rev. A* **8,** 2670 (1973).